Journal of Computational Physics 300 (2015) 533–573

Contents lists available at ScienceDirect

Journal of Computational Physics

www.elsevier.com/locate/jcp

The linking number in systems with Periodic Boundary Conditions

E. Panagiotou

Department of Mathematics, University of California, Santa Barbara, CA 93106, USA

ARTICLE INFO

Article history:
Received 23 October 2014
Received in revised form 11 April 2015
Accepted 27 July 2015
Available online 31 July 2015

Keywords:
Linking number
Periodic Boundary Conditions
Knot theory
Polymer physics
Fluid mechanics
Entanglement

ABSTRACT

Periodic Boundary Conditions (PBC) are often used for the simulation of complex physical systems. Using the Gauss linking number, we define the periodic linking number as a measure of entanglement for two oriented curves in a system employing PBC. In the case of closed chains in PBC, the periodic linking number is an integer topological invariant that depends on a finite number of components in the periodic system. For open chains, the periodic linking number is an infinite series that accounts for all the topological interactions in the periodic system. In this paper we give a rigorous proof that the periodic linking number is defined for the infinite system, i.e., that it converges for one, two, and three PBC models. It gives a real number that varies continuously with the configuration and gives a global measure of the geometric complexity of the system of chains. Similarly, for a single oriented chain, we define the periodic self-linking number and prove that it also is defined for open chains. In addition, we define the cell periodic linking and self-linking numbers giving localizations of the periodic linking numbers. These can be used to give good estimates of the periodic linking numbers in infinite systems. We also define the local periodic linking number associated to chains in the immediate cell neighborhood of a chain in order to study local linking measures in contrast to the global linking measured by the periodic linking numbers. Finally, we study and compare these measures when applied to a PBC model of polyethylene melts.

1. Introduction

The entanglement of filaments arises in many physical systems, such as polymer melts or fluid flows. The rheological properties of polymer melts are determined primarily by the random-walk-like structure of the constituent chains and the fact that the chains cannot cross [1]. Edwards suggested that entanglements effectively restrict individual chain conformations to a curvilinear tubelike region enclosing each chain [1]. For very short time scales, chain segments are allowed to freely fluctuate in all directions until their displacements become commensurate with the tube diameter, a, which is related to the average distance between entanglements, N_e, by $a^2 = N_e b$, where b is the bond length [2–4]. The axis of the tube is a coarse-grained representation of the chain, called the *primitive path* (PP). Several methods have been developed for extracting the PP network [5–11]. Two geometrical methods capable of efficiently reducing computer generated polymer models to entanglement networks are the Z1-code [7,6,12,13] and the CReTA algorithm [8]. The tube model is very successful and provides a unified view of networks and entangled polymer melts on a mean-field level. Simulations as well as experiments back up the microscopic picture of a tube [14]. Despite these advances, our understanding of entanglement is incomplete

E-mail address: panagiotou@math.ucsb.edu.

http://dx.doi.org/10.1016/j.jcp.2015.07.058
0021-9991/

and it is an open question whether these simpler models can be derived from more fundamental topological considerations. The reason is the difficulty to connect the entanglement properties of the chains at two different scales. Indeed, one can distinguish between the local obstacles to the motion of the chains, and the conformational complexity of the entire conformations of the chains in the melt. Similarly, vortex lines in a fluid flow may be seen as mathematical curves that are entangled [15–17]. Helmholtz discovered that the vortex lines move with the fluid in a perfectly inviscid flow [18]. Helmholtz' theorem implied that the global topology of vortex lines remains unchanged throughout the flow evolution. The helicity of a fluid flow confined to a domain D (bounded or unbounded) of three-dimensional Euclidean space $\mathbb{R}^3$ is the integrated scalar product of the velocity field $\vec{u}(\vec{x},t)$ and the vorticity field $\vec{\omega}(\vec{x},t)=\nabla\times\vec{u}$, $H=\int_D \vec{u}\cdot\vec{\omega}dV$ [19,20,15]. Helicity is important at a fundamental level in relation to flow kinematics because it admits topological interpretation in relation to the linking of vortex lines of the flow [15] (see discussion on the linking number in the next paragraph). Invariance of the helicity is then directly associated with invariance of the topology of the vorticity field. Similarly, any solenoidal vector field that is convected without diffusion by a flow will have conserved topology and an associated helicity invariant. Helicity plays a crucial role in the problem of relaxation to magnetostatic equilibrium, a problem of central importance in the context of thermonuclear fusion plasmas [19,16]. Helicity is also related to transition to turbulence [21–23]. When the fluid is conducting, magnetic helicity is an invariant in the ideal case and is central to minimum energy equilibria in plasmas such as in spheromaks, or in solar coronal mass ejections. It is also known that the generation of large-scale magnetic fields occurs due to small-scale mechanic helicity and that in the presence of both rotation and stratification, helicity is created and thus a dynamo is facilitated in a wide variety of astrophysical settings [24,22,25]. Polymer and vortex entanglement share some common features, especially when there is mutual interference, as in the case of polymer solutions. The addition of small amounts of long chain polymers to flowing fluids produces large effects on a wide range of phenomena such as the stability of laminar motion, transition to turbulence, vortex formation and break-up, turbulent transport of heat, mass and momentum, and surface pressure fluctuations [26].

Edwards first pointed out that in the case of ring polymers, the global entanglement of the chains can be studied by using tools from mathematical topology [27,28]. A knot (or link) is one (or more) simple closed curve(s) in space. Knots and links are classified with respect to their complexity by topological invariants, such as knot or link polynomials [29–31]. Since Edwards, many studies have been devoted to the topology of polymer rings and its relation to physical properties [32,5,33–35]. In [34] a direct relation between distinct topological states and N_e has been revealed. However, most of these methods cannot be applied to systems of open chains. The study of global entanglement has been very useful especially in the study of biopolymers [36,37]. Indeed, open curves are not knotted in the topological sense, but they can form complex conformations, which we call *entangled*. Unfortunately, it is not easy to relate intuitive notions of entanglement with topology [38,39]. A classical measure of entanglement that extends naturally to open chains is the Gauss linking integral, *lk*. In the case of closed chains the Gauss linking number is a classical topological integer invariant [40] that is related to the helicity of fluid flows and magnetic fields [41]. More precisely, consider an inviscid incompressible fluid, where the vorticity field is zero except in two closed vortex filaments of strengths (associated circulations) κ_1, κ_2, whose axes are C_1, C_2. Then the *helicity* is $H=2lk(C_1,C_2)\kappa_1\kappa_2$. For pairs of "frozen" open chains, or for a mixed frozen pair, the Gauss linking integral can be applied to calculate an average linking number. For open or mixed pairs, the calculated quantity is a real number that is characteristic of the conformation and changes continuously under continuous deformations of the constituent chains [42]. Thus, the application of the Gauss linking integral to open chains is very clearly not a topological invariant, but a quantity that depends on the specific geometry of the chains. In a similar manner, the Gauss linking integral can be applied to calculate the writhe or the self-linking number of a "frozen" configuration of one open chain. It is true that a complicated tangle and a really untangled curve can have essentially the same writhe, but it takes special effort to construct untangled complicated looking curves with high absolute writhe. Exactly the same considerations apply for the linking number and the self-linking number. Indeed, computer experiments indicate that the linking number and the writhe are effective indirect measures of whatever one might call "entanglement", especially in systems of "random" filaments [41,27,43–48,42,49–54] and it has been shown that they can provide information relevant to the tube model [52,53].

One of the reasons why knots in polymer melts and turbulent flows have not been studied extensively is the problem of handling systems employing PBC [34,55]. Notice that the entire system is created by infinite copies of the simulation cell, and so, applying a traditional measure of entanglement would imply computations involving an infinite number or, at least, a very large number of chains. Furthermore, there exists an infinite number of pairs of chains in the same relative position, giving infinite repetitions of a same pattern. Ideally, one would like to compute a linking measure directly from one cell, but the arcs of the chains inside the cell are relatively short (see Fig. 1). In order to capture the greater degrees of entanglement, or even complex knotting, a large number of arcs must be employed in the creation of a complex chain. In [34,56] the Jones polynomial for systems employing one or two PBC was used to study entanglement in ring polymers. The method presented therein cannot be extended to systems employing 3 PBC. Moreover, the definition of the Jones polynomial is not meaningful when one deals with open chains. In this paper we propose to use the Gauss linking number and its extension to open chains to define a measure of entanglement for chains in one, two or three PBC. This gives a measure of global entanglement of the chains and could be used in the estimation of a topological energy in a system of open, closed or mixed chains with PBC.

In [57], the basis for the study of entanglement in systems employing PBC was introduced, and the *local periodic linking number* was defined and applied to samples of polyethylene (PE) melts. In this paper the *periodic linking number* is defined and its properties for closed, open or infinite chains, and its relation to the Gauss linking number and the local periodic

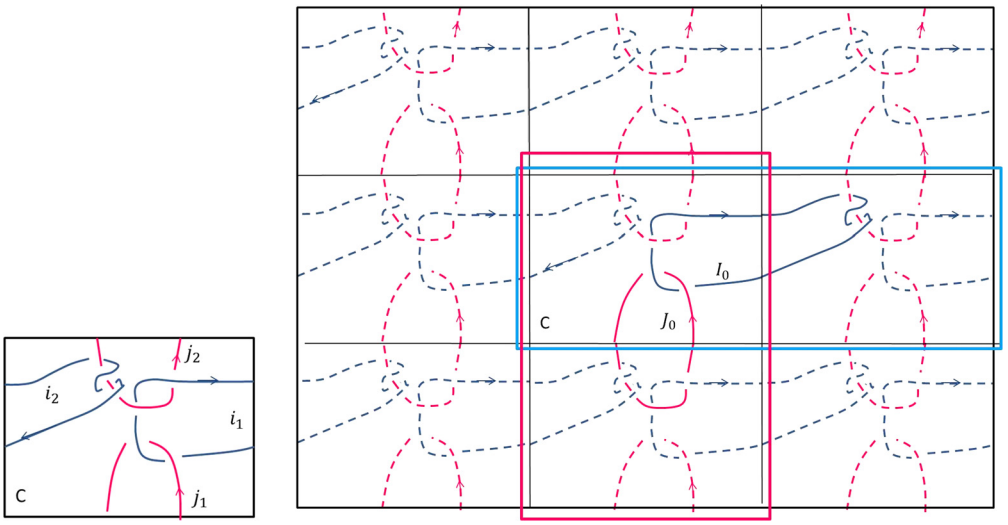

Fig. 1. The central cell C and a portion of the periodic system it generates in the case of closed chains in a system with 2PBC. Left: The central cell C. The generating chain i (resp. j) is composed by the blue (resp. red) arcs in C, i.e. the arcs i_1, i_2 (j_1, j_2, resp.). Right: The free chain I (resp. J) is the set of dotted blue (resp. red) chains in the periodic system. Highlighted are the parent images I_0 and J_0 and the highlighted blue and red cells are their minimal unfoldings. (For interpretation of the references to color in this figure legend, the reader is referred to the web version of this article.)

linking number are studied. More precisely, in Section 2 the structure of the PBC model and its relation to identification spaces is described. In Section 3, the definitions of the periodic linking number and the periodic self-linking measures are introduced. In Section 4 the properties of the periodic linking number and the periodic self-linking number for closed chains are studied. Sections 5 and 6 deal with the properties of the periodic linking number for open or infinite chains. More precisely, in Section 5 a sketch of proof of convergence of the periodic linking number for open or infinite chains is presented and some background material is given. In Section 6 the convergence of the periodic linking number is presented and its properties in the case of open or infinite chains in systems employing PBC are studied. For the purpose of application to polymers, in Section 7, the cell periodic linking number is defined and it is compared to the periodic linking number and the local periodic linking number by applying them to PE melt samples in Section 8.

2. PBC systems

In this section we give some definitions that form the basis for our study of entanglement in PBC.

We study a system consisting of a collection of polygonal chains of length n (i.e. of n edges), by dividing the space into a family of cubic boxes of volume l^3, where l is the edge length of the cube, so that the structure of the melt in each cube is identical, i.e. we impose PBC on the system [14]. Specifically, we make the following definition:

Definition 1. A *cell* consists of a cube with embedded arcs (i.e. parts of curves) whose endpoints lie only in the interior of the cube or on the interior of one of its faces, but not on an edge or corner, and those arcs which meet a face satisfy the PBC requirement. That is, to each ending point corresponds a starting point at exactly the same position on the opposite face of the cube. See Fig. 1 for an illustrative example.

A cell generates a *periodic system* in 3-space by tiling 3-space with the cubes so that they fill space and only intersect on their faces. This allows an arc in one cube to be continued across a face into an adjacent cube and so on. Notice that the resulting chains may be closed, open or infinite.

Without loss of generality, we choose a cell of the periodic system that we call *generating cell*. A *generating chain* is the union of all the arcs inside the cell the translations of which define a connected component in the periodic system. For each arc of a generating chain we choose an orientation such that the translations of all the arcs would define an oriented curve in the periodic system. For each generating chain we choose without loss of generality an arc and a point on it to be its *base point* in the generating cell. For generating chains we shall use the symbols $i, j, \ldots$. For the arcs of a generating chain, say i, we use the symbols $i_1, \ldots, i_k$. An *unfolding* of a generating chain is a connected arc in the periodic system composed by exactly one translation of each arc of the generating chain. Then an unfolding contains exactly one translation of the base point of the generating chain. A generating chain is said to be closed (resp. open) when its unfolding is a closed (resp. open) chain. The smallest union of the copies of the cell needed for one unfolding of a generating chain shall be called the *minimal unfolding*. The smaller number of copies of the cell whose union contains the convex hull of the complete unfolding of a generating chain shall be called the *minimal topological cell*.

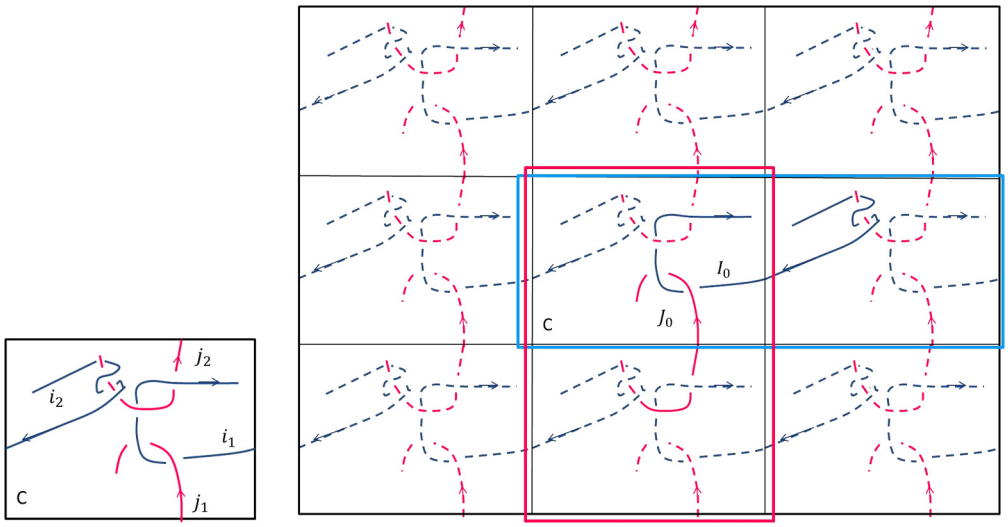

Fig. 2. The central cell C and a portion of the periodic system it generates in the case of closed chains in a system with 2PBC. Left: The central cell C. The generating chain i (resp. j) is composed by the blue (resp. red) arcs in C, i.e. the arcs i_1, i_2 (j_1, j_2, resp.). Right: The free chain I (resp. J) is the set of dotted blue (resp. red) chains in the periodic system. Highlighted are parent images I_0 and J_0 and the highlighted blue and red cells are their minimal unfoldings. (For interpretation of the references to color in this figure legend, the reader is referred to the web version of this article.)

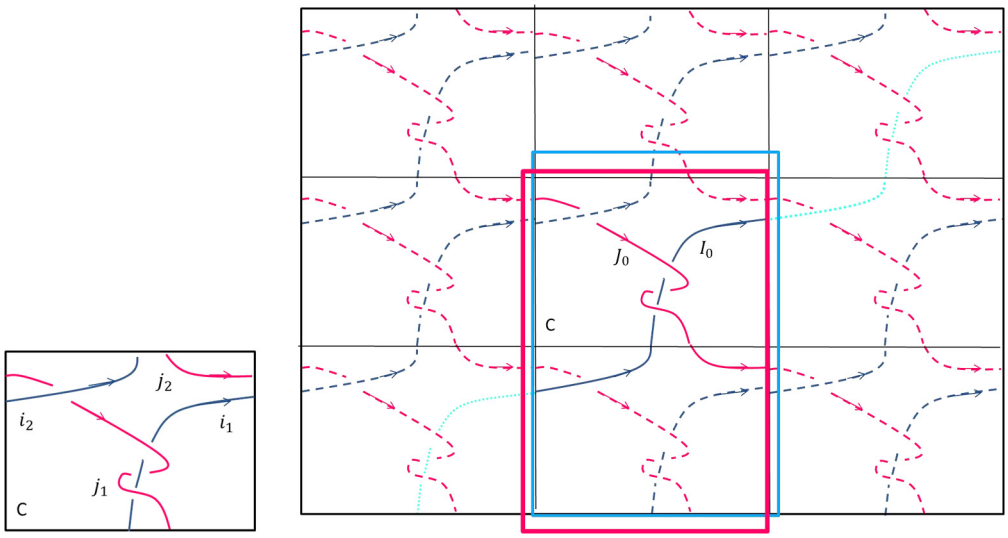

Fig. 3. The central cell C and a portion of the periodic system it generates in the case of closed chains in a system with 2PBC. Left: The central cell C. The generating chain i (resp. j) is composed by the blue (resp. red) arcs in C, i.e. the arcs i_1, i_2 (j_1, j_2, resp.). Right: The free chain I (resp. J) is composed by all the dotted blue (resp. red) arcs in the periodic system. Each connected component in a system of infinite free chains defines an infinite curve, which we call an infinite image. The images of I are now parts of infinite images. For example, the highlighted arc in blue is the parent image I_0 of I and the dotted cyan curve of which I_0 is an arc, is an infinite image of I, $\mathcal{I}_0$. The highlighted blue and red cells are the minimal unfoldings of the parent images I_0 and J_0. (For interpretation of the references to color in this figure legend, the reader is referred to the web version of this article.)

The collection of all translations of the same generating chain i shall be called a *free chain*, denoted I. A free chain is a union of connected components, each of which is equivalent to any other under translation. For free chains we will use the symbols $I, J, \ldots$. An *image* of a free chain is any arc of a free chain that is the unfolding of a generating chain. The minimal unfolding of I containing an image I_u of I, will be denoted $mu(I_u)$. For example, in Figs. 1 and 2, the blue closed curves are some of the images of the free chain I and the highlighted blue cells compose $mu(I_0)$. In the particular case where the images of a free chain form infinite components in the periodic system, this free chain shall be called *infinite free chain*. We call an infinite connected component of an infinite free chain I an *infinite image* of I. Note that an image of an infinite free chain is still a finite arc, an unfolding of a generating chain, lying on an infinite image of I. For example in Fig. 3 the infinite curve on which the image I_0 lies is an infinite image of I, called $\mathcal{I}_0$. The image of I whose base point lies in the generating cell shall be called the *parent image* and it shall be denoted I_0. Then any other image of I can be defined as a translation

of I_0 by a vector $\vec{v}$ based on the base point of the parent image. That is:

$$I_v = I_0 + \vec{v}. \tag{1}$$

3. Linking in PBC

In this section we use the Gauss linking number to define a new measure of linking for chains in PBC. Similarly, we define a new measure of self-linking of a chain in PBC. These measures capture the global entanglement of the chains. Their properties in the cases of closed and open or infinite chains will be discussed in Sections 4 and 6, respectively.

3.1. The Gauss linking number

The Gauss linking number is a traditional measure of the algebraic entanglement of two disjoint oriented closed curves that extends directly to disjoint oriented open chains [43,42,27].

Definition 2. The Gauss *linking number* of two disjoint (closed or open) oriented curves l_1 and l_2, whose arc-length parametrizations are $\gamma_1(t)$, $\gamma_2(s)$ respectively, is defined as a double integral over l_1 and l_2 [40]:

$$L(l_1, l_2) = \frac{1}{4\pi} \int_{[0,1]} \int_{[0,1]} \frac{(\dot{\gamma}_1(t), \dot{\gamma}_2(s), \gamma_1(t) - \gamma_2(s))}{||\gamma_1(t) - \gamma_2(s)||^3} dtds, \tag{2}$$

where $(\dot{\gamma}_1(t), \dot{\gamma}_2(s), \gamma_1(t) - \gamma_2(s))$ is the triple product of $\dot{\gamma}_1(t)$, $\dot{\gamma}_2(s)$ and $\gamma_1(t) - \gamma_2(s)$.

In the case of closed chains the Gauss linking number is a topological invariant. If it is equal to zero, the two chains are said to be algebraically unlinked. The Gauss linking number can be computed for a fixed configuration of two open chains to give a real number that is equal to half the average algebraic sum of crossings between the two chains over all projection directions.

Let Ω denote the space of configurations of all open chains with no intersections in general position. Then L is a continuous function $L : \Omega \to \mathbb{R}$, and as the endpoints of the chains tend to coincide, the linking numbers tend to the linking numbers of the closed chains. For two open chains, the Gauss linking number may be non-zero, even if their convex hulls do not intersect. But as the distance between their convex hulls increases, the Gauss linking number tends to zero.

For applications, where the chains are simulated by open or closed polygonal chains which satisfy some conditions (for example restrictions on bond angles and length), the Gauss linking number can be used to compute an average absolute linking number over the space of configurations [44,48,42]. This quantity then is of special interest, since it is independent of any particular configuration and can be related to other physical properties of the system [27].

The Gauss linking integral can be applied to one chain to measure its entanglement with itself. The *self-linking number* is defined as the linking number between a curve l and a translated image of that curve l_ϵ at a small distance ϵ, called the *normal variation curve* of l, that is, $Sl(l) = L(l, l_\epsilon)$ [58]. This can be expressed by the Gauss integral over $[0,1]^* \times [0,1]^* = \{(x, y) \in [0,1] \times [0,1] \,|\, x \neq y\}$ by adding to it a correction term, so that it is a topological invariant of closed curves [59] under regular isotopy,

$$Sl(l) = \frac{1}{4\pi} \int_{[0,1]^*} \int_{[0,1]^*} \frac{(\dot{\gamma}(t), \dot{\gamma}(s), \gamma(t) - \gamma(s))}{||\gamma(t) - \gamma(s)||^3} dtds + \frac{1}{2\pi} \int_{[0,1]} \frac{(\gamma'(t) \times \gamma''(t)) \cdot \gamma'''(t)}{||\gamma'(t) \times \gamma''(t)||^2} dt. \tag{3}$$

The first integral is the *writhe* of a chain, denoted as $Wr(l)$, and expresses the average algebraic self-crossing number of the chain over all possible projection directions. The second term is the *total torsion* of a chain, denoted as $\tau(l)$ and measures the "extent" to which a curve deviates from being planar. Thus, $Sl(l) = Wr(l) + \tau(l)$.

3.2. The periodic linking number

In a periodic system we must define linking at the level of free chains (see Appendix B for an analysis of the motivation for this definition). Two free chains are two infinite collections of chains, so we return to the beginning of our discussion: how can we measure the linking of only the different pairs of chains? Looking at the periodic system we notice that, due to the periodicity, the linking imposed by all the images of one free chain, say J, to one image of another free chain, say I, are the same for any image of I. Based on this observation we give the following definition of a measure of entanglement between two free chains:

Definition 3 *(Periodic linking number).* Let I and J denote two (closed, open or infinite) free chains in a periodic system. Suppose that I_u is an image of the free chain I in the periodic system. The *periodic linking number*, LK_P, between two free chains I and J is defined as:

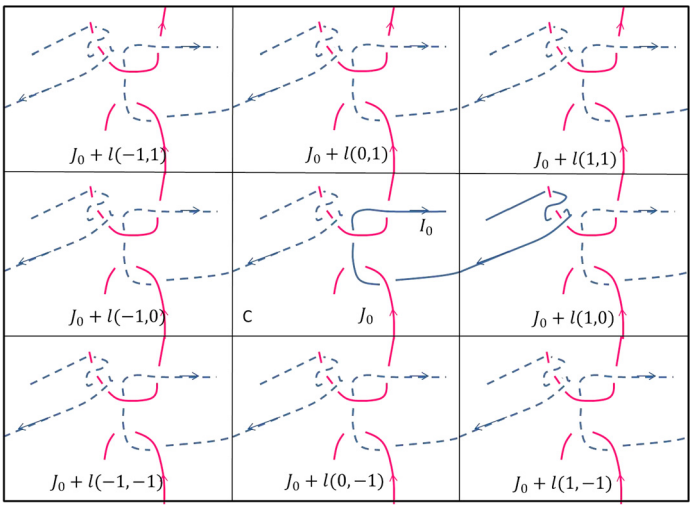

Fig. 4. A portion of a projection of a periodic system with 2 PBC generated by two open free chains. The periodic linking number $LK_P(I, J)$ is the sum of all the linking numbers between I_0 and every image of J. The images of J can be seen as translations of the parent image, i.e. as $J_0 + \vec{v}$, where $\vec{v}$ in $l\mathbb{Z}^2$ and l is the length of an edge of the simulation cell. Notice that since the chains are open, $L(I_0, J_0 + \vec{v}) \neq 0$, no matter how far $J_0 + \vec{v}$ is from I_0. Therefore, the periodic linking number of open chains is an infinite sum.

$$LK_P(I, J) = \sum_v L(I_u, J_v), \tag{4}$$

where the sum is taken over all the images J_v of the free chain J in the periodic system.

The periodic linking number has the following properties with respect to the structure of the cell, which follow directly by its definition:

(i) LK_P captures all the linking that all the images of a free chain impose to an image of the other.
(ii) LK_P is independent of the choice of the image I_u of the free chain I in the periodic system.
(iii) LK_P is independent of the choice, the size and the shape of the generating cell.

From observation (ii) above, the definition of the periodic linking number is equivalent to using the parent image I_0 for the free chain I:

$$LK_P(I, J) = \sum_v L(I_0, J_v) = \sum_v L(I_0, J_0 + \vec{v}). \tag{5}$$

We notice that the periodic linking number is an infinite summation of Gauss linking numbers (see Fig. 4 for an illustrative example). In the case of closed chains we observe in Section 4.1 that LK_P is reduced to a finite summation and in Appendix C we show that it is equal to the linking number of two chains in a manifold other that $\mathbb{R}^3$. However, the periodic linking number of open or infinite chains is indeed an infinite summation since the Gauss linking number is in general non-zero even if the chains are far from each other. Thus, the definition of the periodic linking number for open or infinite chains is meaningful only if the infinite summation converges. In Section 6 we show that LK_P indeed converges and that it is a continuous function of the chain coordinates.

The following important property holds for closed, open or infinite free chains and it shows that the periodic linking number is appropriate for the study of pairwise linking between free chains:

Proposition 4. *The periodic linking number, LK_P, between two free chains I and J of a system with PBC is symmetric.*

Proof. For any pair of images I_0, $J_0 + \vec{v}$ in Eq. (5), then the pair of images $I_0 - \vec{v}$, J_0 are in the same relative position. Thus $L(I_0, J_0 + \vec{v}) = L(I_0 - \vec{v}, J_0)$, and we have:

$$LK_P(I, J) = \sum_{\vec{v}} L(I_0, J_0 + \vec{v}) = \sum_{\vec{v}} L(I_0 - \vec{v}, J_0) = LK_P(J, I). \qquad \square \tag{6}$$

3.2.1. The periodic self-linking number

As we discussed in the Introduction, the periodic system consists of an infinite number of chains. Measuring the self-linking number of all the chains in the system requires an infinite calculation. However, infinitely many chains have the

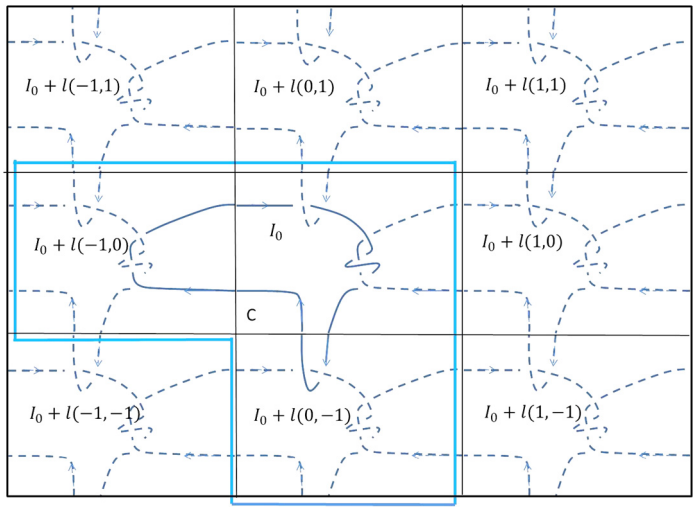

Fig. 5. A projection of a periodic system with 2 PBC generated by one chains. The periodic self-linking number $SL_P(I, J)$ is the sum of the self-linking of I_0 and all the linking numbers between I_0 and every other image of I. The images of I can be seen as translations of the parent image by vectors, $\vec{v}$, in $l\mathbb{Z}^2$, where l is the length of an edge of the simulation cell.

same conformation, thus their self-linking is the same and we would like to compute only the self-linking number of all the different conformations. On the other hand we know that the periodic system is generated by one cell, containing only a finite number of generating chains. These give rise to a finite number of free chains in the periodic system. Inspired by the definition of the periodic linking number at the level of free chains we define a measure of self-linking number at the level of free chains. We notice that an image of a free chain may be entangled with other images of itself (see Fig. 5 for an illustrative example). Thus a measure of self-entanglement of a free chain must capture this information. We introduce the following definition of self-linking for chains in PBC:

Definition 5 *(Periodic self-linking number).* Let I denote a free chain in a periodic system and let I_u be an image of I, then the *periodic self-linking number* of I is defined as:

$$SL_P(I) = Sl(I_u) + \sum_{v \neq u} L(I_u, I_v), \tag{7}$$

where the index v runs over all the images of I, except I_u, in the periodic system.

The periodic self-linking number has the following properties with respect to the structure of the cell, which follow directly by its definition:

(i) SL_P captures the linking that all the images of a free chain impose to one image of it.
(ii) SL_P is independent of the choice of the image I_u of the free chain I in the periodic system.
(iii) SL_P is independent of the choice, the size and the shape of the generating cell.

From observation (ii) above, the definition of the periodic self-linking number is equivalent to using the parent image I_0 for the free chain I:

$$SL_P(I) = Sl(I_0) + \sum_{v} L(I_0, I_v) = Sl(I_0) + \sum_{\vec{v}} L(I_0, I_0 + \vec{v}). \tag{8}$$

We give the following definition:

Definition 6 *(Periodic linking with self-images).* The *periodic linking with self-images* of a free chain I is defined as:

$$SLK_P(I) = \sum_{\vec{v}} L(I_0, I_0 + \vec{v}). \tag{9}$$

We notice that the periodic self-linking number can be expressed as

$$SL_P(I) = Sl(I_0) + SLK_P(I) = Wr(I_0) + \tau(I_0) + \sum_{\vec{v}} L(I_0, I_0 + \vec{v}), \tag{10}$$

where the sum $Wr(I_0) + \sum_v L(I_0, I_0 + \vec{v})$ is equal to the average algebraic self-crossing number of an image of I with itself, and with the other images of I. So, it measures the average algebraic self-crossing number of a free chain I. We give the following definition

Definition 7 *(Periodic writhe).* The *periodic writhe* of a free chain I is defined as:

$$WR_P(I) = Wr(I_0) + \sum_{\vec{v}} L(I_0, I_0 + \vec{v}). \tag{11}$$

Thus, $SL_P(I) = WR_P(I) + \tau(I_0)$.

4. Properties of LK_P for closed free chains

In this section we study some properties of the periodic linking number and the periodic self-linking number in the case of closed free chains. Namely, that the periodic linking number is a topological invariant and that it coincides with the linking number of the corresponding realized chains and that of the corresponding identification chains. These properties are rather obvious, resulting from the use of the Gauss linking number in the definition. Throughout this section I and J denote closed free chains.

4.1. Connecting LK_P with the Gauss linking number

We recall that for any closed curve in S^3 or $\mathbb{R}^3$ there is a surface of which it is the boundary. Thus there is a surface Σ, such that $\partial\Sigma = I_0$. Then for each image of J, say J_k, that does not intersect Σ, $L(I_0, J_k) = 0$. Thus the periodic linking number of closed chains can be expressed in terms of the Gauss linking number as

$$LK_P(I, J) = \sum_{\vec{v} \in S} L(I_0, J_0 + \vec{v}), \tag{12}$$

where S denotes the set of vectors for which $J_0 + \vec{v}$, intersects Σ.

It follows that the periodic linking number has the following properties in the case of closed free chains:

(i) LK_P is a topological invariant.
(ii) LK_P is an integer and it is equal to half the algebraic number of intersections between the projection of an image of I and the projection of all the images of J in any projection direction.
(iii) When the chains do not touch the faces of the cell, then LK_P equal to the linking number of their parent images.

The following proposition shows that in the case of one and two PBC, it is possible to compute LK_P only from the generating chains. In the following let us call the pair of right–left faces *x-faces* and the closing arcs that connect endpoints on these faces *x-closing arcs*. Similarly we define the *y-faces* and the *y-closing arcs*, and the *z-faces* and the *z-closing arcs*.

Proposition 8. *Let us consider a cell with one or two PBC imposed on the x- or/and y-faces of the cell. Then the following holds:*

$$LK_P(I, J) = \Big(L(i, j)\Big)_{xy}, \tag{13}$$

where $\Big(L(i, j)\Big)_{xy}$ *is equal to half the algebraic sum of crossings between i and j when projected on the xy-plane.*

Proof. We will focus in the case of two PBC, since, the result for a system with one PBC follows easily from this case. Let us project the periodic system on the xy-plane. In the following let $cr(f, g)$ denote the crossings between the projections of two arcs f and g to the xy-plane. We notice that the base point of I_0 is also the base point of the generating chain in the generating cell. Then we can define a translation of the generating chain in any other cell in the periodic system with a vector based on that base point. Let $i_1, \ldots, i_k$ denote the arcs that compose the generating chain i, and let $j_1, \ldots, j_l$ denote the arcs that compose the generating chain j. We can also define a base point on each arc of a generating chain in order to determine their translation. Let then $i_1 + \vec{u}_1, \ldots, i_k + \vec{u}_k$ denote the translations of the arcs of the generating chain i that compose the image I_0 and let $j_1 + \vec{v}_1, \ldots, j_k + \vec{v}_l$ denote the translations of the arcs of the generating chain j that compose the image J_0. (By definition, there is exactly one translation of an arc of i (resp. j) in I_0 (resp. J_0).) Then

$$\begin{aligned} LK_P(I, J) &= \sum_{\vec{v}} L(I_0, J_0 + \vec{v}) = \frac{1}{2} \sum_{\vec{v}} \sum_{c \in cr(I_0, J_0 + \vec{v})} sign(c) \\ &= \frac{1}{2} \sum_{\vec{v}} \sum_{1 \le m \le l} \sum_{c \in cr(I_0, j_m + \vec{v})} sign(c). \end{aligned} \tag{14}$$

Let $mu(I_0)$ denote the minimal unfolding of I_0. We denote $j+\vec{v} \in mu(I_0)$ if the translation of the arc j by $\vec{v}$ lies in the minimal unfolding of I_0. We notice that at the chosen projection direction, it is impossible to have crossings between I_0 and translations of arcs of j that do not lie in $mu(I_0)$, thus the LK_P is equal to the following summation:

$$\begin{aligned} LK_P(I, J) &= \sum_{\substack{\vec{v} \\ j+\vec{v}\in mu(I_0)}} \sum_{1\le m\le l} \sum_{c\in cr(I_0, j_m+\vec{v})} sign(c) \\ &= \sum_{\substack{\vec{v} \\ j+\vec{v}\in mu(I_0)}} \sum_{1\le m\le l} \sum_{1\le n\le k} \sum_{c\in cr(i_n+\vec{u}_n, j_m+\vec{v})} sign(c). \end{aligned} \tag{15}$$

But we notice that the projection of $i_n+\vec{u}_n$ may intersect the projection of $j_m+\vec{v}$ on the xy-plane if and only if they lie in the same cell, that is, if $\vec{u}_n = \vec{v}$. Thus

$$\begin{aligned} LK_P(I, J) &= \sum_{1\le m\le l} \sum_{1\le n\le k} \sum_{c\in cr(i_n+\vec{u}_n, j_m+\vec{u}_n)} sign(c) \\ &= \sum_{1\le m\le l} \sum_{1\le n\le k} \sum_{c\in cr(i_n, j_m)} sign(c) = \sum_{c\in cr(i,j)} sign(c) = \Big(L(i, j)\Big)_{xy}. \qquad \square \end{aligned} \tag{16}$$

4.2. Properties of SL_P for closed free chains

We notice that for closed chains, the periodic self-linking number can be expressed as

$$SL_P(I) = Sl(I_0) + SLK_P(I) = Sl(I_0) + \sum_{\vec{v}\in S} L(I_0, I_0+\vec{v}), \tag{17}$$

where S contains all the vectors $\vec{v}$ for which $I_0+\vec{v}$ intersects Σ.

It follows that the periodic self-linking number has the following properties in the case of closed free chains:

(i) SL_P is a finite summation.
(ii) If the chain I_0 does not touch the faces of the cell, then $SL_P(I) = Sl(I_0)$.
(iii) SL_P is an integer invariant up to regular isotopy.

In Section 3.2.1 we mentioned that the self-linking number of a closed chain l is equal to the linking number between l and its normal variation curve l_ϵ, i.e. $Sl(l) = L(l, l_\epsilon)$ [58,59]. Let us give the corresponding definition in PBC:

Definition 9. Let I denote a free chain in a periodic system. We define its *normal variation free curve* to be the free chain I_ϵ in the periodic system, such that every translated image of I_ϵ is the normal variation curve of a translated image of I.

Then in analogy with the Calugareanu formula for chains in $\mathbb{R}^3$, the following holds for chains in PBC:

Corollary 10. *Let I denote a closed free chain in PBC, and let I_ϵ denote its free variation curve. Then $SL_P(I) = LK_P(I, I_\epsilon)$.*

Proof. By Definition 9 we have

$$\begin{aligned} LK_P(I, I_\epsilon) &= \sum_{\vec{v}} L\left(I_0, (I_0)_\epsilon + \vec{v}\right) = L(I_0, (I_0)_\epsilon) + \sum_{\vec{v}} L(I_0, (I_0)_\epsilon + \vec{v}) \\ &= Sl(I_0) + \sum_{\vec{v}} L(I_0, (I_0)_\epsilon + \vec{v}). \end{aligned} \tag{18}$$

We notice that we can choose ϵ small enough so that the deformation of the link I_0, $I_0+\vec{v}$ to I_0, $(I_0)_\epsilon+\vec{v}$ is an isotopy. So, $L(I_0, I_0+\vec{v}) = L(I_0, (I_0)_\epsilon+\vec{v})$ for all $\vec{v}$. Thus we have the following expression for the periodic self-linking number of the free chain I in the periodic system

$$LK_P(I, I_\epsilon) = Sl(I_0) + \sum_{\vec{v}} L(I_0, (I_0)_\epsilon + \vec{v}) = Sl(I_0) + \sum_{\vec{v}} L(I_0, I_0+\vec{v}) = SL_P(I). \qquad \square \tag{19}$$

Remark 11. Corollary 10 implies that the Fuller–White formula [60,61] can be extended to a closed ribbon in a system with PBC as follows:

$$LK_P(I, I_\epsilon) = WR_P(I) + \tau(I_0). \tag{20}$$

Similarly, one could envision that some generalizations of the Fuller spherical area formula, and the Fuller Writhe difference formula [62] are possible in PBC.

4.2.1. Properties of SLK_P for closed free chains

Notice that the periodic linking number with self images can be expressed as

$$SLK_P(I) = \sum_{\vec{v}\in S} L(I_0, I_0 + \vec{v}), \tag{21}$$

where S contains all the vectors $\vec{v}$ for which $I_0 + \vec{v}$ intersects Σ.

It follows that the periodic linking number with self-images has the following properties in the case of closed free chains:

(i) SLK_P is a finite summation.
(ii) If the chain I_0 does not touch the faces of the cell, then $SLKP(I) = 0$.
(iii) SLK_P is an integer invariant.

Corollary 12. *SLK_P is an even number.*

Proof. We have that $SLK_P(I) = \sum_{\vec{v}\in S} L(I_0, I_0 + \vec{v})$. Notice that for every image of I that intersects Σ, say $I_0 + \vec{v}$, then the image $I_0 - \vec{v}$ also intersects Σ. More precisely, the pairs I_0, $I_0 + \vec{v}$ and I_0, $I_0 - \vec{v}$ are in the same relative position, thus $L(I_0, I_0 + \vec{v}) = L(I_0, I_0 - \vec{v})$. □

5. Sketch of proof and basic tools for the convergence of LK_P for open or infinite free chains

In this section we study the convergence of the periodic linking number of open or infinite free chains and we show that LK_P indeed converges. We observe first that if LK_P of two free chains in three PBC converges, then it also converges in one and two PBC. Similarly, convergence in two PBC implies convergence in one PBC. Indeed, LK_P in one and two PBC is computed from Eq. (5) by using only the terms that correspond to the vectors that lie on a line (say the x-axis), or the vectors that lie in a plane (say the xy-plane), respectively. The proof of convergence in three PBC is gradually built up from the proofs of convergence in one and two PBC using a collection of lemmas and observations. We chose to present our proof for three PBC gradually from that of one and two PBC for the following reasons: There are physical problems that involve only one or two PBC. As we show here convergence in one PBC is straightforward while for showing convergence in two PBC we need to use additional geometric methods. Finally, convergence in two PBC plays an important role for proving convergence in three PBC. Moreover, in the course of our proof we give explicit upper bounds for $LK_P(I, J)$ in one, two and three PBC, we denote $LK_P^{(1)}$, $LK_P^{(2)}$ and $LK_P^{(3)}$ respectively, which give an estimate on the amount of global entanglement of the system and on how LK_P compares to the Gauss linking number of two chains in 3-space.

As the proofs are rather technical and elaborate we shall first give a sketch of our proofs. The detailed proofs are presented in Section 6.

Let I and J denote two free chains. Also let $l\mathbb{Z}^3$ denote the *integer lattice of unit length* l, where l is the edge-length of the cubic cell. Thus one can express the periodic linking number (Eq. (5)) as:

$$LK_P(I, J) = \sum_{\vec{v}\in l\mathbb{Z}^3} L(I_0, J_0 + \vec{v}) \tag{22}$$

In our study, we will focus on the case where I and J are formed by piecewise linear arcs, edges, of length $b_I = b_J = b < l/2$ each. Let $e_{i,1}$, $e_{j,1}$ be a pair of edges in i and j respectively, and consider the cell with only those edges inside. The periodic space generated by this cell contains translations of these two edges. Then the linking of $e_{i,1}$ with each one of the translations of $e_{j,1}$ must be taken into consideration in $LK_P(I, J)$. Therefore, if we imagine $e_{i,1}$, $e_{j,1}$ as generating chains of free chains $E_{i,1}$, $E_{j,1}$, we notice that $LK_P(E_{i,1}, E_{j,1})$ must be contained in $LK_P(I, J)$. We will show that $LK_P(I, J)$ is the summation of the periodic linking numbers between the edges that form I and J.

Lemma 13. *Let $e_{i,k}, k = 1, \ldots, n_i$ be the edges that form the generating chain i and let $e_{j,k'}, k' = 1, \ldots, n_j$ be the edges that form the generating chain j. Two edges $e_{i,k}$, $e_{j,k'}$ generate two free chains $E_{i,k}$, $E_{j,k'}$ resp. in the periodic system. LK_P is expressed as:*

$$LK_P(I, J) = \sum_{k}\sum_{k'} LK_P(E_{i,k}, E_{j,k'}). \tag{23}$$

Proof. Let $\beta_{i,k}$, $\beta_{j,k'}$ denote the base points of the edges $e_{i,k}$, $e_{j,k'}$, $k = 1, \ldots, n_i$, $k' = 1, \ldots, n_j$. Let also $e_{i,1} + \vec{u}_1, \ldots, e_{i,n_i} + \vec{u}_{n_i}$ denote the images of the free chains $E_{i,k}$, $k = 1, \ldots, n_i$, that form I_0, and let $e_{j,1} + \vec{w}_1, \ldots, e_{j,n_j} + \vec{w}_{n_j}$ denote the images of the free chains $E_{j,k'}$, $k' = 1, \ldots, n_j$, that form J_0 (see Fig. 6 for an illustrative example). Then $LK_P(I, J)$ can be expressed as

$$LK_P(I, J) = \sum_{\vec{v}\in l\mathbb{Z}^3} \sum_{1\le k\le n_i} \sum_{1\le k'\le n_j} L(e_{i,k} + \vec{u}_k, e_{j,k'} + \vec{w}_{k'} + \vec{v})$$

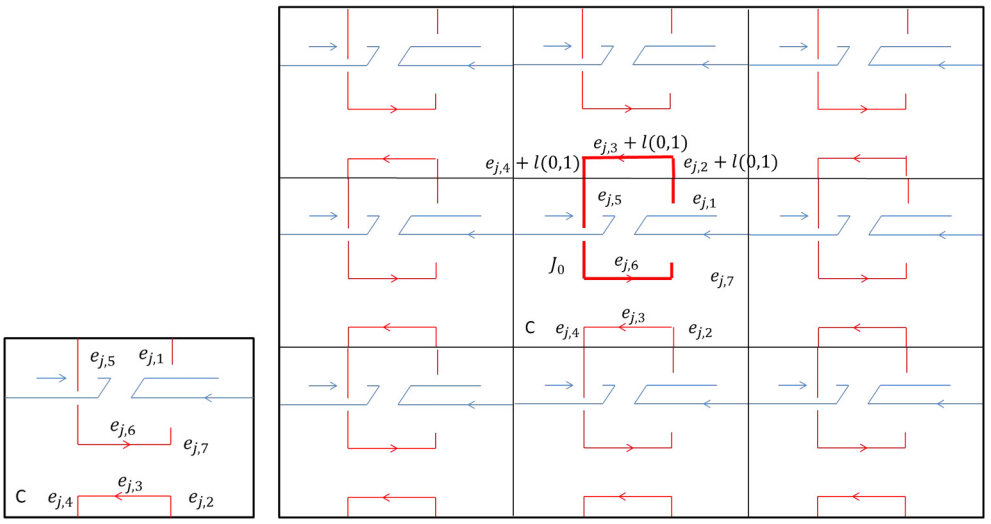

Fig. 6. An image of J contains translations of edges of j by different vectors. In this example J_0 is composed by the arcs $e_{j,1}, e_{j,2}+l(0,1), e_{j,3}+l(0,1), e_{j,4}+l(0,1), e_{j,5}, e_{j,6}$.

$$= \sum_{1\le k\le n_i} \sum_{1\le k'\le n_j} \sum_{\vec{v}\in l\mathbb{Z}^3} L(e_{i,k}+\vec{u}_k, e_{j,k'}+\vec{w}_{k'}+\vec{v}). \tag{24}$$

Since the lengths of I_0 and J_0 are finite (i.e. $n_i, n_j < \infty$), in order to prove convergence of LK_P it suffices from Eq. (24) to prove convergence for every summand of the form

$$\sum_{\vec{v}\in l\mathbb{Z}^3} L(e_{i,k}+\vec{u}_k, e_{j,k'}+\vec{w}_{k'}+\vec{v}), \tag{25}$$

which is equal to the periodic linking number of the free chains $E_{i,k}$, $E_{j,k'}$, $LK_P(E_{i,k}, E_{j,k'})$. □

Notation 14. For the rest of the proof, in order to avoid unnecessarily complicated indices we will use the notation I, J for the free chains $E_{i,k}$, $E_{j,k'}$. Notice that these are free chains whose images are straight arcs (edges). We will call such free chains *free edges*.

5.1. Sketch of proof of convergence

Let Ω denote the space of all possible configurations of two disjoint oriented edges in general position. Let $\vec{x} = (I_0, J_0)$ denote a point in Ω. Then the Gauss linking integral is a function $L : \Omega \to \mathbb{R}$.

Grouping together in Eq. (22) all the terms with vectors $\vec{v} \in l\mathbb{Z}^3$ that have the same norm, $||\vec{v}||^2 = n \in \mathbb{N}$, results in the following expression for $LK_P(I, J)$:

$$LK_P(I, J) = L(I_0, J_0) + \sum_{n\in\mathbb{N}} \sum_{\substack{\vec{v}\in l\mathbb{Z}^3 \\ ||\vec{v}||^2 = l^2 n}} L(I_0, J_0+\vec{v}). \tag{26}$$

Denoting:

$$q_n(\vec{x}) := \sum_{\substack{\vec{v}\in l\mathbb{Z}^3 \\ ||\vec{v}||^2 = l^2 n}} L(I_0, J_0+\vec{v}), \tag{27}$$

we obtain:

$$LK_P(I, J) = L(I_0, J_0) + \sum_n q_n(\vec{x}). \tag{28}$$

Thus LK_P is a series over n of the functions $q_n : \Omega \to \mathbb{R}$. By using bounding expressions Q_n that depend only on n such that $|q_n(\vec{x})| < Q_n$ for all $\vec{x} \in \Omega$, we prove the convergence of LK_P by proving the convergence of the series $\sum_n Q_n$. Thus the proof of convergence of LK_P is reduced to finding appropriate upper bounds Q_n of $q_n(\vec{x})$, for which $\sum_n Q_n$ converges. For this purpose, one needs to know the number of terms in $q_n(\vec{x})$ and upper bounds of each one of these terms.

Concerning the number of terms in $q_n(\vec{x})$: In the case of a system with one PBC where there are translations along the x-axis, we have $q_n = L(I_0, J_0 + l\sqrt{n}(1,0,0)) + L(I_0, J_0 - l\sqrt{n}(1,0,0))$ if $n = m^2$, $m \in \mathbb{N}$ and $q_n = 0$ if n is squarefree. In

the case of systems with two (resp. three) PBC, where we consider translations in a plane (resp. in 3-space), the vectors $\vec{v} \in l\mathbb{Z}^3$ such that $||\vec{v}||^2 = n \in \mathbb{N}$, correspond to lattice points on a circle (resp. sphere) of radius $\sqrt{n}$ with unit length l. More precisely, they correspond to representations of a number $n \in \mathbb{N}$ as a sum of two (resp. three) squares, denoted $r_2(n)$ (resp. $r_3(n)$), which is the number of terms in $q_n(\vec{x})$. The estimation of $r_2(n)$ and $r_3(n)$ is an old and challenging problem in number theory and will be discussed in Section 5.2. We will see that $r_2(n) \approx O(n^{7/22})$ and $r_3(n) \approx O(\sqrt{n}(\log n)^2)$.

Concerning upper bounds for $q_n(\vec{x})$: We will show in Lemma 17 that each term in q_n is bounded by:

$$|L(I_0, J_0 + \vec{v})| < O\left(\frac{1}{||\vec{v}||^2}\right) = O\left(\frac{1}{l^2 n}\right). \tag{29}$$

This upper bound proves convergence in the case of one PBC, since Eq. (29) then gives $Q_n^{(1)} = O\left(\frac{1}{l^2 n}\right)$ and for $n = m^2$, $m \in \mathbb{N}$, $Q_n^{(1)} = O\left(\frac{1}{l^2 n}\right) = O\left(\frac{1}{l^2 m^2}\right) = Q_m^{(1)}$. Thus $LK_P^{(1)}(I, J) < L(I_0, J_0) + \sum_{n,n=m^2} Q_n^{(1)} = L(I_0, J_0) + \sum_m Q_m^{(1)} = L(I_0, J_0) + \sum_m O\left(\frac{1}{l^2 m^2}\right)$ which converges.

In the case of systems with two or three PBC, Eq. (29) gives $Q_n^{(1)} = O\left(\frac{r_2(n)}{n}\right)$ and $Q_n^{(1)} = O\left(\frac{r_3(n)}{n}\right)$ respectively. Unfortunately, $\sum_n Q_n^{(1)}$ diverges. So, in order to prove convergence in two and three PBC, a stronger upper bound must be used. This is achieved by taking into consideration the signs of the terms in $q_n(\vec{x})$ (Eq. (27)). For this purpose, in Section 6.2, $q_n(\vec{x})$ is expressed as:

$$q_n(\vec{x}) = \frac{1}{2} \sum_{\substack{\vec{v} \in l\mathbb{Z}^3 \\ |\vec{v}|^2 = l^2 n}} (L(I_0, J_0 + \vec{v}) + L(I_0, J_0 - \vec{v})). \tag{30}$$

Note that, even though all translation vectors appear in opposite pairs, the linking numbers of these pairs in Eq. (30) do not cancel, as shown in Fig. 10. We show (Lemma 23) that there exists a natural number $n_0 \in \mathbb{N}$ such that for all $\vec{v}$ with $||\vec{v}||^2 = n > n_0$

$$|L(I_0, J_0 + \vec{v}) + L(I_0, J_0 - \vec{v})| < O\left(\frac{1}{n\sqrt{n}}\right). \tag{31}$$

Thus for $n > n_0$, the following upper bound of $q_n(\vec{x})$ can be used:

$$Q_n^{(2)} = O\left(\frac{r_2(n)}{n\sqrt{n}}\right) \quad \text{and} \quad Q_n^{(2)} = O\left(\frac{r_3(n)}{n\sqrt{n}}\right)$$

in the case of two and three PBC respectively. Then

$$LK_P^{(2)}(I, J) < \sum_{n \le n_0} Q_n^{(1)} + \sum_{n > n_0} Q_n^{(2)},$$

which converges (Theorem 24) but, unfortunately, this estimation is not strong enough to prove convergence in the case of three PBC.

Thus another method is needed in order to prove convergence of $LK_P^{(3)}$. Indeed, the proof of convergence in three PBC is given in two steps: first we prove that $LK_P^{(3)}(\vec{x}_0)$ converges for all $\vec{x}_0 \in \Omega_1 \subset \Omega$, where Ω_1 is a subset of the configuration space, defined in Section 6.3.1, and, next, using this, we prove that $LK_P^{(3)}$ converges for all $\vec{x} \in \Omega$. More precisely, we show (Lemma 27) that for $\vec{x}_0 = (I', J') \in \Omega_1$ we have:

$$q_n(\vec{x}_0) \approx \sum_{\vec{v} \notin V} L(I'_0, J'_0 + \vec{v}), \tag{32}$$

where V denotes the set of vectors $\vec{v} = (v_1, v_2, v_3) \in l\mathbb{Z}^3$ for which $|v_1|, |v_2|, |v_3| > l\sqrt{n_0}$, and such that not all $|v_1| = |v_2| = |v_3|$. Now the upper bounds $Q_n^{(1)}$ and $Q_n^{(2)}$ are sufficient to prove that $LK_P^{(3)}(\vec{x}_0)$ converges (Lemma 29). For the next step we prove (Lemma 32) that for any given configuration, $\vec{x} = (I, J) \in \Omega$, there exists a configuration $\vec{x}_0 \in \Omega_1$ such that:

$$|LK_P^{(3)}(\vec{x}) - LK_P^{(3)}(\vec{x}_0)| < R \in \mathbb{R}. \tag{33}$$

Hence, $LK_P(I, J)$ converges in three PBC (Theorem 33).

Remark 15. Notice that the proof in one, two or three PBC would be simplified if one could prove convergence of $DLK_P^{(3)}(\vec{r}(t))$ in the space Ω' of configurations of polygonal chains of three edges. Then, starting from two unlinked closed polygons, say $\vec{x}_0 \in \Omega'$, one could find a path $\vec{r}(\tau) \in \Omega'$, $\tau \in [0, 1]$ to any two straight arcs $\vec{x} \in \Omega$ by opening the polygons and straightening them. Then, since $LK_P(\vec{x}_0) = 0$ we could prove convergence of $LK_P(\vec{x})$ by proving convergence of $DLK_P^{(3)}(\vec{r}(t))$. The proof of convergence of $DLK_P^{(3)}(\vec{r}(t))$ however, is not yet possible.

5.2. Arithmetic functions

In this section we give some known results on arithmetic functions that will be used in the following sections to prove convergence.

Lattice points on a circle or a sphere

Let us denote $r_2(n) = \sharp\{(v_1, v_2) \in \mathbb{Z}^2 | v_1^2 + v_2^2 = n\}$, the number of representations of a natural number as a sum of two squares, $R_2(n) = \sharp\{(v_1, v_2) \in \mathbb{Z}^2 | \gcd(v_1, v_2) = 1, v_1^2 + v_2^2 = n\}$ the number of primitive representations of a number as a sum of two squares, $r_3(n) = \sharp\{(v_1, v_2, v_3) \in \mathbb{Z}^3 | v_1^2 + v_2^2 + v_3^2 = n\}$ the number of representations of a number as a sum of three squares, and $R_3(n) = \sharp\{(v_1, v_2, v_3) \in \mathbb{Z}^3 | \gcd(v_1, v_2, v_3) = 1, v_1^2 + v_2^2 + v_3^2 = n\}$, the number of primitive representations of a number as a sum of three squares. Recall that $r_2(n)$ and $r_3(n)$ were used in Section 5.1 and will also be used in Section 6 in the proof of convergence. Analytic expressions for these functions can be found in [63–67]. More precisely, Jacobi [66] proved that

$$r_2(n) = 4(d_1(n) - d_3(n)), \tag{34}$$

where $d_i(n) = i \bmod 4$, and Bateman in 1950 [63] has proved that

$$r_3(n) = \frac{16}{\pi}\sqrt{n}\, L(1, \chi)\, q(n)\, P(n), \tag{35}$$

where $n = 4^a n_1$, for $a, n_1 \in \mathbb{N}$; $q(n) = 0$, if $n_1 = 7 \bmod 8$, or $q(n) = 2^{-a}$ if $n_1 = 3 \bmod 8$, or $q(n) = 3 \cdot 2^{-a-1}$ if $n_1 = 1, 2, 5$ or $6 \bmod 8$; and finally

$$P(n) = \prod_{\substack{p^{2b} | n \\ p \text{odd}}} \left[1 + \sum_{j=1}^{b-1} p^{-f} + p^{-b}\left(1 - \left[\frac{(-n/p^{2b})}{p}\right]\frac{1}{p}\right)^{-1}\right], \tag{36}$$

where $P(n) = 1$ for square-free n. Also, $\chi(m)$, is the Legendre–Jacobi–Kronecker symbol defined as $\chi(m) = \left(\frac{-4}{m}\right)$, $\chi(m) = 1$ if $m = 1 \bmod 4$, $\chi(m) = 0$ if $m = 0 \bmod 2$ and $\chi(m) = -1$ if $m = 3 \bmod 4$, and finally, $L(S, \chi) = \sum_{m=1}^{\infty} \chi(m) m^{-S}$.

For $R_2(n)$, $R_3(n)$, let the prime factorization of n be given by

$$n = 2^{\lambda_2} \prod_p p^{\lambda_p}, \tag{37}$$

where the product is taken over all odd primes p which divide n. Then

$$R_2(n) = c_2(n) \prod_p (1 + (-1)^{(p-1)/2}), \tag{38}$$

where $c_2(n) = 0$ if $n = 0 \bmod 4$ and $c_2(n) = 4$ if $n \neq 0 \bmod 4$, [67].

Let m denote the square-free part of n, let $k \geq 1$ and let $\left(\frac{a}{p}\right)$ denote the Legendre symbol: $\left(\frac{a}{p}\right) = 1$ if a is a quadratic residue modulo p and $a \not\equiv 0 \bmod p$, $\left(\frac{a}{p}\right) = -1$ if a is a quadratic non-residue modulo p and $\left(\frac{a}{p}\right) = 0$ if $a \equiv 0 \bmod p$. Then

$$R_3(n) = c_3(n) R_3(m) \frac{n^{1/2}}{m^{1/2}} \prod_{p | \frac{n}{m}} \left(1 - \frac{\left(\frac{-m}{p}\right)}{p}\right), \tag{39}$$

where $c_3(n) = 1$ if $n \neq 0 \bmod 4$ or $c_3(n) = 0$ if $n = 0 \bmod 4$, [67]. Moreover, $r_3(n)$ and $R_3(n)$ are related by the following [63]:

$$r_3(n) = \sum_{d^2 | n} R_3(n/d^2). \tag{40}$$

In the proof of convergence we will be interested in the growth of these functions, something that is not evident in the previous expressions of $r_2(n)$, $R_2(n)$, $r_3(n)$, $R_3(n)$. A naive approach for finding the order of magnitude of $r_d(n)$ for $d = 2, 3$, is to take the volume of the ball of radius $\sqrt{n}$ divided by the number of spheres of radius $\sqrt{m}, m \in \mathbb{N}$, contained in the ball. The volume of a ball of radius $\sqrt{n}$ grows as $n^{d/2}$ whilst the number of concentric spheres of radius $\sqrt{m}, m \in \mathbb{N}$, enclosed in the ball of radius $\sqrt{n}$ is n. For $d = 2$ this leads us to expect a constant number of lattice points on a circle, while for $d = 3$ we expect a growth proportional to $\sqrt{n}$. However, as it is shown in Eq. (34), the growth is quite irregular and depends on the divisor structure of n. For example, for $d = 2$, most circles of radius $\sqrt{n}$ have no lattice points at all. In fact, Landau proved that the number of circles with at least one lattice point, of integer squared radius smaller than x, grows as $Cx/\sqrt{\log x}$ [68]. Moreover, there are infinite families of circles with very few lattice points. On the other hand, the number

of lattice points on a circle of radius $\sqrt{n}$ is not bounded. For $d = 3$, the ratio between the number of points and the naive estimate above is bounded, up to constants only depending on ϵ, from above by n^{ϵ} and from below by $n^{-\epsilon}$, for all $\epsilon > 0$. More precisely, in [69], we see that

$$r_3(n) = O(\sqrt{n}(\log n)^2). \tag{41}$$

It has been shown that the distribution of the lattice points on the sphere of radius $\sqrt{n}$ is uniform [70–73].

Lattice points inside a circle or a sphere

A related problem is the estimation of the number of lattice points inside a circle or a sphere. Estimates for the number of lattice points inside a circle or sphere can be found in [74,75]. More precisely, by [74] we know that the number of lattice points inside the circle of radius $\sqrt{n}$ is:

$$\sum_{1\le m\le n} r_2(m) = \pi n + O(n^{7/22}). \tag{42}$$

Also, by [74] we know that the number of primitive lattice points inside a circle of radius $\sqrt{n}$ is:

$$\sum_{1\le m\le n} R_2(m) = \frac{6}{\pi} n + O(n^{(51+\epsilon)/100}), \tag{43}$$

for all $\epsilon > 0$. By [75] we know that the number of lattice points inside a sphere of radius $\sqrt{n}$ is equal to:

$$\sum_{1\le m\le n} r_3(m) = \frac{4\pi}{3} n\sqrt{n} + O(n^{21/32+\epsilon}), \tag{44}$$

for all $\epsilon > 0$. Again, by [75] we know that the number of primitive lattice points inside a sphere of radius $\sqrt{n}$ is:

$$\sum_{1\le m\le n} R_3(m) = \frac{4\pi}{3\zeta(3)} n\sqrt{n} + O(\sqrt{n}(\log\sqrt{n})^{1/2}), \tag{45}$$

where ζ is the Riemann zeta function.

Remark 16. Using the above estimates, we obtain rough estimates for $r_2(n)$, $R_2(n)$ as follows:

$$\begin{aligned} r_2(n) &= \sum_{1\le m\le n} r_2(m) - \sum_{1\le m\le n-1} r_2(m) = \pi + O(n^{7/22}) - O((n-1)^{7/22}) \\ &< \pi + O(n^{7/22}), \end{aligned} \tag{46}$$

and:

$$R_2(n) = \sum_{1\le m\le n} R_2(m) - \sum_{1\le m\le n-1} R_2(m) < \frac{6}{\pi} + O(n^{(51+\epsilon)/100}), \tag{47}$$

which we will use in our proof of convergence.

For our numerical estimates in Remarks 25, 31 and 34, we will use the averaging process described above to make the following approximations for large n: $r_2(n) \approx \pi$, $R_2(n) \approx \frac{6}{\pi}$, $r_3(n) = \frac{4\pi}{3}\sqrt{n}$ and $R_3(n) \approx \frac{4\pi}{3\zeta(3)}\sqrt{n}$, where ζ denotes the Riemann zeta function.

5.3. The Gauss linking integral of two edges

Let e_1, e_2 denote two edges in 3-space with arc-length parametrizations $\gamma_1(t)$, $\gamma_2(s)$, $t, s \in [0,1]$, and let $\vec{\alpha}$ denote the vector that connects the base point of e_1 to the base point of e_2. Let us assume that e_1, e_2 have the same length, b. By definition, the Gauss linking integral of e_1, e_2 is expressed by

$$\begin{aligned} L(e_1,e_2) &= \frac{1}{4\pi}\int\int \frac{(\dot\gamma_1(t), \dot\gamma_2(s), \gamma_1(t)-\gamma_2(s))}{||\gamma_1(t)-\gamma_2(s)||^3} dt\,ds \\ &= \frac{1}{4\pi}\int\int \frac{||\dot\gamma_1(t)||||\dot\gamma_2(s)||||\gamma_1(t)-\gamma_2(s)||\sin\phi\cos\theta(s,t)}{||\gamma_1(t)-\gamma_2(s)||^3} dt\,ds \\ &= \frac{1}{4\pi}\int\int \frac{\sin\phi\cos\theta(s,t)}{||\gamma_1(t)-\gamma_2(s)||^2} dt\,ds, \end{aligned} \tag{48}$$

where ϕ is the angle between the two edges and $\theta(s,t)$ is the angle between $\dot\gamma_1 \times \dot\gamma_2$ and $\gamma_1(t) - \gamma_2(s)$. A general upper bound for L is: $|L(e_1,e_2)| < 1/2$. Next, we can give an estimate of an upper bound depending on the distance of the base points of the two edges.

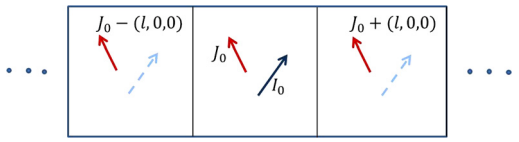

Fig. 7. The projection of two free edges in a system employing one PBC. For the computation of $LK_P^{(1)}(I, J)$ we add the linking numbers of I_0 with all the images of J.

Lemma 17. *For two edges e_1, e_2 of length b whose base points are connected by a vector $\vec{\alpha}$, such that $||\vec{\alpha}|| > b$, then*

$$|L(e_1, e_2)| \leq \frac{1}{4\pi} \frac{1}{(||\vec{\alpha}|| - b)^2}. \tag{49}$$

Proof. By Eq. (48),

$$\begin{aligned} |L(e_1, e_2)| &\leq \frac{1}{4\pi} \frac{1}{\min_{t,s}\{||\gamma_1(t) - \gamma_2(s)||^2\}} \left| \int \int \sin\phi \cos\theta(s,t) dt\, ds \right| \\ &\leq \frac{1}{4\pi} \frac{1}{(||\vec{\alpha}|| - b)^2}. \quad \square \end{aligned} \tag{50}$$

6. Convergence of LK_P for open and infinite free chains

In this section we present the convergence of LK_P for open or infinite free chains. In the following, let I, J denote two free edges whose images are straight arcs of length $b < l/2$, where l is the length of an edge of the cubic cell. (The analysis follows similarly when the edges do not have the same length.)

6.1. Convergence in one PBC

Without loss of generality, let us consider the case of one PBC imposed on the x-axis (right–left faces of the cell). Then the periodic linking number of two free edges, we denote $LK_P^{(1)}$, can be expressed as (see Fig. 7)

$$LK_P^{(1)}(I, J) = \sum_{m \in \mathbb{Z}} L(I_0, J_0 + m(l, 0, 0)). \tag{51}$$

Let $\vec{\alpha}$ denote the vector that connects the base point of I_0, β_i, to the base point of J_0, β_j. Let $\gamma_1(t)$, $\gamma_2(s)$, $t, s \in [0, 1]$ denote the arc-length parametrizations of the images I_0 and J_0 respectively. Then,

Proposition 18. *The periodic linking number between two free edges, I and J, in one PBC, denoted $LK_P^{(1)}(I, J)$, converges uniformly and is bounded above by*

$$LK_P^{(1)}(I, J) < L(I_0, J_0) + \frac{1}{2\pi} \sum_{m \in \mathbb{N}} \frac{1}{(ml - ||\vec{\alpha}|| - b)^2}, \tag{52}$$

where $\vec{\alpha}$ is the vector that connects the base points of the parent images, I_0 and J_0, b is the length of an image of I and J, and l is the length of an edge of the cell.

Proof. The periodic linking number is bounded above by

$$\begin{aligned} LK_P^{(1)}(I, J) &\leq \sum_{m \in \mathbb{Z}} |L(I_0, J_0 + ml(1, 0, 0))| \\ &= \sum_{m \in \mathbb{N}} |L(I_0, J_0 - ml(1, 0, 0))| + |L(I_0, J_0)| + \sum_{m \in \mathbb{N}} |L(I_0, J_0 + ml(1, 0, 0))|. \end{aligned} \tag{53}$$

Note that $||\gamma_1(t) - \gamma_2(s) \pm ml\vec{v}|| \geq \min_{t,s}\{||\gamma_1(t) - \gamma_2(s) \pm ml\vec{v}||\} \geq ml||\vec{v}|| - ||\vec{\alpha}|| - b$. So, by Eq. (50)

$$\begin{aligned} |L(I_0, J_0 + ml(1, 0, 0))| &\leq \frac{1}{4\pi} \frac{1}{(ml - ||\vec{\alpha}|| - b)^2} \left| \int \int \sin\phi \cos\theta(s,t) dt ds \right| \\ &\leq \frac{1}{4\pi} \frac{1}{(ml - ||\vec{\alpha}|| - b)^2} = Q_m^{(1)}, \end{aligned} \tag{54}$$

and similarly for $|L(I_0, J_0 - ml(1, 0, 0))|$. So,

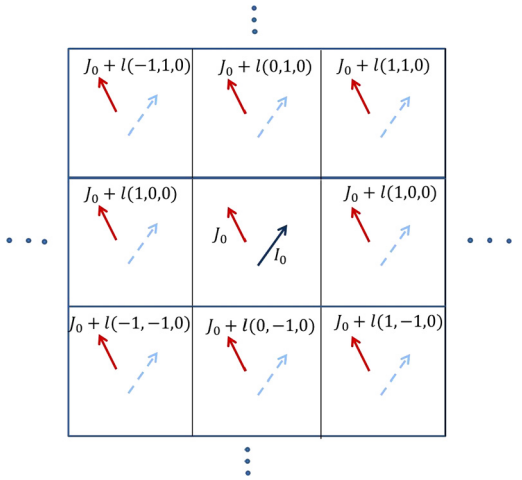

Fig. 8. The projection of two free edges in a system employing two PBC. For the computation of $LK_P^{(1)}(I, J)$ we add the linking numbers of I_0 with all the images of J.

$$\sum_{m\in\mathbb{Z}} |L(I_0, J_0 + ml(1,0,0))| < L(I_0, J_0) + \sum_{m\in\mathbb{Z}, m\neq 0} Q_m^{(1)}$$
$$\leq L(I_0, J_0) + \frac{1}{2\pi}\sum_{m\in\mathbb{N}} \frac{1}{(ml - ||\vec{\alpha}|| - b)^2}, \tag{55}$$

which converges and the convergence is uniform. □

Remark 19. Notice that for a system with one PBC we can adjust the position of the cell to ensure that $||\vec{\alpha}|| < \frac{3l}{2}$. In applications to polymers, where the edges correspond to monomer bonds, $||\vec{\alpha}|| > b$. Notice that $L(I_0, J_0)$ increases as $||\vec{\alpha}||$ decreases, and the same holds for $LK_P^{(1)}(I, J)$. For $||\vec{\alpha}|| = b$ we obtain the following upper bound

$$LK_P^{(1)}(I, J) < \frac{1}{2} + \frac{1}{2\pi l^2}\sum_{m\in\mathbb{N}} \frac{1}{(m - 2b/l)^2} \tag{56}$$

Notice that for a cell employing one PBC of edge length $l = 50$ and for edges of length $b = 1$ (which are reasonable sizes for simulation of polymer melts), Eq. (56) gives $LK_P^{(1)}(I, J) < 0.500111$.

Corollary 20. *The periodic linking number of two open or infinite chains in one PBC is a continuous function almost everywhere in the space of configurations.*

Proof. Since the convergence of LK_P is uniform, it follows from the fact that the Gauss linking integral is a continuous function almost everywhere in the space of configurations. □

6.2. Convergence in two PBC

Without loss of generality, let us consider the case of two PBC imposed on the x- and y-axis (right–left and top–bottom faces of the cell). In order to prove convergence of $LK_P(I, J)$ in the case of two PBC we need to take into consideration the signs of the linking numbers involved in its computation (see Fig. 8). In the following the translations of J_0 by $\vec{v}$ and by $-\vec{v}$ shall be called *opposite translations*, and the pairs of edges $(I_0, J_0 + \vec{v}), (I_0, J_0 - \vec{v})$ will be called a *pair of opposite translations*. As we shall see, the linking number of I_0 with these may have opposite sign.

Lemma 21. *Let e_1, e_2 denote two edges whose base points get connected by a vector $\vec{\alpha}$, then $L(e_1, e_2) = -L(e_1, e_2 - 2\vec{\alpha})$.*

Proof. Let us consider a mirror M placed on the plane with normal vector $\vec{\alpha}$ which contains β_1, as shown in Fig. 9, and let $(e_1)_M$ and $(e_2)_M$ denote the mirror images of e_1 and e_2 (shown in blue in Fig. 9). Then $L\Big((e_1)_M, (e_2)_M\Big) = -L(e_1, e_2)$.

Next we rotate $(e_1)_M$ and $(e_2)_M$ by π around the axis that contains $\vec{\alpha}$. Let $((e_2)_M)_R$ and $((e_1)_M)_R$ denote the resulting edges (shown in light blue in Fig. 9). During the rotation the relative position of the two edges does not change, so $L\Big(((e_1)_M)_R, (((e_2)_M)_R)\Big) = L\Big((e_1)_M, (e_2)_M\Big) = -L(e_1, e_2)$. Notice that $((e_2)_M)_R$ and $((e_1)_M)_R$, lie exactly on the edges $e_2 - 2\vec{\alpha}$

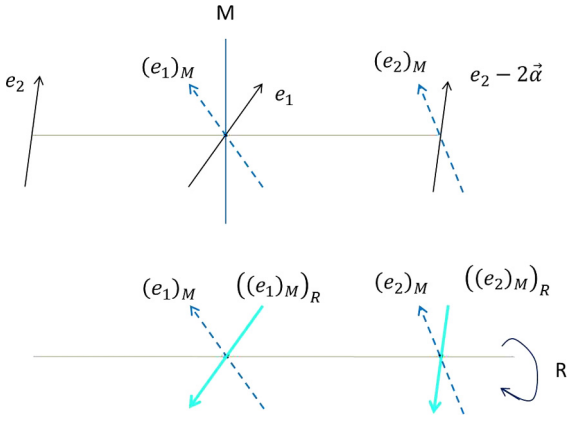

Fig. 9. Above: $L(e_1, e_2) = -L((e_1)_M, (e_2)_M)$. Below: $L((e_1)_M, (e_2)_M) = L(((e_1)_M)_R, ((e_2)_M)_R) = L(e_1, e_2 - 2\vec{\alpha})$. (For interpretation of the references to color in this figure, the reader is referred to the web version of this article.)

and e_1 respectively, but they have opposite orientation compared to $e_2 - 2\vec{\alpha}$ and e_1. If the orientation on both $((e_2)_M)_R$ and $((e_1)_M)_R$ is reversed, their linking number does not change. Thus $L(e_1, e_2 - 2\vec{\alpha}) = L\Big(-((e_1)_M)_R, -(((e_2)_M)_R)\Big) = L\Big(((e_1)_M)_R, (((e_2)_M)_R)\Big) = -L(e_1, e_2)$. □

Corollary 22. *Let e_1, e_2 denote two edges whose base points are connected by a vector $\vec{\alpha}$, then*

$$L(e_1, e_2 + \vec{\nu}) + L(e_1, e_2 - \vec{\nu}) = L(e_1, e_2 + \vec{\nu}) - L(e_1, e_2 + \vec{\nu} - 2\vec{\alpha}). \tag{57}$$

Proof. Notice that the base points of the edges e_1 and $e_2' = e_2 - \vec{\nu}$ get connected by a vector $\vec{\alpha}' = \vec{\alpha} - \vec{\nu}$ (see Fig. 10). Thus, by Lemma 21

$$\begin{aligned} L(e_1, e_2 - \vec{\nu}) &= L(e_1, e_2') = -L(e_1, e_2' - 2\vec{\alpha}') = -L(e_1, e_2 - \vec{\nu} - 2\vec{\alpha}') \\ &= -L(e_1, e_2 - \vec{\nu} - 2(\vec{\alpha} - \vec{\nu})) = -L(e_1, e_2 + \vec{\nu} - 2\vec{\alpha}). \end{aligned} \tag{58}$$

□

For the sum of the linking integrals of two opposite translations, we have the following important lemma:

Lemma 23. *Let e_1, e_2 denote two edges whose base points are connected by a vector $\vec{\alpha}$, then for $||\vec{\nu}|| >> ||\vec{\alpha}||$,*

$$|L(e_1, e_2 + \vec{\nu}) + L(e_1, e_2 - \vec{\nu})| < \frac{2}{\pi}||\vec{\alpha}||\frac{1}{(||\vec{\nu}|| - ||\vec{\alpha}||)^3} \tag{59}$$

Proof. Let $\gamma_1(\tau)$, $\gamma_2(s)$, $t, s \in [0, 1]$ denote the arc-length parametrizations of the edges e_1, e_2 respectively. By Lemma 22:

$$\begin{aligned} &L(e_1, e_2 + \vec{\nu}) + L(e_1, e_2 - \vec{\nu}) \\ &= L(e_1, e_2 + \vec{\nu}) - L(e_1, e_2 + \vec{\nu} - 2\vec{\alpha}) \\ &= \frac{1}{4\pi}\Big(\int\int \frac{(\dot{\gamma_1} \times \dot{\gamma_2}) \cdot (\gamma_1(t) - \gamma_2(s) + \vec{\nu})}{||\gamma_1(t) - \gamma_2(s) + \vec{\nu}||^3} dsdt - \int\int \frac{(\dot{\gamma_1} \times \dot{\gamma_2}) \cdot (\gamma_1(t) - \gamma_2(s) + \vec{\nu} - 2\vec{\alpha})}{||\gamma_1(t) - \gamma_2(s) + \vec{\nu} - 2\vec{\alpha}||^3} dsdt\Big). \end{aligned} \tag{60}$$

For $||\vec{\nu}||$ large, the integrands can be approximated, for all (s, t) values, by their values at (t_1, s_1), where $\gamma_1(t_1) = \beta_1$ and $\gamma_2(s_1) = \beta_2$. For simplicity we will denote $\gamma_1(t_1) = \gamma_1$, $\gamma_2(s_2) = \gamma_2$. Notice that $\vec{\alpha} = \gamma_1 - \gamma_2$, so Eq. (60) becomes:

$$\begin{aligned} &L(e_1, e_2 + \vec{\nu}) - L(e_1, e_2 + \vec{\nu} - 2\vec{\alpha}) \\ &= \frac{1}{4\pi}\Big(\frac{(\dot{\gamma_1} \times \dot{\gamma_2}) \cdot (\vec{\alpha} + \vec{\nu})}{||\vec{\alpha} + \vec{\nu}||^3} - \frac{(\dot{\gamma_1} \times \dot{\gamma_2}) \cdot (\vec{\alpha} + \vec{\nu} - 2\vec{\alpha})}{||\vec{\alpha} + \vec{\nu} - 2\vec{\alpha}||^3}\Big) \\ &= \frac{1}{4\pi}\Big(\frac{(\dot{\gamma_1} \times \dot{\gamma_2}) \cdot (\vec{\alpha} + \vec{\nu})}{||\vec{\alpha} + \vec{\nu}||^3} - \frac{(\dot{\gamma_1} \times \dot{\gamma_2}) \cdot (\vec{\alpha} + \vec{\nu})}{||\vec{\alpha} + \vec{\nu} - 2\vec{\alpha}||^3} + \frac{(\dot{\gamma_1} \times \dot{\gamma_2}) \cdot 2\vec{\alpha}}{||\vec{\alpha} + \vec{\nu} - 2\vec{\alpha}||^3}\Big) \\ &= \frac{1}{4\pi}\Big((\dot{\gamma_1} \times \dot{\gamma_2}) \cdot (\vec{\alpha} + \vec{\nu})\Big(\frac{1}{||\vec{\alpha} + \vec{\nu}||^3} - \frac{1}{||\vec{\alpha} + \vec{\nu} - 2\vec{\alpha}||^3}\Big) + \frac{(\dot{\gamma_1} \times \dot{\gamma_2}) \cdot 2\vec{\alpha}}{||\vec{\alpha} + \vec{\nu} - 2\vec{\alpha}||^3}\Big). \end{aligned} \tag{61}$$

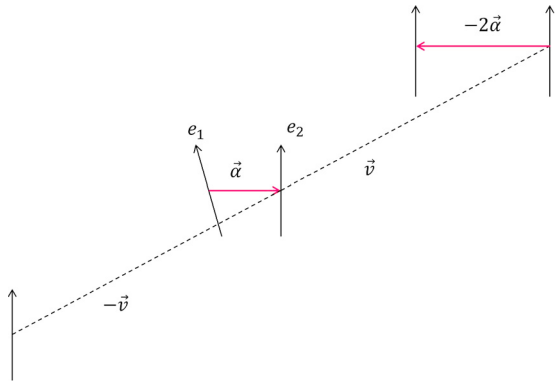

Fig. 10. The base points of the translations of e_2 by $\pm\vec{v}$, get connected to the base point of e_1 by $\vec{v}+\vec{\alpha}$ and $-\vec{v}+\vec{\alpha}$. Thus, in general, they do not have the same distance from the base point of e_1, and thus $L(e_1, e_2+\vec{v}) \neq L(e_1, e_2-\vec{v})$. By Lemma 21, $L(e_1, e_2+\vec{v})+L(e_1, e_2-\vec{v}) = L(e_1, e_2+\vec{v})-L(e_1, e_2+\vec{v}-2\vec{\alpha})$.

Then, using the Mean Value Theorem of Calculus, for the function

$$h(\vec{v}) = \frac{1}{||\vec{\alpha}+\vec{v}||^3} \tag{62}$$

for $||\vec{v}|| >> ||\vec{\alpha}||$, the expression $\frac{1}{||\vec{\alpha}+\vec{v}||^3} - \frac{1}{||\vec{\alpha}+\vec{v}-2\vec{\alpha}||^3}$ in Eq. (61) can be approximated by the directional derivative of $h(\vec{v})$ with respect to $\vec{a}$:

$$2||\vec{\alpha}||D_{\vec{\alpha}}(h(\vec{v})) \approx \frac{-6||\vec{\alpha}||\cos\theta_1}{||\vec{\alpha}+\vec{v}||^4}, \tag{63}$$

where θ_1 denotes the angle between $\vec{\alpha}$ and $\vec{\alpha}+\vec{v}$. Thus:

$$\begin{aligned} &L(e_1, e_2+\vec{v}) + L(e_1, e_2-\vec{v}) \\ &\approx \frac{1}{4\pi}\Big((\dot{\gamma}_1\times\dot{\gamma}_2)\cdot(\vec{\alpha}+\vec{v})\frac{-6||\vec{\alpha}||\cos\theta_1}{||\vec{\alpha}+\vec{v}||^4} + \frac{(\dot{\gamma}_1\times\dot{\gamma}_2)\cdot 2\vec{\alpha}}{||\vec{\alpha}+\vec{v}-2\vec{\alpha}||^3}\Big) \\ &= \frac{1}{4\pi}\Big(\sin\phi\cos\theta\frac{-6||\vec{\alpha}||\cos\theta_1}{||\vec{\alpha}+\vec{v}||^3} + \sin\phi\cos\psi\frac{2||\vec{\alpha}||}{||\vec{v}-\vec{\alpha}||^3}\Big), \end{aligned} \tag{64}$$

where ϕ denotes the angle between $\dot{\gamma}_1$ and $\dot{\gamma}_2$, θ denotes the angle between $\dot{\gamma}_1\times\dot{\gamma}_2$ and $\vec{\alpha}+\vec{v}$, and ψ denotes the angle between $\dot{\gamma}_1\times\dot{\gamma}_2$ and $\vec{\alpha}$. So,

$$\begin{aligned} &|L(e_1, e_2+\vec{v}) + L(e_1, e_2-\vec{v})| \\ &< \frac{1}{2\pi}||\vec{\alpha}||\,|\sin\phi|\Big(\frac{3|\cos\theta\cos\theta_1|}{||\vec{v}+\vec{\alpha}||^3} + \frac{|\cos\psi|}{||\vec{v}-\vec{\alpha}||^3}\Big) \\ &< \frac{1}{2\pi}||\vec{\alpha}||\,|\sin\phi|\Big(\frac{3|\cos\theta\cos\theta_1|}{(||\vec{v}||-||\vec{\alpha}||)^3} + \frac{|\cos\psi|}{(||\vec{v}||-||\vec{\alpha}||)^3}\Big) \\ &\leq \frac{2}{\pi}||\vec{\alpha}||\frac{1}{(||\vec{v}||-||\vec{\alpha}||)^3}. \qquad \square \end{aligned} \tag{65}$$

Using these results, convergence in two PBC is proved in the next theorem:

Theorem 24. *The periodic linking number between two free edges I and J in a system with two PBC, denoted $LK_P^{(2)}(I, J)$, converges uniformly and is bounded above by*

$$\begin{aligned} &LK_P^{(2)}(I, J) \\ &< L(I_0, J_0) + \Big(LK_P^{(1)}(I, J) - L(I_0, J_0)\Big)\sum_{n\leq n_0} R_2(n) + \frac{1}{\pi}||\vec{\alpha}||^2\sum_{n>n_0}\frac{r_2(n)}{(l\sqrt{n}-||\vec{\alpha}||)^3} \\ &< L(I_0, J_0) + \Big(\frac{1}{2\pi}\sum_{m\in\mathbb{N}}\frac{1}{(ml-||\vec{\alpha}||-b)^2}\Big)\sum_{n\leq n_0} R_2(n) + \frac{1}{\pi}||\vec{\alpha}||^2\sum_{n>n_0}\frac{r_2(n)}{(l\sqrt{n}-||\vec{\alpha}||)^3}, \end{aligned} \tag{66}$$

where $\vec{\alpha}$ is the vector that connects the base points of the parent images, I_0 and J_0, b denotes the length of an image of I and J, l denotes the length of an edge of the cubic cell and $n_0 >> \left(\frac{||\vec{\alpha}||}{l}\right)^2 \in \mathbb{N}$.

Proof. Let $\vec{\alpha}$ denote the vector that connects the base points of the parent images of I and J. Let $n_0 \in \mathbb{N}$ be such that $n_0 >> \left(\frac{||\vec{\alpha}||}{l}\right)^2$. Then LK_P can be expressed as:

$$LK_P^{(2)}(I,J) = L(I_0,J_0) + \sum_{n\le n_0\in\mathbb{N}} \sum_{\substack{\vec{v}\in l\mathbb{Z}^2 \\ ||\vec{v}||^2=l^2n}} L(I_0,J_0+\vec{v}) + \frac{1}{2}\sum_{n>n_0\in\mathbb{N}} \sum_{\substack{\vec{v}\in l\mathbb{Z}^2 \\ ||\vec{v}||^2=l^2n}} (L(I_0,J_0+\vec{v}) + L(I_0,J_0-\vec{v})). \tag{67}$$

Let us denote these sums as Σ_1, Σ_2 respectively.

For the terms in Σ_2 Lemma 23 can be applied, giving

$$\begin{aligned}\sum_{\substack{\vec{v}\in l\mathbb{Z}^2 \\ ||\vec{v}||^2=l^2n}} |L(I_0,J_0+\vec{v}) + L(I_0,J_0-\vec{v})| &= \sum_{\substack{\vec{v}\in \mathbb{Z}^2 \\ ||\vec{v}||^2=n}} |L(I_0,J_0+l\vec{v}) + L(I_0,J_0-l\vec{v})| \\ &\le \sum_{\substack{\vec{v}\in \mathbb{Z}^2 \\ ||\vec{v}||^2=n}} \left(\frac{2}{\pi}||\vec{\alpha}||\frac{1}{(l||\vec{v}|| - ||\vec{\alpha}||)^3}\right) = \frac{2}{\pi}||\vec{\alpha}||\frac{r_2(n)}{(l\sqrt{n}-||\vec{\alpha}||)^3} = Q_n^{(2)}.\end{aligned} \tag{68}$$

By Eq. (46), $r_2(n) < O(n^{7/22})$, thus $\Sigma_2 < \frac{1}{2}\sum_{n>n_0} Q_n^{(2)} < \infty$, and the convergence is uniform.

Notice that, Σ_1 is a finite summation, thus we have proved that $LK_P^{(2)}$ converges uniformly.

To find an upper bound for Σ_1 we proceed as follows: Note that any non-zero vector $\vec{v}$ in $l\mathbb{Z}^2$ can be expressed as $\vec{v} = ml(v_1, v_2)$ where $m \in \mathbb{N}$, $v_i \in \mathbb{Z}$ and $\gcd(v_1, v_2) = 1$, where by $\gcd(v_1, v_2)$ we mean the gcd of the non-zero coordinates among the v_1, v_2. Thus we can express Σ_1 as:

$$\begin{aligned}\Sigma_1 &= \sum_{n\le n_0\in\mathbb{N}} \sum_{\substack{\vec{v}\in l\mathbb{Z}^2 \\ ||\vec{v}||^2=l^2n}} L(I_0,J_0+\vec{v}) \\ &= \sum_{n\le n_0} \sum_{\substack{\vec{v}\in \mathbb{Z}^2 \\ ||\vec{v}||^2=n,\gcd(v_1,v_2)=1}} \sum_{m\in\mathbb{N}} L(I_0,J_0+ml\vec{v}) \\ &< \sum_{n\le n_0} \sum_{\substack{\vec{v}\in \mathbb{Z}^2 \\ ||\vec{v}||^2=n,\gcd(v_1,v_2)=1}} \sum_{m\in\mathbb{N}} Q_m^{(1)},\end{aligned} \tag{69}$$

where $Q_m^{(1)}$ was defined in the proof of Theorem 18 as $\sum_{m\in\mathbb{N}} Q_m^{(1)} = LK_P^{(1)}(I,J) - L(I_0,J_0) < \infty$, and thus:

$$\begin{aligned}\Sigma_1 &< \sum_{n\le n_0} \sum_{\substack{\vec{v}\in \mathbb{Z}^3 \\ ||\vec{v}||^2=n,\gcd(v_1,v_2)=1}} \left(LK_P^{(1)}(I,J) - L(I_0,J_0)\right) \\ &= \left(LK_P^{(1)}(I,J) - L(I_0,J_0)\right)\sum_{n\le n_0} R_2(n).\end{aligned} \tag{70}$$

Thus LK_P converges uniformly, and is bounded above by:

$$\begin{aligned}LK_P^{(2)}(I,J) &< L(I_0,J_0) + \left(LK_P^{(1)}(I,J) - L(I_0,J_0)\right)\sum_{n\le n_0} R_2(n) + \frac{1}{\pi}||\vec{\alpha}||^2 \sum_{n>n_0} \frac{r_2(n)}{(l\sqrt{n}-||\vec{\alpha}||)^3} \\ &< L(I_0,J_0) + \left(\frac{1}{2\pi}\sum_{m\in\mathbb{N}} \frac{1}{(ml-||\vec{\alpha}||-b)^2}\right)\sum_{n\le n_0} R_2(n) + \frac{1}{\pi}||\vec{\alpha}||^2 \sum_{n>n_0} \frac{r_2(n)}{(l\sqrt{n}-||\vec{\alpha}||)^3}.\end{aligned} \tag{71}$$

□

Remark 25. Notice that in a system with two PBC, we can adjust the position of the cell to ensure that $||\vec{\alpha}|| < \sqrt{\frac{3}{2}}l$. In applications to polymers, where the edges correspond to monomer bonds, $||\vec{\alpha}|| > b$. Notice that $L(I_0,J_0)$ increases as $||\vec{\alpha}||$ decreases, and the same holds for $LK_P^{(2)}(I,J)$. For $||\vec{\alpha}|| = b$ we get the following upper bound

$$LK_P^{(2)}(I,J) < 1/2 + \left(\frac{1}{2\pi l^2}\sum_{m\in\mathbb{N}} \frac{1}{(m-2b/l)^2}\right)\sum_{n\le n_0} R_2(n) + \frac{2b}{\pi l^3}\sum_{n>n_0} \frac{r_2(n)}{(\sqrt{n}-b/l)^3}. \tag{72}$$

Using the approximations $r_2(n) \approx \pi$, $\sum_{n\le n_0} R_2(n) \approx \frac{6}{\pi}n_0$, Eq. (72) becomes:

$$LK_P^{(2)}(I,J) < 1/2 + \Big(\frac{1}{2\pi l^2}\sum_{m\in\mathbb{N}}\frac{1}{(m-2b/l)^2}\Big)\frac{6}{\pi}n_0 + \frac{2b}{l^3}\sum_{n>n_0}\frac{1}{(\sqrt{n}-b/l)^3}. \tag{73}$$

For $l = 50, b = 1$ (which are reasonable sizes for the simulation of PE melts) and for $n_0 = 10$ (which is much larger than $(b/l)^2 = 4 * 10^{-4}$), Eq. (73) gives $LK_P^{(2)}(I,J) < 0.502133$.

Corollary 26. *For two open or infinite chains in two PBC, LK_P is a continuous function almost everywhere in the space of configurations.*

6.3. Convergence in three PBC

In order to prove convergence of the periodic linking number of two free edges in three PBC, we denote $LK_P^{(3)}$, the convergence of $LK_P^{(3)}$ for a special type of configuration of two free edges is proved first and then this result is used to prove convergence for an arbitrary configuration of two free edges.

6.3.1. Convergence for two special free edges

Let Ω_1 denote the subset of Ω composed by pairs of edges, say (I'_0, J'_0), whose arc-length parametrizations are $\gamma_1(t)$, $\gamma_2(s)$, $t, s \in [0,1]$ respectively, such that $\dot\gamma_1 \times \dot\gamma_2$ is parallel to the x-axis, that is, $\dot\gamma_1 \times \dot\gamma_2 = (||\dot\gamma_1 \times \dot\gamma_2||, 0, 0)$ (see Fig. 11 for an illustrative example). Let I', J' be two free edges in three PBC with parent images $(I'_0, J'_0) \in \Omega_1$. In this section we prove that $LK_P^{(3)}(I', J')$ converges.

For any vector $\vec v = (v_1, v_2, v_3) \in l\mathbb{Z}^3$, let us group together all the distinct vectors whose coordinates are permutations of the coordinates of $\vec v$ with all possible combinations of signs. For any $\vec v$ let $pm(\vec v)$ denote this collection of vectors. Then $LK_P^{(3)}(I', J')$ can be expressed as:

$$\begin{aligned} LK_P^{(3)}(I',J') &= L(I'_0,J'_0) + \sum_{\substack{\vec v\in l\mathbb{N}^3\\ v_1^2=v_2^2=v_3^2}} L(I'_0,J'_0+\vec v) + \sum_{\substack{\vec v\in l\mathbb{N}^3\\ v_1\le v_2\le v_3^*}}\ \sum_{\vec u\in pm(\vec v)} L(I'_0,J'_0+\vec u)\\ &= L(I'_0,J'_0) + \sum_{\substack{\vec v\in l\mathbb{N}^3\\ v_1^2=v_2^2=v_3^2}} L(I'_0,J'_0+\vec v) + \sum_{\substack{\vec v\in l\mathbb{N}^3\\ v_1\le v_2\le v_3^*}} G_{\vec v}(I'_0,J'_0), \end{aligned} \tag{74}$$

where $v_1 \le v_2 \le v_3^*$ denotes all the vectors with $v_1 \le v_2 \le v_3$ except those with $v_1 = v_2 = v_3$, and $G_{\vec v}(I'_0, J'_0) = \sum_{\vec u\in pm(\vec v)} L(I'_0, J'_0 + \vec u)$.

This can be expressed more precisely as follows: Let $\rho(\vec v)$ denote a vector whose coordinates result from a combination of signs of the coordinates of $\vec v$ without changing the absolute values of the coordinates. For each vector there are 8 such combinations. Let $\rho_1(\vec v) = (v_1, v_2, v_3) = -\rho_5(\vec v)$, $\rho_2(\vec v) = (v_1, v_2, -v_3) = -\rho_6(\vec v)$, $\rho_3(\vec v) = (v_1, -v_2, v_3) = -\rho_7(\vec v)$, $\rho_4(\vec v) = (v_1, -v_2, -v_3) = -\rho_8(\vec v)$. Next, let τ denote a cyclic permutation in S_3. Then for a vector $\vec v$ let $\tau_1(\vec v) = (v_1, v_2, v_3)$, $\tau_2(\vec v) = (v_2, v_3, v_1)$ and $\tau_3(\vec v) = (v_3, v_1, v_2)$. Let also $\vec z = (v_1, v_3, v_2)$. Then LK_P can be expressed as

$$\begin{aligned} LK_P^{(3)}(I',J') &= L(I'_0,J'_0) + \sum_{\substack{\vec v\in l\mathbb{N}^3\\ v_1^2=v_2^2=v_3^2}} L(I'_0,J'_0+\vec v)\\ &\quad + \frac{1}{2}\sum_{\substack{\vec v\in l\mathbb{N}^3\\ v_1\le v_2\le v_3^*}}\Big(\sum_{j=1}^{4}\sum_{i=1}^{3}\Big(L(I'_0,J'_0+l\tau_i(\rho_j(\vec v))) + L(I'_0,J'_0-l\tau_i(\rho_j(\vec v)))\Big)\\ &\quad + \sum_{j=1}^{4}\sum_{i=1}^{3}\Big(L(I'_0,J'_0+l\tau_i(\rho_j(\vec z))) + L(I'_0,J'_0-l\tau_i(\rho_j(\vec z)))\Big)\Big)\\ &= L(I'_0,J'_0) + \sum_{\substack{\vec v\in l\mathbb{N}^3\\ v_1^2=v_2^2=v_3^2}} L(I'_0,J'_0+\vec v) + \frac{1}{2}\sum_{v_1\le v_2\le v_3^*\in l\mathbb{N}}\Big(\sum_{j=1}^{4}\Sigma(\rho_j(\vec v)) + \sum_{j=1}^{4}\Sigma(\rho_j(\vec z))\Big), \end{aligned} \tag{75}$$

where $\Sigma(\rho_j(\vec v)) = \sum_{i=1}^{3}\Big(L(I'_0, J'_0 + l\tau_i(\rho_j(\vec v))) + L(I'_0, J'_0 - l\tau_i(\rho_j(\vec v)))\Big)$ and $\Sigma(\rho_j(\vec z)) = \sum_{i=1}^{3}\Big(L(I'_0, J'_0 + l\tau_i(\rho_j(\vec z))) + L(I'_0, J'_0 - l\tau_i(\rho_j(\vec z)))\Big)$. So, $G_{\vec v}(I'_0, J'_0) = \frac{1}{2}\Big(\sum_{j=1}^{4}\Sigma(\rho_j(\vec v)) + \sum_{j=1}^{4}\Sigma(\rho_j(\vec z))\Big)$. (Notice that the vectors in $\Sigma(\rho_j(\vec v)), j = 1,\dots,4$, are the only vectors in $pm(\vec v)$ in the case where two coordinates of $\vec v$ are the same.)

Then:

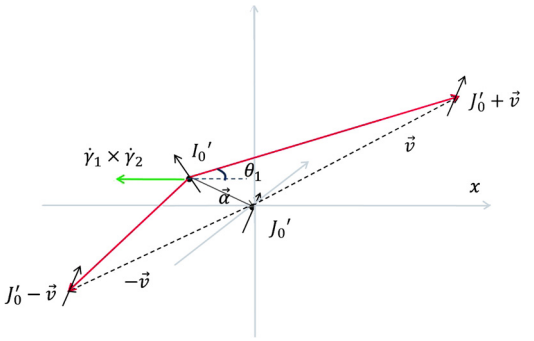

Fig. 11. In this configuration $\dot{\gamma}_1 \times \dot{\gamma}_2$ is parallel to the x-axis. Let $\vec{v} = (v_1, v_2, v_3)$, then for the angle θ_1 between $\dot{\gamma}_1 \times \dot{\gamma}_2$ and $\vec{\alpha} + \vec{v}$, we have $\cos\theta_1 = \frac{v_1+\alpha_1}{(v_1+\alpha_1)^2+(v_2+\alpha_2)^2+(v_3+\alpha_3)^2}$.

Lemma 27. *Let I', J' be two free edges with parent images I_0', J_0' with arc-length parametrizations $\gamma_1(t)$, $\gamma_2(s)$ $t, s \in [0,1]$ respectively, such that $\dot{\gamma}_1 \times \dot{\gamma}_2 = (\gamma, 0, 0)$, where $\gamma = \pm||\dot{\gamma}_1 \times \dot{\gamma}_2||$. Let the base points of I_0', J_0' be connected by a vector $\vec{\alpha} = (\alpha_1, \alpha_2, \alpha_3)$ and let $\vec{v} = (v_1, v_2, v_3)$ be a vector such that $v_1, v_2, v_3 >> \alpha = \max\{|\alpha_1|, |\alpha_2|, |\alpha_3|\}$ and not all $v_1^2 = v_2^2 = v_3^2$. Then $G_{\vec{v}}(I_0', J_0') \approx 0$.*

Proof. In the following we prove that $\sum_{j=1}^{4} \Sigma(\rho_j(\vec{v})) \approx 0$. Similarly one can prove that $\sum_{j=1}^{4} \Sigma(\rho_j(\vec{z})) \approx 0$, thus $G_{\vec{v}}(I', J') \approx 0$.

Notice that $\Sigma(\rho_j(\vec{v}))$ is equal to

$$\begin{aligned}\Sigma(\rho_j(\vec{v})) = {} & L(I_0', J_0' + \tau_1(\rho_j(\vec{v}))) + L(I_0', J_0' - \tau_1(\rho_j(\vec{v}))) + L(I_0', J_0' + \tau_2(\rho_j(\vec{v}))) \\ & + L(I_0', J_0' - \tau_2(\rho_j(\vec{v}))) + L(I_0', J_0' + \tau_3(\rho_j(\vec{v}))) + L(I_0', J_0' - \tau_3(\rho_j(\vec{v}))),\end{aligned} \tag{76}$$

which is a sum of linking numbers of three pairs of opposite translations.

Recall that the sign of $L(I_0', J_0' + \tau_i(\rho_j(\vec{v})))$ is positive/negative if the projection of $\vec{\alpha} + \tau_i(\rho_j(\vec{v}))$ on $\dot{\gamma}_1 \times \dot{\gamma}_2$ has the same orientation/or not, as $\dot{\gamma}_1 \times \dot{\gamma}_2$. For this special type of configuration, where $\dot{\gamma}_1 \times \dot{\gamma}_2 = (\gamma, 0, 0)$, this can be determined by examining the first coordinate of $\vec{\alpha} + \tau_i(\rho_j(\vec{v}))$ and γ. Let $\tau_i(\rho_j(\vec{v})) = (w_x, w_y, w_z)$, then $L(I_0, J_0 + \tau_i(\rho_j(\vec{v}))) > 0$ if and only if $(w_x + a_1)\gamma > 0$, that is, if γ and $w_x + a_1$ have the same sign. Since $v_1, v_2, v_3 > |\alpha_1|$ and $w_x = v_1, v_2$, or v_3, $L(I_0, J_0 + \tau_i(\rho_j(\vec{v})))$ and $L(I_0, J_0 - \tau_i(\rho_j(\vec{v})))$ have opposite signs for all i, j. Without loss of generality, let us suppose that $\gamma < 0$, then $L(I_0, J_0 + \tau_i(\rho_j(\vec{v}))) < 0$ and $L(I_0, J_0 - \tau_i(\rho_j(\vec{v}))) > 0$.

Thus the sum of opposite translations can be expressed as:

$$\begin{aligned}& L(I_0', J_0' + \tau_i(\rho_j(\vec{v}))) + L(I_0', J_0' - \tau_i(\rho_j(\vec{v}))) \\ & = -\frac{1}{4\pi}\int\int\Big(\frac{|\cos\theta_{ij}^{+}(t,s)\sin\phi|}{||\gamma_1(t) - \gamma_2(s) + \tau_i(\rho_j(\vec{v}))||^2} - \frac{|\cos\theta_{ij}^{-}(t,s)\sin\phi|}{||\gamma_1(t) - \gamma_2(s) - \tau_i(\rho_j(\vec{v}))||^2}\Big)dsdt,\end{aligned} \tag{77}$$

where $\theta_{ij}^{+}(t,s)$ is the smallest angle between $\gamma_1(t) - \gamma_2(s) + \tau_i(\rho_j(\vec{v}))$ with $\dot{\gamma}_1 \times \dot{\gamma}_2$, and similarly $\theta_{ij}^{-}(t,s)$ is the smallest angle between $\gamma_1(t) - \gamma_2(s) - \tau_i(\rho_j(\vec{v}))$ with $\dot{\gamma}_1 \times \dot{\gamma}_2$ and ϕ is the angle between I_0' and J_0'.

For $v_1, v_2, v_3 >> \alpha$ the value of the integrands in Eq. (77) for all s, t can be approximated by the value for (s_1, t_1), where $\gamma_1(t_1)$ is the base point of I_0 and $\gamma_2(s_1)$ is the base point of J_0, as follows:

$$L(I_0', J_0' + \tau_i(\rho_j(\vec{v}))) + L(I_0', J_0' - \tau_i(\rho_j(\vec{v}))) \approx -\frac{1}{4\pi}\sin\phi\Big(\frac{|\cos\theta_{ij}^{+}|}{||\vec{\alpha} + \tau_i(\rho_j(\vec{v}))||^2} - \frac{|\cos\theta_{ij}^{-}|}{||\vec{\alpha} - \tau_i(\rho_j(\vec{v}))||^2}\Big). \tag{78}$$

Thus,

$$\begin{aligned}\Sigma(\rho_j(\vec{v})) \approx -\frac{1}{4\pi}\Big[& \Big(\frac{|\cos\theta_{1j}^{+}|}{||\vec{\alpha} + \tau_1(\rho_j(\vec{v}))||^2} - \frac{|\cos\theta_{1j}^{-}|}{||\vec{\alpha} - \tau_1(\rho_j(\vec{v}))||^2}\Big) \\ & + \Big(\frac{|\cos\theta_{2j}^{+}|}{||\vec{\alpha} + \tau_2(\rho_j(\vec{v}))||^2} - \frac{|\cos\theta_{2j}^{-}|}{||\vec{\alpha} - \tau_2(\rho_j(\vec{v}))||^2}\Big) \\ & + \Big(\frac{|\cos\theta_{3j}^{+}|}{||\vec{\alpha} + \tau_3(\rho_j(\vec{v}))||^2} - \frac{|\cos\theta_{3j}^{-}|}{||\vec{\alpha} - \tau_3(\rho_j(\vec{v}))||^2}\Big)\Big].\end{aligned} \tag{79}$$

Without loss of generality, let us suppose that $\alpha_1, \alpha_2, \alpha_3 > 0$, then (see for example Fig. 11)

$$|\cos\theta_{11}^{+}(t_1,s_1)| = \frac{v_1+\alpha_1}{||\vec{\alpha}+\vec{v}||} = \frac{v_1+\alpha_1}{\sqrt{(v_1+\alpha_1)^2+(v_2+\alpha_2)^2+(v_3+\alpha_3)^2}}, \tag{80}$$

and

$$|\cos\theta_{11}^{-}(t_1,s_1)| = \frac{v_1-\alpha_1}{||\vec{\alpha}-\vec{v}||} = \frac{v_1-\alpha_1}{\sqrt{(v_1-\alpha_1)^2+(v_2-\alpha_2)^2+(v_3-\alpha_3)^2}}. \tag{81}$$

Thus Eq. (79) can be expressed as:

$$\begin{aligned}\Sigma(\rho_1(\vec{v})) = -\frac{1}{4\pi}\Big(&\frac{v_1+\alpha_1}{((v_1+\alpha_1)^2+(v_2+\alpha_2)^2+(v_3+\alpha_3)^2)^{3/2}} - \frac{v_1-\alpha_1}{((v_1-\alpha_1)^2+(v_2-\alpha_2)^2+(v_3-\alpha_3)^2)^{3/2}}\\ &+\frac{v_2+\alpha_1}{((v_2+\alpha_1)^2+(v_3+\alpha_2)^2+(v_1+\alpha_3)^2)^{3/2}} - \frac{v_2-\alpha_1}{((v_2-\alpha_1)^2+(v_3-\alpha_2)^2+(v_1-\alpha_3)^2)^{3/2}}\\ &+\frac{v_3+\alpha_1}{((v_3+\alpha_1)^2+(v_1+\alpha_2)^2+(v_2+\alpha_3)^2)^{3/2}} - \frac{v_3-\alpha_1}{((v_3-\alpha_1)^2+(v_1-\alpha_2)^2+(v_2-\alpha_3)^2)^{3/2}}\Big).\end{aligned} \tag{82}$$

Let $f:\mathbb{R}^3\to\mathbb{R}$ be defined as $f(x,y,z) = -\frac{1}{||(x,y,z)||}$. Then the first two terms in Eq. (82) can be expressed as $\frac{\partial f}{\partial x}(v_1+\alpha_1, v_2+\alpha_2, v_3+\alpha_3) - \frac{\partial f}{\partial x}(v_1-\alpha_1, v_2-\alpha_2, v_3-\alpha_3)$. For $v_1, v_2, v_3 >> \alpha$, this can be approximated by the directional derivative of $\frac{\partial f}{\partial x}$ in the direction $\vec{\alpha}$ by applying the Mean Value Theorem of calculus:

$$\begin{aligned}&\frac{v_1+\alpha_1}{((v_1+\alpha_1)^2+(v_2+\alpha_2)^2+(v_3+\alpha_3)^2)^{3/2}} - \frac{v_1-\alpha_1}{((v_1-\alpha_1)^2+(v_2-\alpha_2)^2+(v_3-\alpha_3)^2)^{3/2}}\\ &= \frac{\partial f}{\partial x}(v_1+\alpha_1, v_2+\alpha_2, v_3+\alpha_3) - \frac{\partial f}{\partial x}(v_1-\alpha_1, v_2-\alpha_2, v_3-\alpha_3)\\ &\approx -2||\vec{\alpha}||\nabla\Big(\frac{\partial f}{\partial x}\Big)(v_1,v_2,v_3)\cdot\vec{\alpha}.\end{aligned} \tag{83}$$

Using the same method for the next pairs of terms in Eq. (82), for $v_1, v_2, v_3 >> \alpha$, Eq. (82) can be approximated by:

$$\Sigma(\rho_1(\vec{v})) \approx \frac{||\vec{\alpha}||}{2\pi}\Big(\nabla\Big(\frac{\partial f}{\partial x}\Big)(\vec{v})\cdot(\alpha_1,\alpha_2,\alpha_3) + \nabla\Big(\frac{\partial f}{\partial y}\Big)(\vec{v})\cdot(\alpha_3,\alpha_1,\alpha_3) + \nabla\Big(\frac{\partial f}{\partial z}\Big)(\vec{v})\cdot(\alpha_2,\alpha_3,\alpha_1)\Big). \tag{84}$$

Following the same method,

$$\Sigma(\rho_2(\vec{v})) \approx \frac{||\vec{\alpha}||}{2\pi}\Big(\nabla\Big(\frac{\partial f}{\partial x}\Big)(\vec{v})\cdot(\alpha_1,\alpha_2,-\alpha_3) + \nabla\Big(\frac{\partial f}{\partial y}\Big)(\vec{v})\cdot(\alpha_3,\alpha_1,-\alpha_2) - \nabla\Big(\frac{\partial f}{\partial z}\Big)(\vec{v})\cdot(\alpha_2,\alpha_3,-\alpha_1)\Big), \tag{85}$$

$$\Sigma(\rho_3(\vec{v})) \approx \frac{||\vec{\alpha}||}{2\pi}\Big(\nabla\Big(\frac{\partial f}{\partial x}\Big)(\vec{v})\cdot(\alpha_1,-\alpha_2,\alpha_3) - \nabla\Big(\frac{\partial f}{\partial y}\Big)(\vec{v})\cdot(\alpha_3,-\alpha_1,\alpha_2) + \nabla\Big(\frac{\partial f}{\partial z}\Big)(\vec{v})\cdot(\alpha_2,-\alpha_3,\alpha_1)\Big), \tag{86}$$

and

$$\Sigma(\rho_4(\vec{v})) \approx \frac{||\vec{\alpha}||}{2\pi}\Big(\nabla\Big(\frac{\partial f}{\partial x}\Big)(\vec{v})\cdot(\alpha_1,-\alpha_2,-\alpha_3) - \nabla\Big(\frac{\partial f}{\partial y}\Big)(\vec{v})\cdot(\alpha_3,-\alpha_1,-\alpha_2) - \nabla\Big(\frac{\partial f}{\partial z}\Big)(\vec{v})\cdot(\alpha_2,-\alpha_3,-\alpha_1)\Big). \tag{87}$$

Finally, adding together Eq. (84), (85), (86) and (87):

$$\sum_{j=1}^{4}\Sigma(\rho_j(\vec{v})) \approx 0. \tag{88}$$

Similarly, $\sum_{\vec{e}'\in p^{(1)}(\vec{v})}\Sigma(\vec{e}') \approx 0$, thus $G_{\vec{v}}(I_0', J_0') \approx 0$. □

Remark 28. Notice that the function $f(x,y,z) = -\frac{1}{||(x,y,z)||}$ defined in the proof of Theorem 27 is the opposite of the electric potential created by a point charge at distance $||(x,y,z)||$.

Now we can prove the following:

Lemma 29. *Let I', J' be two free edges in three PBC, with parent images I_0', J_0' with arc-length parametrizations $\gamma_1(t)$, $\gamma_2(s)$ $t,s\in[0,1]$ respectively, such that $\dot{\gamma}_1\times\dot{\gamma}_2 = (\gamma,0,0)$, where $\gamma = \pm||\dot{\gamma}_1\times\dot{\gamma}_2||$. Then their periodic linking number, denoted $LK_P^{(3)}(I', J')$, converges uniformly.*

Proof. Let $n_0 \in \mathbb{N}$ be such that $n_0 >> \left(\frac{||\vec{\alpha}||}{l}\right)^2$. Let V denote the set of vectors $\vec{v} = (v_1, v_2, v_3) \in l\mathbb{Z}^3$, with $|v_1|, |v_2|, |v_3| > l\sqrt{n_0}$, and such that not all $|v_1| = |v_2| = |v_3|$. Then $LK_P^{(3)}$ can be expressed as

$$LK_P^{(3)}(I', J') = \sum_{\vec{v}\in V} L(I'_0, J'_0 + \vec{v}) + \sum_{\vec{v}\notin V} L(I'_0, J'_0 + \vec{v}). \tag{89}$$

By Lemma 27 this can be expressed as

$$LK_P^{(3)}(I', J') \approx \sum_{\vec{v}\notin V} L(I'_0, J'_0 + \vec{v}). \tag{90}$$

Notice that the terms that do not belong in V correspond to the lattice points in the regions $A = \{-l\sqrt{n_0} \le x \le l\sqrt{n_0}\}$, $B = \{-l\sqrt{n_0} \le y \le l\sqrt{n_0}\}$ and $C = \{-l\sqrt{n_0} \le z \le l\sqrt{n_0}\}$, and all vectors (v_1, v_2, v_3), such that $|v_1| = |v_2| = |v_3|$. Notice that these regions contain points that lie in planes parallel to the xy-, xz- and yz-planes around the origin. The sum of the terms that correspond to the lattice points in A are bounded above by $2n_0 LK_P^{(2)}(I', J')$, since there are $2n_0$ planes containing these lattice points. Also, there are 8 vectors with $|v_1| = |v_2| = |v_3| = 1$. Thus, the terms in the direction of these vectors are bounded above by $LK_P^{(1)}(I', J')$. Thus, we have the following upper bound

$$\begin{aligned} LK_P^{(3)}(I', J') &< L(I'_0, J'_0) + 4(LK_P^{(1)}(I', J') - L(I'_0, J'_0)) + \sum_{\vec{v}\in A} L(I'_0, J'_0 + \vec{v}) + \sum_{\vec{v}\in B} L(I'_0, J'_0 + \vec{v}) + \sum_{\vec{v}\in C} L(I'_0, J'_0 + \vec{v}) \\ &< L(I'_0, J'_0) + 4(LK_P^{(1)}(I', J') - L(I'_0, J'_0)) + 6n_0 \left(LK_P^{(2)}(I', J') - L(I'_0, J'_0)\right). \end{aligned} \tag{91}$$

Since $LK_P^{(1)}(I', J')$ and $LK_P^{(2)}(I', J')$ converge uniformly (Theorems 18 and 24), $LK_P^{(3)}(I', J')$ is uniformly convergent. □

Notice that in the above proof of a finite upper bound of $LK_P^{(3)}(I', J')$, some terms are encountered several times. The following lemma provides a smaller upper bound of $LK_P^{(3)}(I', J')$:

Lemma 30. *Let I', J' be two free edges in three PBC, with parent images I'_0, J'_0 with arc-length parametrizations $\gamma_1(t)$, $\gamma_2(s)$ $t, s \in [0, 1]$ respectively, such that $\dot{\gamma}_1 \times \dot{\gamma}_2 = (\gamma, 0, 0)$, where $\gamma = \pm||\dot{\gamma}_1 \times \dot{\gamma}_2||$. Then $LK_P^{(3)}(I', J')$ is bounded above by*

$$\begin{aligned} &LK_P^{(3)}(I', J') \\ &< L(I'_0, J'_0) + 6(LK_P^{(1)}(I'_0, J'_0) - L(I'_0, J'_0)) + \frac{3}{\pi}||\vec{\alpha}||n_0 \sum_{n>n_0} \frac{r_2(n) + 2n_0}{(l\sqrt{n} - ||\vec{\alpha}||)^3} + \frac{1}{4\pi} \sum_{n\le 3n_0} \frac{r_3(n)}{(l\sqrt{n} - ||\vec{\alpha}|| - b)^2} \\ &< L(I'_0, J'_0) + \frac{3}{\pi} \sum_{m\in\mathbb{N}} \frac{1}{(ml - ||\vec{\alpha}|| - b)^2} + \frac{3}{\pi}||\vec{\alpha}||n_0 \sum_{n>n_0} \frac{r_2(n) + 2n_0}{(l\sqrt{n} - ||\vec{\alpha}||)^3} + \frac{1}{4\pi} \sum_{n\le 3n_0} \frac{r_3(n)}{(l\sqrt{n} - ||\vec{\alpha}|| - b)^2}, \end{aligned} \tag{92}$$

where $\vec{\alpha}$ is the vector that connects the base points of the parent images, I'_0, J'_0, b is the length of an image of I, J, l is the length of an edge of the cell and $n_0 >> \left(\frac{||\vec{\alpha}||}{l}\right)^2 \in \mathbb{N}$.

Proof. The periodic linking number can be expressed as:

$$LK_P^{(3)}(I', J') = \sum_{\vec{v}\notin V} L(I'_0, J'_0 + \vec{v}) \tag{93}$$

where V is defined as in the proof of Lemma 29. This can be expressed as

$$\begin{aligned} LK_P^{(3)}(I', J') \approx L(I'_0, J'_0) &+ \sum_{\substack{\vec{v}\in l\mathbb{Z}^3 \\ v_1^2 = v_2^2 = v_3^2}} L(I'_0, J'_0 + \vec{v}) + \sum_{\vec{v}\in V_1} L(I'_0, J'_0 + \vec{v}) \\ &+ \sum_{\vec{v}\in V_2} L(I'_0, J'_0 + \vec{v}) + \sum_{\substack{\vec{v}\in l\mathbb{Z}^3 \\ (v_1^2, v_2^2, v_3^2 \le l^2 n_0)^*}} L(I'_0, J'_0 + \vec{v}), \end{aligned} \tag{94}$$

where V_1 is the set of vectors in $l\mathbb{Z}^3$ with one coordinate of absolute value smaller than or equal to $l\sqrt{n_0}$ and two of absolute value larger than $l\sqrt{n_0}$, a V_2 is the set of vectors in $l\mathbb{Z}^3$ with two coordinates of absolute value smaller than or equal to $l\sqrt{n_0}$ and one of absolute value larger than $l\sqrt{n_0}$. The expression $(v_1^2, v_2^2, v_3^2 \le l^2 n_0)^*$ denotes the vectors with $v_1^2, v_2^2, v_3^2 \le l^2 n_0$, where not all $v_1 = v_2 = v_3$. Let us denote these sums as U_0, U_1, U_2, U_3 respectively. For U_0 we have $U_0 < 4(LK_P^{(1)}(I', J') - L(I'_0, J'_0))$.

To obtain an upper bound for U_1, U_2, we will apply Lemma 23. More precisely, we can bound U_1 by:

$$U_1 < \frac{1}{2}\Big(\sum_{\substack{\vec{v}\in l\mathbb{Z}^3 \\ v_1^2\le l^2n_0, v_2^2, v_3^2 > l^2n_0}} |L(I_0', J_0'+\vec{v}) + L(I_0', J_0'-\vec{v})| + \sum_{\substack{\vec{v}\in l\mathbb{Z}^3 \\ v_2^2\le l^2n_0, v_1^2, v_3^2 > l^2n_0}} |L(I_0', J_0'+\vec{v}) + L(I_0', J_0'-\vec{v})| + \sum_{\substack{\vec{v}\in l\mathbb{Z}^3 \\ v_3^2\le l^2n_0, v_1^2, v_2^2 > l^2n_0}} |L(I_0', J_0'+\vec{v}) + L(I_0', J_0'-\vec{v})|\Big) \tag{95}$$

By Lemma 23 we have:

$$\begin{aligned} U_1 &< \frac{1}{2}\Big(\sum_{\substack{\vec{v}\in l\mathbb{Z}^3 \\ v_1^2\le l^2n_0, v_2^2, v_3^2 > l^2n_0}} \frac{2}{\pi}||\vec{\alpha}|| \frac{1}{(l||\vec{v}|| - ||\vec{\alpha}||)^3} + \sum_{\substack{\vec{v}\in l\mathbb{Z}^3 \\ v_2^2\le l^2n_0, v_1^2, v_3^2 > l^2n_0}} \frac{2}{\pi}||\vec{\alpha}|| \frac{1}{(l||\vec{v}|| - ||\vec{\alpha}||)^3} \\ &\quad + \sum_{\substack{\vec{v}\in l\mathbb{Z}^3 \\ v_3^2\le l^2n_0, v_1^2, v_2^2 > l^2n_0}} \frac{2}{\pi}||\vec{\alpha}|| \frac{1}{(l||\vec{v}|| - ||\vec{\alpha}||)^3}\Big) \\ &< \frac{3}{2} \sum_{\substack{\vec{v}\in\mathbb{Z}^2 \\ v_1^2, v_2^2 > n_0}} \frac{2}{\pi}||\vec{\alpha}|| \frac{1}{(l||\vec{v}|| - ||\vec{\alpha}||)^3} \\ &< \frac{3}{2}n_0 \sum_{\substack{\vec{v}\in\mathbb{Z}^2 \\ v_1^2, v_2^2 > n_0}} |L(I_0', J_0'+\vec{v}) + L(I_0', J_0'-\vec{v})| \\ &< \frac{3}{2}n_0 \sum_{\substack{\vec{v}\in\mathbb{Z}^2 \\ v_1^2, v_2^2 > n_0}} \frac{2}{\pi}||\vec{\alpha}|| \frac{1}{(l||\vec{v}|| - ||\vec{\alpha}||)^3} < \frac{3}{2}n_0 \sum_{n>2n_0} \sum_{\substack{\vec{v}\in\mathbb{Z}^2 \\ ||\vec{v}||^2 = n}} \frac{2}{\pi}||\vec{\alpha}|| \frac{1}{(l\sqrt{n} - ||\vec{\alpha}||)^3} \\ &= \frac{3}{\pi}||\vec{\alpha}||n_0 \sum_{n>2n_0} \frac{r_2(n)}{(l\sqrt{n} - ||\vec{\alpha}||)^3} = \frac{3}{2}n_0 \sum_{n>2n_0} Q_n^{(2)} < \frac{3}{2}n_0 \sum_{n>n_0} Q_n^{(2)} \end{aligned} \tag{96}$$

Similarly, for U_2 we have:

$$\begin{aligned} U_2 &< \frac{1}{2}\Big(\sum_{\substack{\vec{v}\in l\mathbb{Z}^3 \\ v_3^2 > l^2n_0, v_1^2, v_2^2 \le l^2n_0}} |L(I_0', J_0'+\vec{v}) + L(I_0', J_0'-\vec{v})| + \sum_{\substack{\vec{v}\in l\mathbb{Z}^3 \\ v_2^2 > l^2n_0, v_1^2, v_3^2 \le l^2n_0}} |L(I_0', J_0'+\vec{v}) + L(I_0', J_0'-\vec{v})| \\ &\quad + \sum_{\substack{\vec{v}\in l\mathbb{Z}^3 \\ v_1^2 > l^2n_0, v_2^2, v_3^2 \le l^2n_0}} |L(I_0', J_0'+\vec{v}) + L(I_0', J_0'-\vec{v})|\Big) \\ &< \frac{3}{2}n_0^2 \sum_{\substack{v_1\in l\mathbb{Z} \\ v_1^2 > l^2n_0}} |L(I_0', J_0'+(v_1,0,0)) + L(I_0', J_0'-(v_1,0,0))| \\ &< \frac{3}{\pi}n_0^2||\vec{\alpha}|| \sum_{n>n_0\in\mathbb{N}} \frac{1}{(l\sqrt{n} - ||\vec{\alpha}||)^3} \end{aligned} \tag{97}$$

For the terms in U_3, we apply Lemma 17 to get:

$$\begin{aligned} U_3 &< \sum_{\substack{\vec{v}\in l\mathbb{Z}^3 \\ v_1^2, v_2^2, v_3^2 \le l^2n_0}} |L(I_0', J_0'+\vec{v})| \\ &< \sum_{n\le 3n_0} \sum_{\substack{\vec{v}\in l\mathbb{Z}^3 \\ ||\vec{v}||^2 = l^2n}} |L(I_0', J_0'+\vec{v})| < \frac{1}{4\pi} \sum_{n\le 3n_0} \sum_{\substack{\vec{v}\in l\mathbb{Z}^3 \\ ||\vec{v}||^2 = l^2n}} \frac{1}{(||\vec{v}|| - ||\vec{\alpha}|| - b)^2} \\ &= \frac{1}{4\pi} \sum_{n\le 3n_0} \frac{r_3(n)}{(l\sqrt{n} - ||\vec{\alpha}|| - b)^2} \end{aligned} \tag{98}$$

Thus $LK_P^{(3)}(I', J') \approx U_0 + U_1 + U_2 + U_3 < \infty$ converges uniformly and is bounded by:

$$LK_P^{(3)}(I', J') < L(I_0', J_0') + \frac{2}{\pi}\sum_{m\in\mathbb{N}}\frac{1}{(ml - ||\vec{\alpha}|| - b)^2} + \frac{3}{\pi}||\vec{\alpha}||n_0\sum_{n>n_0}\frac{r_2(n)+n_0}{(l\sqrt{n} - ||\vec{\alpha}||)^3} + \frac{1}{4\pi}\sum_{n\le 3n_0}\frac{r_3(n)}{(l\sqrt{n} - ||\vec{\alpha}|| - b)^2}. \quad \square \tag{99}$$

Remark 31. Notice that in a system with three PBC we can adjust the position of the cell to ensure that $||\vec{\alpha}|| < \frac{\sqrt{3}l}{2}$. In applications to polymers, where the edges correspond to monomer bonds, $||\vec{\alpha}|| > b$. Notice that $L(I_0', J_0')$ increases as $||\vec{\alpha}||$ decreases, and the same holds for $LK_P^{(3)}(I', J')$. For $||\vec{\alpha}|| = b$ and using the approximations $r_2(n) \approx \pi$, $r_3(n) \approx \frac{4\pi}{3}\sqrt{n}$, we have the following upper bound:

$$LK_P^{(3)}(I', J') < 1/2 + \frac{3}{\pi l^2}\sum_{m\in\mathbb{N}}\frac{1}{(m - 2b/l)^2} + \frac{3b}{l^3\pi}n_0(\pi + n_0)\sum_{n>n_0}\frac{1}{(\sqrt{n} - b/l)^3} + \frac{1}{3l^2}\sum_{n\le 3n_0}\frac{\sqrt{n}}{(\sqrt{n} - 2b/l)^2}. \tag{100}$$

Notice that for $l = 50, b = 1$ (which is a reasonable size for the simulation of polymer melts) and for $n_0 = 10$ (which is much larger than $(b/l)^2 = 10^{-4}$), Eq. (100) gives $LK_P^{(3)}(I', J') < 0.502386$.

6.3.2. Convergence for any two free edges

In the following, we will prove that for any configuration I, J with parent images in Ω there exists a configuration I', J' with parent images in Ω_1, with $|LK_P^{(3)}(I, J) - LK_P^{(3)}(I', J')| < R \in \mathbb{R}$. Since by Theorem 30, $LK_P^{(3)}(I', J')$ converges, $LK_P^{(3)}$ converges for any configuration.

Lemma 32. *Let I', J' be two free edges in three PBC, with parent images I_0', J_0' having arc-length parametrizations $\gamma_1(t)$, $\gamma_2(s)$ $t, s \in [0, 1]$ respectively, such that $\dot{\gamma}_1 \times \dot{\gamma}_2 = (\gamma, 0, 0)$, where $\gamma = \pm||\dot{\gamma}_1 \times \dot{\gamma}_2||$. For any configuration of two free edges, I, J there exists a configuration I', J' such that*

$$|LK_P^{(3)}(I, J) - LK_P^{(3)}(I', J')| < \frac{1}{4\pi}\sum_{n\le n_0}\frac{r_3(n)}{(l\sqrt{n} - ||\vec{\alpha}|| - b)^2} + \sum_{n>n_0}\frac{3r_3(n)||\vec{\alpha}||}{\pi}\frac{1}{(l\sqrt{n} - ||\vec{\alpha}|| - b)^3}\left(\frac{6}{n^{1/2}} + \frac{\sqrt{6}}{n^{1/4}}\right) \tag{101}$$

Proof. Let Ω denote the space of all possible configurations of two generating edges in a cell. Let $(I_0, J_0) \in \Omega$ denote the parent images of the free edges I, J, with arc-length parametrizations $\gamma_1(t)$, $\gamma_2(s)$ $t, s \in [0, 1]$ respectively. We can transform a configuration of two free edges, I, J, in time $\tau \in [0, 1]$, by transforming the configuration of their parent images, I_0, J_0, so that for any τ, any image of $I(\tau)$ ($J(\tau)$, resp.) is a translation of $I_0(\tau)$ ($J_0(\tau)$, resp.). Any two free edges I, J can be transformed to two special free edges I', J' (i.e. such that $(I_0', J_0') \in \Omega_1$) by rigid rotation of I_0, J_0 around the base point of J_0, until $\dot{\gamma}_1 \times \dot{\gamma}_2$ becomes perpendicular to the yz-plane. Equivalently, the configuration I', J' described above can also be derived by leaving I, J fixed in space and rotating the coordinate axes x, y, z, to x', y', z', until $\dot{\gamma}_1 \times \dot{\gamma}_2$ becomes perpendicular to the $y'z'$-plane. Then we have

$$LK_P^{(3)}(I, J) = L(I_0, J_0) + \sum_n \sum_{\substack{\vec{v}\in l\mathbb{Z}^3 \\ ||\vec{v}||^2 = n}} L(I_0, J_0 + \vec{v}) \tag{102}$$

and

$$LK_P^{(3)}(I', J') = L(I_0, J_0) + \sum_n \sum_{\substack{\vec{v}'\in l\mathbb{Z}^3 \\ ||\vec{v}'||^2 = n}} L(I_0, J_0 + \vec{v}'), \tag{103}$$

where $\vec{v}'$ denotes a vector in the xyz-coordinate system from the origin to a lattice point in the x', y', z' coordinate system.

The number of lattice points on a sphere of radius $\sqrt{n}$, denoted $S_{\sqrt{n}}$, can be approximated by $r_3(n) = \frac{4\pi}{3}\sqrt{n}$. By [70–73] it is known that, as $n \to \infty$, the lattice points on $S_{\sqrt{n}}$ are uniformly distributed. Thus, for n large enough, we may partition $S_{\sqrt{n}}$, into elementary areas, of size l^2Area of $S_{\sqrt{n}}/r_3(n) \approx 3l^2\sqrt{n}$ each of which contains one lattice point of the xyz coordinate system (where l denotes the unit length of the lattice of our system). Similarly, each lattice point of the $x'y'z'$ coordinate system on $S_{\sqrt{n}}$, will lie in exactly one of these elementary areas and will be of distance less than $\sqrt{6}ln^{1/4}$ from a lattice point of the xyz coordinate system. Therefore, we can express every vector $\vec{v}'$ as $\vec{v}' = \vec{v} + \vec{h}$, where $||\vec{h}|| \le \sqrt{6}ln^{1/4}$.

We can write the periodic linking number as:

$$LK_P^{(3)}(I, J) = L(I_0, J_0) + \frac{1}{2}\sum_n \sum_{\substack{\vec{v}\in l\mathbb{Z}^3 \\ ||\vec{v}||^2=n}} \Big(L(I_0, J_0+\vec{v}) + L(I_0, J_0-\vec{v})\Big). \tag{104}$$

By the proof of Lemma 23, Eq. (64), we have

$$L(I_0, J_0+\vec{v}) + L(I_0, J_0-\vec{v}) = \frac{1}{4\pi}\Big(\sin\phi\cos\theta\frac{-6||\vec{\alpha}||\cos\theta_1}{||\vec{\alpha}+\vec{v}||^3} + \sin\phi\cos\psi\frac{2||\vec{\alpha}||}{||\vec{v}-\vec{\alpha}||^3}\Big), \tag{105}$$

where ϕ denotes the angle between $\dot{\gamma}_1$ and $\dot{\gamma}_2$, θ denotes the angle between $\dot{\gamma}_1\times\dot{\gamma}_2$ and $\vec{\alpha}+\vec{v}$, θ_1 denotes the angle between $\vec{\alpha}$ and $\vec{\alpha}+\vec{v}$, and ψ denotes the angle between $\dot{\gamma}_1\times\dot{\gamma}_2$ and $\vec{\alpha}$.

Thus, we want to compare the terms

$$S_1 = \frac{1}{4\pi}\Big(\sin\phi\cos\theta\frac{-6||\vec{\alpha}||\cos\theta_1}{||\vec{\alpha}+\vec{v}||^3} + \sin\phi\cos\psi\frac{2||\vec{\alpha}||}{||\vec{v}-\vec{\alpha}||^3}\Big) \tag{106}$$

and

$$S_2 = \frac{1}{4\pi}\Big(\sin\phi\cos\theta'\frac{-6||\vec{\alpha}||\cos\theta_1'}{||\vec{\alpha}+\vec{v}+\vec{h}||^3} + \sin\phi\cos\psi\frac{2||\vec{\alpha}||}{||\vec{v}+\vec{h}-\vec{\alpha}||^3}\Big), \tag{107}$$

where θ' denotes the angle between $\dot{\gamma}_1\times\dot{\gamma}_2$ and $\vec{\alpha}+\vec{v}+\vec{h}$, θ_1' denotes the angle between $\vec{\alpha}$ and $\vec{\alpha}+\vec{v}+\vec{h}$. Note that ϕ and ψ are the same for both configurations.

For n large enough, we may assume that $||\vec{\alpha}+\vec{v}+\vec{h}||\approx||\vec{\alpha}+\vec{v}||$. Thus we have

$$S_2 \approx \frac{\sin\phi}{4\pi}\Big(\cos\theta'\frac{-6||\vec{\alpha}||\cos\theta_1'}{||\vec{\alpha}+\vec{v}||^3} + \cos\psi\frac{2||\vec{\alpha}||}{||\vec{v}-\vec{\alpha}||^3}\Big). \tag{108}$$

Let θ_ϵ denote the angle between $\vec{v}$ and $\vec{v}'$. Then $\theta_\epsilon \le \frac{\sqrt{6}}{n^{1/4}}$ and we have $|\theta-\theta'| = x$, where $0\le x\le\theta_\epsilon$. Without loss of generality, we assume that $\theta'>\theta$ and $\theta_1'>\theta_1$. Thus, $\theta'\approx\theta+x$. Similarly, we have $\theta_1'\approx\theta_1+x$. Thus, we have $\cos\theta' = \cos\theta\cos x - \sin\theta\sin x$ and similarly, $\cos\theta_1' = \cos\theta_1\cos x - \sin\theta_1\sin x$. For large n, $\theta_\epsilon << 1$, we may assume that the signs of S_1 and S_2 are the same. Thus, we have

$$\begin{aligned}
|S_1-S_2| &\approx \frac{3||\vec{\alpha}||\sin\phi}{2\pi||\vec{\alpha}+\vec{v}||^3}\Big|\cos\theta\cos\theta_1 - \cos\theta'\cos\theta_1'\Big| \\
&= \frac{3||\vec{\alpha}||\sin\phi}{2\pi||\vec{\alpha}+\vec{v}||^3}\Big|\cos\theta\cos\theta_1 - (\cos\theta\cos x - \sin\theta\sin x)(\cos\theta_1\cos x - \sin\theta_1\sin x)\Big| \\
&= \frac{3||\vec{\alpha}||\sin\phi}{2\pi||\vec{\alpha}+\vec{v}||^3}\Big|(\cos\theta\cos\theta_1 - \cos\theta\cos\theta_1\cos^2 x) \\
&\quad - (-\cos\theta\sin\theta_1\cos x\sin x - \sin\theta\cos\theta_1\sin x\cos x + \sin\theta\sin\theta_1\sin^2 x)\Big| \\
&\le \frac{3||\vec{\alpha}||\sin\phi}{2\pi||\vec{\alpha}+\vec{v}||^3}\Big(|\cos\theta\cos\theta_1|(1-\cos^2 x) \\
&\quad + |\cos\theta\sin\theta_1\cos x\sin x| + |\sin\theta\cos\theta_1\sin x\cos x| + |\sin\theta\sin\theta_1\sin^2 x|\Big) \\
&\le \frac{3||\vec{\alpha}||\sin\phi}{2\pi||\vec{\alpha}+\vec{v}||^3}\Big(|\cos\theta\cos\theta_1|\sin^2\theta_\epsilon \\
&\quad + |\cos\theta\sin\theta_1||\sin\theta_\epsilon| + |\sin\theta\cos\theta_1||\sin\theta_\epsilon| + |\sin\theta\sin\theta_1|\sin^2\theta_\epsilon\Big) \\
&\le \frac{3||\vec{\alpha}||\sin\phi}{\pi||\vec{\alpha}+\vec{v}||^3}(|\sin\theta_\epsilon| + \sin^2\theta_\epsilon).
\end{aligned} \tag{109}$$

For n large we can use the small angle approximation: $\sin\theta_\epsilon = \sin\frac{\sqrt{6}}{n^{1/4}} \approx \frac{\sqrt{6}}{n^{1/4}}$. (Note that a lower upper bound could be obtained by using the small angle approximation for $\cos\theta_\epsilon$.)

Thus, we have

$$\begin{aligned}
|S_1-S_2| &\le \frac{3||\vec{\alpha}||}{\pi||\vec{\alpha}+\vec{v}||^3}\Big(\frac{6}{n^{1/2}} + \frac{\sqrt{6}}{n^{1/4}}\Big) \\
&\le \frac{3||\vec{\alpha}||}{\pi}\frac{1}{(l\sqrt{n}-||\vec{\alpha}||-b)^3}\Big(\frac{6}{n^{1/2}} + \frac{\sqrt{6}}{n^{1/4}}\Big).
\end{aligned} \tag{110}$$

So, we have

$$|LK_P^{(3)}(I,J) - LK_P^{(3)}(I',J')| \leq \frac{1}{4\pi}\sum_{n\leq n_0}\frac{r_3(n)}{(l\sqrt{n}-||\vec{\alpha}||-b)^2} + \sum_{n>n_0}\frac{3r_3(n)||\vec{\alpha}||}{\pi}\frac{1}{(l\sqrt{n}-||\vec{\alpha}||-b)^3}\Big(\frac{6}{n^{1/2}}+\frac{\sqrt{6}}{n^{1/4}}\Big). \quad \square \tag{111}$$

Theorem 33. *The periodic linking number of two free edges I, J in three PBC, we denote $LK_P^{(3)}$, converges uniformly and is bounded above by*

$$LK_P^{(3)}(I,J) < L(I_0,J_0) + \frac{3}{\pi}\sum_{m\in\mathbb{N}}\frac{1}{(ml-||\vec{\alpha}||-b)^2} + \frac{3}{\pi}||\vec{\alpha}||n_0\sum_{n>n_0}\frac{r_2(n)+n_0}{(l\sqrt{n}-||\vec{\alpha}||)^3} + \frac{1}{4\pi}\sum_{n\leq 3n_0}\frac{r_3(n)}{(l\sqrt{n}-||\vec{\alpha}||-b)^2} + \frac{1}{4\pi}\sum_{n\leq n_0}\frac{r_3(n)}{(l\sqrt{n}-||\vec{\alpha}||-b)^2} + \sum_{n>n_0}\frac{3r_3(n)||\vec{\alpha}||}{\pi}\frac{1}{(l\sqrt{n}-||\vec{\alpha}||-b)^3}\Big(\frac{6}{n^{1/2}}+\frac{\sqrt{6}}{n^{1/4}}\Big) \tag{112}$$

where $\vec{\alpha}$ is the vector that connects the base points of the parent images, I_0, J_0, b is the length of an image of I, J, l is the length of an edge of the cell and $n_0 >> \left(\frac{||\vec{\alpha}||}{l}\right)^2 \in \mathbb{N}$.

Proof. By Lemma 32, we know that there exists a configuration I', J' such that

$$LK_P^{(3)}(I',J') < L(I_0,J_0) + \frac{2}{\pi}\sum_{m\in\mathbb{N}}\frac{1}{(ml-||\vec{\alpha}||-b)^2} + \frac{3}{\pi}||\vec{\alpha}||n_0\sum_{n>n_0}\frac{r_2(n)+n_0}{(l\sqrt{n}-||\vec{\alpha}||)^3} + \frac{1}{4\pi}\sum_{n\leq 3n_0}\frac{r_3(n)}{(l\sqrt{n}-||\vec{\alpha}||-b)^2} \tag{113}$$

and

$$|LK_P^{(3)}(I,J) - LK_P^{(3)}(I',J')| \leq \frac{1}{4\pi}\sum_{n\leq n_0}\frac{r_3(n)}{(l\sqrt{n}-||\vec{\alpha}||-b)^2} + \sum_{n>n_0}\frac{4r_3(n)||\vec{\alpha}||}{3\pi}\frac{1}{(l\sqrt{n}-||\vec{\alpha}||-b)^3}\Big(\frac{6}{n^{1/2}}+\frac{\sqrt{6}}{n^{1/4}}\Big) \tag{114}$$

Thus, we have

$$LK_P^{(3)}(I,J) \leq L(I_0,J_0) + \frac{2}{\pi}\sum_{m\in\mathbb{N}}\frac{1}{(ml-||\vec{\alpha}||-b)^2} + \frac{3}{\pi}||\vec{\alpha}||n_0\sum_{n>n_0}\frac{r_2(n)+n_0}{(l\sqrt{n}-||\vec{\alpha}||)^3} + \frac{1}{4\pi}\sum_{n\leq 3n_0}\frac{r_3(n)}{(l\sqrt{n}-||\vec{\alpha}||-b)^2} + \frac{1}{4\pi}\sum_{n\leq n_0}\frac{r_3(n)}{(l\sqrt{n}-||\vec{\alpha}||-b)^2} + \sum_{n>n_0}\frac{3r_3(n)||\vec{\alpha}||}{\pi}\frac{1}{(l\sqrt{n}-||\vec{\alpha}||-b)^3}\Big(\frac{6}{n^{1/2}}+\frac{\sqrt{6}}{n^{1/4}}\Big) \tag{115}$$

So, $LK_P^{(3)}$ converges uniformly. $\square$

Remark 34. Notice that in a system with three PBC we can adjust the position of the cell to ensure that $||\vec{\alpha}|| < \frac{\sqrt{3}l}{2}$. In applications to polymers, where the edges correspond to monomer bonds, $||\vec{\alpha}|| > b$. Notice that $L(I_0,J_0)$ increases when $||\vec{\alpha}||$ decreases, and the same holds for $LK_P^{(3)}(I,J)$. For $||\vec{\alpha}|| = b$ and using the approximations $r_2(n) \approx \pi$ and $r_3(n) \approx \frac{4\pi}{3}\sqrt{n}$, the following approximate upper bound results

$$LK_P^{(3)}(I,J) < 1/2 + \frac{2}{\pi l^2}\sum_{m\in\mathbb{N}}\frac{1}{(m-2b/l)^2} + \frac{3b}{\pi l^3}n_0\sum_{n>n_0}\frac{\pi+n_0}{(\sqrt{n}-b/l)^3} + \frac{1}{3l^2}\sum_{n\leq 3n_0}\frac{\sqrt{n}}{(\sqrt{n}-2b/l)^2} + \frac{1}{3l^2}\sum_{n\leq n_0}\frac{1}{(\sqrt{n}-2b/l)^2} + \frac{4b}{l^3}\sum_{n>n_0}\frac{6+\sqrt{6}n^{1/4}}{(\sqrt{n}-2b/l)^3} \tag{116}$$

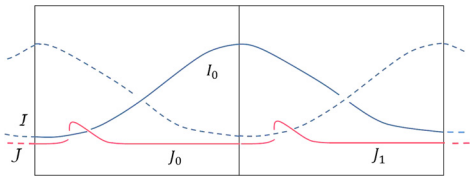

Fig. 12. The linking number between the two infinite lines $\mathcal{I}$ and $\mathcal{J}$ is related to the periodic linking number in one PBC as: $LK_P(I, J) = \lim_{T\to\infty} \frac{L(\mathcal{I}_T, \mathcal{J})}{T}$, where $\mathcal{I}_T$ is the arc formed by T concatenated copies of I_1.

Notice that for $l = 50, l = 1$ (which are appropriate sizes for the simulation of polymer melts) and $n_0 = 10$ (which is much larger than $(b/l)^2 = 10^{-4}$), Eq. (116) gives $LK_P^{(3)}(I, J) < 0.502824$.

Corollary 35. *The periodic linking number of open or infinite free chains is a continuous function almost everywhere of the chains coordinates.*

Corollary 36. *The periodic self-linking number and the periodic linking number with self-images of a chain in one, two, or three PBC converges and are continuous functions almost everywhere of the chain coordinates.*

6.4. The periodic linking number of infinite free chains

The study of linking of infinite chains in PBC is a difficult topological problem. The periodic linking number is a well-defined measure for two infinite free chains in PBC. In this section the periodic linking number of infinite chains is studied.

6.4.1. Connection of LK_P of infinite free chains with the Gauss linking number

There is a connection between the periodic linking number of two infinite free chains and the Gauss linking number of two infinite images of these free chains.

Consider the example of two infinite free chains I, J in a system with one PBC shown in Fig. 12. Let $\mathcal{I}$, $\mathcal{J}$ denote two infinite images of I and J respectively. Then:

$$L(\mathcal{I}, \mathcal{J}) = \sum_{t=1}^{\infty}\sum_{u=1}^{\infty} L(I_t, J_u) = \lim_{T\to\infty} \sum_{t=1}^{T}\sum_{u=1}^{\infty} L(I_t, J_u) = \lim_{T\to\infty} \sum_{t=1}^{T} LK_P(I, J), \tag{117}$$

since $LK_P(I, J)$ is independent of the image of I (or J) used for its computation. Thus, in this example, the periodic linking number between I and J is related to the linking number of $\mathcal{I}$, $\mathcal{J}$ as follows:

$$LK_P(I, J) = \lim_{T\to\infty} \frac{L(\mathcal{I}_T, \mathcal{J})}{T}, \tag{118}$$

where $\mathcal{I}_T$ denotes the arc that is formed by taking T consecutive copies of I_1 in $\mathcal{I}$. Notice that by Theorem 18 we know that for finite T, $L(\mathcal{I}_T, \mathcal{J})$ is a real number.

In the general case of a system with two or three PBC, where the system is composed by translations of infinite images of I, J, then an analogous expression is

$$LK_P(I, J) = \sum_{k} \lim_{T\to\infty} \frac{L(\mathcal{I}_T, \mathcal{J}_k)}{T}, \tag{119}$$

where $\mathcal{J}_k$ denotes an infinite image of J.

6.4.2. Connection of LK_P of infinite free chains with the intersection number in identification spaces

If the free chains are infinite then they represent non-trivial elements in $H_1(\mathbb{R}^3)$ and they project to non-trivial elements in the identification space (ST, $T^2 \times I$, or T^3). In that case, $\sigma_{\bar{I}}$ (or $\sigma_{\bar{J}}$) are not contained in the identification space, and we say that $\bar{I}$ (or $\bar{J}$) is an essential knot in ST, $T^2 \times I$, or T^3 respectively. Then the usual definition of intersection number cannot be applied to measure the linking between $\bar{I}$ and $\bar{J}$. In that case $\bar{i}$, $\bar{j}$ are intrinsically linked with the auxiliary curves that represent the identification space. Thus $L(\bar{i}, \bar{j})$ is not sufficient to describe the linking between $\bar{I}$ and $\bar{J}$. This is why a relative intersection number with respect to the manifold is needed [76–82].

The periodic linking number provides an alternative definition of linking number in the identification space that is computed in the universal cover of the identification space. In Appendix C we saw that the periodic linking number of closed chains is equal to the linking number of two chains in the identification space (ST, $T^2 \times I$, or T^3). It would be interesting to examine if the periodic linking number of infinite free chains is an integer topological invariant and how it may be related to the alternative definitions of linking number in manifolds.

6.5. Helicity in periodic domains

The Gauss linking number is related to the helicity of a fluid flow as follows [16]: Let $\vec{u}(\vec{x},t)$ be the velocity field in an inviscid incompressible fluid, and let $\vec{\omega}(\vec{x},t)=\nabla\times\vec{u}$ be the corresponding vorticity field, which is zero except in two closed vortex filaments of strengths (associated circulations) κ_1, κ_2, whose axes are C_1, C_2. Let S be any closed orientable surface, bounding a volume V, moving with the fluid on which $\vec{u}\cdot\vec{n}=0$. Then the *helicity* is

$$H=\int_V \vec{u}\cdot\vec{\omega}dV=2lk(C_1,C_2)\kappa_1\kappa_2. \tag{120}$$

For the simulation of turbulence periodic boundary conditions are applied and one needs to measure helicity in periodic domains [16,55]. For a system of two closed vortex filaments in PBC the helicity in a volume bounded by a surface on which $\vec{u}\cdot\vec{n}=0$, inside the identification space is related to the periodic linking number as follows [51]:

$$H=\int_V \vec{u}\cdot\vec{\omega}dV=2LK_P(C_1,C_2)\kappa_1\kappa_2. \tag{121}$$

In the case of vortices that form infinite free chains in [55] is shown that in general, the total helicity is not even definable, much less conserved. It was believed that expressions based on linking numbers fail when confronted with periodic field lines. So the question remained whether some new quantity, H_P, exists which extends helicity to a periodic domain. For two infinite vortex lines, C_1, C_2 of strength κ_1, κ_2, we propose to define the *periodic helicity* as:

$$H_P=2\kappa_1\kappa_2LK_P(C_1,C_2). \tag{122}$$

The periodic helicity reduces to the usual H for a field without periodic lines, since LK_P reduces to the Gauss linking number in the case of chains that do not touch the faces of the cell. It would be interesting to examine its relation with the asymptotic linking number [83].

7. Computation of the periodic linking number: the cell periodic linking number and the local periodic linking number

The estimation of the periodic linking number in the case of open or infinite chains is computationally difficult since it consists of infinite summations requiring us to use numerical methods and analyze the convergence of the infinite summation. In studies of polymer physics, the influence of chains in a neighborhood of another is of greater interest than the contribution of distant chains. Moreover, in turbulent flows, turbulent activity is concentrated at locations where the vortex lines are closer. Thus, we may be more interested in the flow lines that are in a neighborhood of a given flow line. In this section we propose two methods which are now going to focus on the contribution of entanglement arising by nearby chains. We propose the cell periodic linking number, which is a rather symmetric cut-off of the contributions around one chain, and the local periodic linking number, which is rather focused on the contributions of the chains in a neighborhood of one chain. We will propose approximations of the periodic linking number that have the following properties: (*i*) provide a good estimation of the periodic linking number in the case of open or infinite free chains and (*ii*) are equal to the periodic linking number in the case of closed chains.

7.1. The cell periodic linking number LK_C

The first method to approximate the periodic linking number is based on a symmetric cell containing the chain:

Definition 37 *(Chain cell).* Let I denote a free chain in the periodic system. We define the *Chain Cell*, $SC(I_u)$, to be the union of the minimum number of cells that are needed in order to create a larger cubic cell that contains an image of I, say I_u, and whose center cell contains the center of mass of I_u.

Definition 38 *(Cell periodic linking number).* Let $J_1, J_2, \ldots, J_m$ denote the images of J that intersect the chain cell of an image of I, say I_0. The *cell periodic linking number between I and J*, $LK_C(I,J)$, is defined as:

$$LK_C(I,J)=\sum_{1\le v\le m} L(I_u,J_v).'' \tag{123}$$

Properties of the cell periodic linking number, LK_C:

(i) LK_C is independent of the choice of the image I_u of the free chain I in the periodic system.
(ii) For closed chains the cell periodic linking number is equal to the (global) periodic linking number, that is, $LK_C(I,J)=LK_P(I,J)$. Thus LK_C is an integer topological invariant for closed chains.
(iii) LK_C captures all the linking that one free chain imposes on an image of the other and does not depend on the image of I used for its computation or on the minimal unfolding of the chain.

(iv) Two drawbacks of the cell periodic linking number are that in the case of open chains, LK_C depends on $SC(I_u)$ and it is not symmetric, i.e. $LK_C(I, J) \neq LK_C(J, I)$. However, we shall see that LK_C provides a good approximation of LK_P for open chains and thus, $LK_C(I, J) \approx LK_P(I, J) = LK_P(J, I) \approx LK_C(J, I)$, so $LK_C(I, J) \approx LK_C(J, I)$.

From observation (i) above, the definition of the cell periodic linking number is equivalent to using the parent image I_0 for the free chain I:

$$LK_C(I, J) = \sum_{1 \leq v \leq m} L(I_0, J_v) = \sum_{1 \leq v \leq m} L(I_0, J_0 + \vec{v}). \tag{124}$$

Remark 39. Similarly, we define the cell periodic self-linking number, the cell periodic linking with self-images and the cell periodic writhe.

The computation of LK_C can be done following the pseudocode described in Algorithm 3.

Algorithm 1: Computation of $mu(I_0)$.

```
mu(I_0) = {(0, 0, 0)} ***the first node of I_0 lies in the (0, 0, 0) cell***.
n_I = number of vertices in I_0
for i = 2 to n_I
  i⃗ = the position vector of the cell in which lies the vertex i
  if i⃗ ∉ mu(I_0) then
    append i⃗ to mu(I_0)
  endif
end
```

Algorithm 2: Computation of $SC(I_0)$.

```
m⃗ = the cell in which lies the center of mass of I_0
SC(I_0) = {m⃗}
d = 0
for i = 1 to |mu(I_0)|
  i⃗ = i-th vector in mu(I_0)
  d⃗ = i⃗ − c m⃗
  for j = 1 to 3
    if abs(d⃗(j)) > d *** where d⃗(j) = j-th coord. of d⃗***
      d = abs(d⃗(j))
    endif
  end
end
for x = m⃗(1) − d to m⃗(1) + d
  for y = m⃗(2) − d to m⃗(2) + d
    for z = m⃗(3) − d to m⃗(3) + d
      Append (x, y, z) to SC(I_0)
    end
  end
end
```

7.2. The local periodic linking number

Another approximation of the periodic linking number comes from focusing only on the local topological constraints seen in a cell. For this purpose in [57] we defined the following measure:

Definition 40 *(Local periodic linking number).* Let I and J denote two free chains in the periodic system. Let $J_1, J_2, \ldots, J_k$ denote the images of J that intersect the minimal unfolding of an image of I, say I_u. The *local periodic linking number*, LK, between two free chains I and J is defined as:

$$LK(I, J) = \sum_{1 \leq v \leq k} L(I_u, J_v). \tag{125}$$

Example 41. Consider the system shown in Fig. 4. Then for the computation of $LK(I, J)$ we need to consider the images of J which intersect the minimal unfolding of I_0: $LK(I, J) = L(I_0, J_0) + L(I_0, J_0 + l(1, 0)) + L(I_0, J_0 + l(1, 1)) + L(I_0, J_0 + l(0, 1))$.

Algorithm 3: Computation of $LK_C(I, J)$.

1. Find the minimal unfoldings of I_0, $mu(I_0)$, and J_0, $mu(J_0)$ (see Algorithm 1).
2. Find the chain cell of I_0, $SC(I_0)$ (see Algorithm 2).
3. Find the images of J which intersect the chain cell of I_0:
$Img = \{(0,0,0)\}$ *** J_0 always intersects $SC(I_0)$***
for $i = 1$ to $|SC(I_0)|$
  $\vec{i} = i$-th vector in $SC(I_0)$
  for $j = 1$ to $|mu(J_0)|$
    $\vec{j} =$ the j-th vector in $mu(J_0)$
    $\vec{v} = \vec{i} + \vec{j}$ *** $J_0 + \vec{v}$ intersects $SC(I_0)$ ***
    if $\vec{v} \notin Img$ then
      append $\vec{v}$ to Img
    endif
  end
end
4. Compute the cell periodic linking number:
$LK_C = 0$
$n_J =$ number of vertices in J_0
for $k = 1$ to $|Img|$
  $\vec{k} = k$-th vector in Img
  *** define $J_k = J_0 + \vec{k}$ ***
  for $j = 1$ to n_J
    $\vec{j}_0 = j$-th vertex of J_0
    $\vec{j}_k = \vec{j}_0 + \vec{k}$ *** this is the j-th vertex of J_k ***
  end
  Compute $L(I_0, J_k)$
  $LK_C = LK_C + L(I_0, J_k)$
end

The properties of LK were studied in [57]. We stress the following:

(i) LK is independent of the choice of the image I_u of the free chain I in the periodic system.
(ii) LK is symmetric, that is, $LK(I, J) = LK(J, I)$.
(iii) LK captures all the local topological constraints (TCs) that one free chain imposes on an image of the other and is independent of the image used for its computation.
(iv) A drawback of the local periodic linking number is that LK depends on the size of the cell both in the case of open and infinite and in the case of closed chains. However, for most physical systems the size of the cell is such that LK is a topological invariant for closed chains.

From observation (i) above, the definition of the local periodic linking number is equivalent to using the parent image I_0 for the free chain I:

$$LK(I, J) = \sum_{1 \le v \le k} L(I_0, J_v) = \sum_{1 \le v \le k} L(I_0, J_0 + \vec{v}). \tag{126}$$

The computation of LK for two free chains I and J can be done by following Algorithm 4.

Remark 42. Similarly, we define the local periodic self-linking number, the local periodic linking with self-images and the local periodic writhe

Remark 43. Notice that $LK_C(I, J)$ and $LK(I, J)$ differ on the images of J used for their computation (see Algorithms 3 and 4). The images of J are those which intersect the chain cell of I_0, denoted $SC(I_0)$, or the minimal unfolding of I_0, denoted $mu(I_0)$, respectively. Notice that $mu(I_0) \subseteq SC(I_0)$. Therefore, the images taken into consideration in $LK(I, J)$ are also in the sum of $LK_C(I, J)$, but $LK_C(I, J)$ takes into consideration more images of J. Both measures capture all the linking with images that may impose TCs to I_0. Moreover, for closed chains, LK_C is a topological invariant and $LK_C = LK_P$. On the other hand, one can imagine conformations for which LK is not a topological invariant even for closed chains and $LK \neq LK_P$, but, for the simulations of the physical systems under study it is expected that for closed chains LK is a topological invariant and it is equal to LK_P. Notice also that LK_C is not symmetric, while LK is symmetric both for open or closed chains. Comparing LK_C and LK with respect to computational cost, we notice that LK requires less computational effort. Recall that for two chains of n edges each, the computation of the Gauss linking number is of the order $O(n^2)$. Let k and m denote the number of pairs of chains (i.e. pairs I_0, J_v) used in the definition of $LK(I, J)$ and $LK_C(I, J)$ respectively. Then the computation of LK is of the order $O(kn^2)$ and that of LK_C of the order $O(mn^2)$. Notice that I_0 has length nb, where b is the bond length. Therefore its minimal unfolding (used for the computation of LK) may consist of up to $\lceil nb/l \rceil$ cells, where l is the length of an edge of the cubic simulation cell. This occurs when I_0 has a rod-like conformation. The chain cell (used for the computation of LK_C)

Algorithm 4: Computation of $LK(I, J)$.

1. Find the minimal unfoldings of I_0, $mu(I_0)$, and J_0, $mu(J_0)$ (see Algorithm 1).
2. Find the images of J which intersect the minimal unfolding of I_0:
$Img = \{(0,0,0)\}$ *** J_0 always intersects $mu(I_0)$ ***
for $i = 1$ to $|mu(I_0)|$
  $\vec{i} =$ the i-th vector in $mu(I_0)$
  for $j = 1$, to $|mu(J_0)|$
    $\vec{j} =$ the j-th vector in $mu(J_0)$
    $\vec{v} = \vec{i} + \vec{j}$ *** $J_0 + \vec{v}$ intersects $mu(I_0)$ ***
    if $\vec{v} \notin Img$ then
      append $\vec{v}$ to Img
    endif
  end
end
4. Finally, compute the local periodic linking number:
$LK = 0$
$n_J =$number of vertices in J_0
for $k = 1$ to $|Img|$
  $\vec{k} = k$-th vector in Img
  *** define $J_k = J_0 + \vec{k}$ ***
  for $j = 1$ to n_J
    $\vec{j}_0 =$the j-th vertex of J_0
    $\vec{j}_k = \vec{j}_0 + \vec{k}$ ***this is the j-th coordinate of J_k***
  end
  Compute $L(I_0, J_k)$
  $LK = LK + L(I_0, J_k)$
end

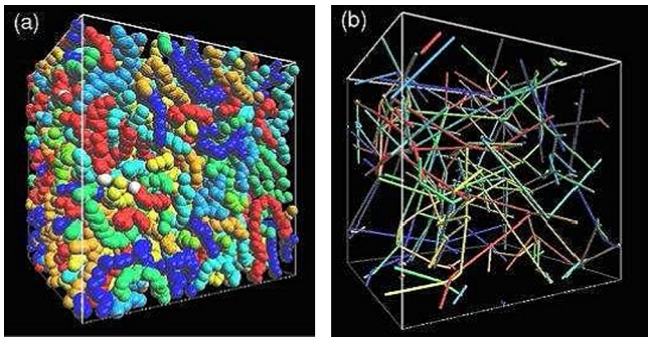

Fig. 13. (a) Representative atomistic PE sample and (b) the corresponding reduced network.

consists of at most $\lceil (nb/2)^2/l \rceil$ cells (again when I_0 has a rod-like conformation). The same holds for J_0. Therefore, there are at most $\lceil nb/l \rceil$ images of J_0 intersecting each cell of the minimal unfolding or the chain cell of I_0. Thus, $k \leq \lceil (nb)^2/l^2 \rceil$ and $m \leq \lceil (nb)^3/4l^2 \rceil$. So, in the worst case, the computation of LK, resp. LK_C, is of the order $O(n^4)$, resp. $O(n^5)$. The density of a system of two generating chains of $n+1$ vertices each is $\rho = \frac{(2n+2)b}{l^3}$. It follows, that the computation of LK, resp. LK_C, scales in a way that depends on the density and the length of the chains as: $O(\rho^{2/3} n^3 n^{1/3})$, resp. $O(\rho^{2/3} n^4 n^{1/3})$, in the worst case. We notice that, since the Gauss linking number of two edges is bounded above by 1/2, then the Gauss linking number of two images is bounded above by $n^2/2$. This indicates that some very rough upper bounds of LK and LK_C in the worst case are $LK \leq \lceil n^4 b^2/l^2 \rceil/2$ and $LK_C \leq \lceil n^5 b^3/4l^2 \rceil/2$. We could get an average upper bound as $\langle |LK| \rangle \leq \lceil (nb)^2/l^2 \rceil \langle |L| \rangle$ and $\langle |LK_C| \rangle \leq \lceil (nb)^3/4l^2 \rceil \langle |L| \rangle$. This suggests that $\langle |LK_C| \rangle - \langle |LK| \rangle \leq \left(\lceil (nb)^3/4l^2 \rceil - \lceil (nb)^2/l^2 \rceil \right) \langle |L| \rangle \approx (nb/4 - 1) \lceil (nb)^2/l^2 \rceil \langle |L| \rangle$. However, these are very rough upper bounds for $\langle |LK| \rangle$, $\langle |LK_C| \rangle$ and $\langle |LK_C| \rangle - \langle |LK| \rangle$, and in order to obtain meaningful upper bounds or even approximations, further study is needed.

8. Application to polymers

In this section we apply the cell and the local periodic linking number to samples of polyethylene (PE) frames. First, we examine how the local periodic linking number captures the entanglement complexity in a polymer melts and use it to estimate the effect of the CReTA (Contour Reduction Topological Analysis) [8] algorithm to the linking of the chains.

Next, we compare the cell periodic linking number and the local periodic linking number to the (global) periodic linking number for the same systems. The data analyzed concerns 80 PE frames [8] of density $\rho \approx 0.77 - 0.78$ g/cm^3. Each frame is generated by 8 PE chains of 1000 beads each, so finally our results on LK are based on 2240 distinct pairs of PE chains.

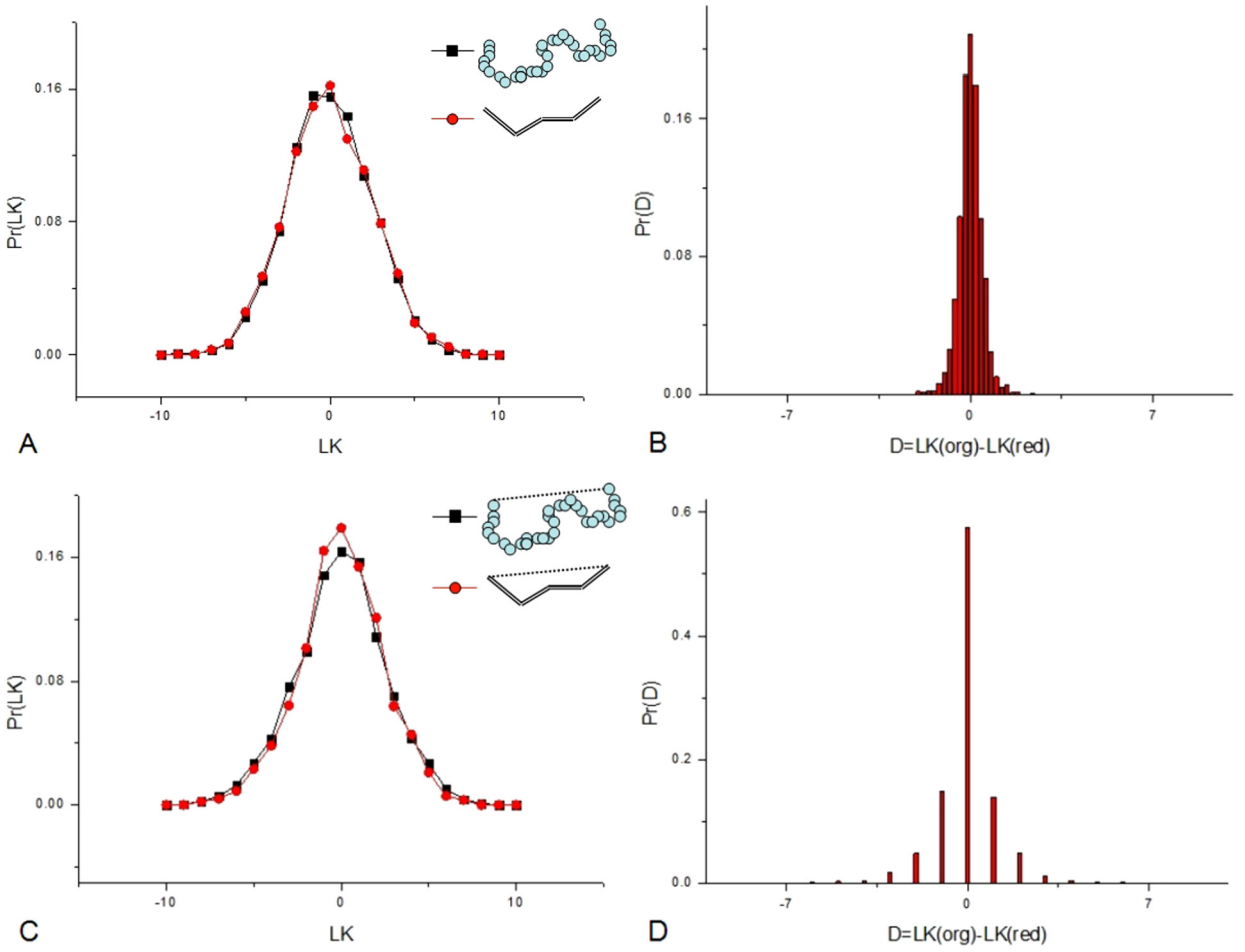

Fig. 14. Figure A shows the normalized probability distribution of *LK* for the original and the corresponding reduced chains in a PE-1000 melt and Figure B the probability distribution of the corresponding differences. Figure C shows the normalized probability distribution of *LK* for the original and reduced chains after end-to-end closure and Figure D shows the corresponding differences.

8.1. The CReTA algorithm and the local periodic linking number

To study the entanglement complexity present in a given polymer system, one has to coarse grain the polymer chains at a level where certain geometrical characteristics relevant to entanglement become evident. The CReTA (Contour Reduction Topological Analysis) [8] algorithm fixes chain ends in space, and while prohibiting chain crossing, it minimizes (shrinks) simultaneously the contour lengths of all chains, until they become sets of rectilinear strands coming together at the nodal points (TCs) of a network of primitive paths. When there are no possible alignments left, then shrink the diameter of the beads of each chain and continue the same process, until a minimum thickness is achieved and no alignment moves are possible. Fig. 13 shows an atomistic polymer sample and the corresponding reduced network.

The CReTA algorithm has been shown [8,84] to give a meaningful representation of the underlying topology of a polymer melt by comparing it to experimental data. In [57], by using the local periodic linking number *LK*, we examined the extent to which the CReTA method preserves that linking measure of entanglement in PE melts, or if critical entanglement information is lost in the reduction process. To do this, we computed the normalized probability distribution of *LK* for pairs of PE chains in a frame and compared it to the *LK* for the corresponding reduced pairs. Fig. 14(A) shows the probability distribution of the pairwise local periodic linking numbers for the original and CReTA reduced PE chains. The two distributions are quite similar and normal centered, as expected for random coils. The mean absolute value of *LK* is 1.97 and the mean absolute value of *LK* of pairs of reduced chains is 2.01. These findings suggest that the TCs present in the system do not only have a local character but the system is non-trivially linked. Moreover, we observe that the maximum value of *LK* is approximately 10, suggesting the presence of pairs with significant linking. Fig. 14(B) shows the probability distribution of the difference of *LK* before and after the application of the CReTA algorithm, i.e. $D = LK_{original} - LK_{reduced}$. We note that the distribution is quite narrow (with standard deviation 0.30), has mean -0.19, and mean absolute difference (i.e. $< |D| >$) of the local periodic linking between original and reduced chains of 0.29, indicating that *LK* is about the same for original and reduced

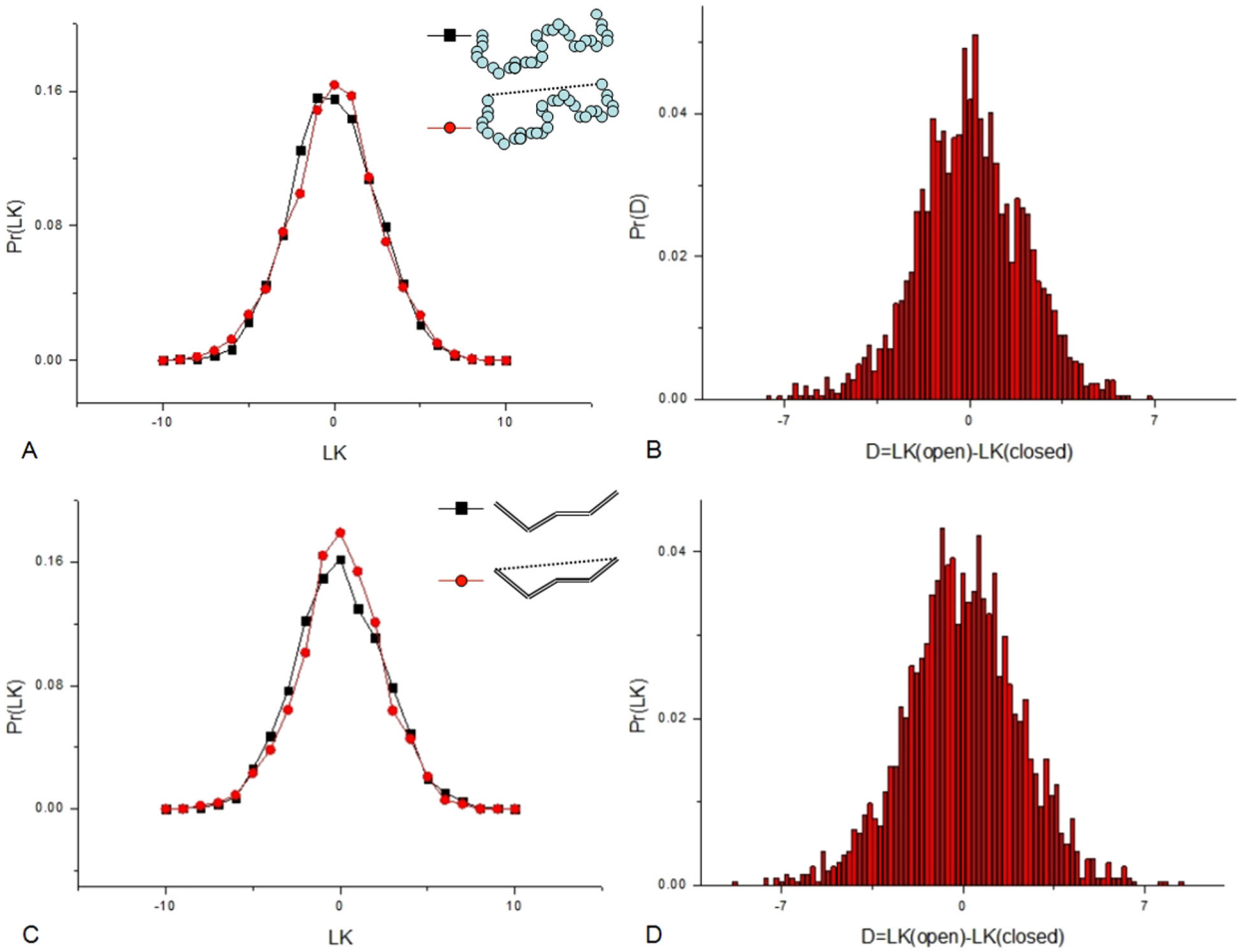

Fig. 15. Figure A shows the normalized probability distribution of *LK* for the original chains before and after end-to-end closure and Figure B the probability distribution of the corresponding differences. Figure C shows the normalized probability distribution of *LK* for the reduced chains before and after end-to-end closure and Figure D shows the corresponding differences.

pairs of chains. Thus, at least with respect to the local linking, one can study the entanglement of a PE melt in its reduced representation after the application of the CReTA algorithm.

Since a popular method to study the entanglement of linear polymers is to perform direct end-to-end closure [33,85,86] of the chains and study them topologically, by using *LK* we have tested whether the method of direct end-to-end closure is reliable and if *LK* can detect topological differences between the open and closed original and reduced systems. In [57] we showed that the method of end-to-end closure retains much but not all the topological information from the original in the reduced systems, by computing the local periodic linking number *LK* after performing end-to-end closure to the original chains and comparing it to the *LK* after performing end-to-end closure to the corresponding reduced chains. Fig. 14(C) shows the normalized *LK* for the end-to-end closures of the original and the corresponding reduced chains. We notice a smaller overlap of the two distributions. The mean absolute value of *LK* for the original closed chains is 2.01 and the mean absolute value of *LK* for the reduced closed chains is 1.86. Fig. 14(D) shows the normalized probability distribution of the difference $D = LK_{OrgClosed} - LK_{RedClosed}$. We can see that the distribution is a bit broader having standard deviation 0.92 in comparison with the open data. The mean absolute difference is 0.57. We could expect *LK* to be invariant for closed chains in most cases. The end-to-end closure is performed, in this case, before and after the application of the CReTA algorithm. Thus the observed differences between the original and reduced chains are most likely due to movements during the reduction algorithm in which a chain crossed the path of the end-to-end closure.

Next we compute the difference between the *LK* for open and closed original chains and the difference between the *LK* for open and closed reduced chains. Figs. 15(A) and 15(C) show the normalized *LK* for the original open and the corresponding original closed chains and the normalized *LK* for the reduced open and the corresponding reduced closed chains respectively. In both cases, we notice an even smaller overlap between the two distributions. In Figs. 15(B) and 15(D) we show the normalized probability distribution of the difference $LK_{OrgOpen} - LK_{OrgClosed}$ and of the difference $LK_{RedOpen} - LK_{RedClosed}$ respectively. We can see that the distributions are broader, with standard deviations 2.00 and 1.91,

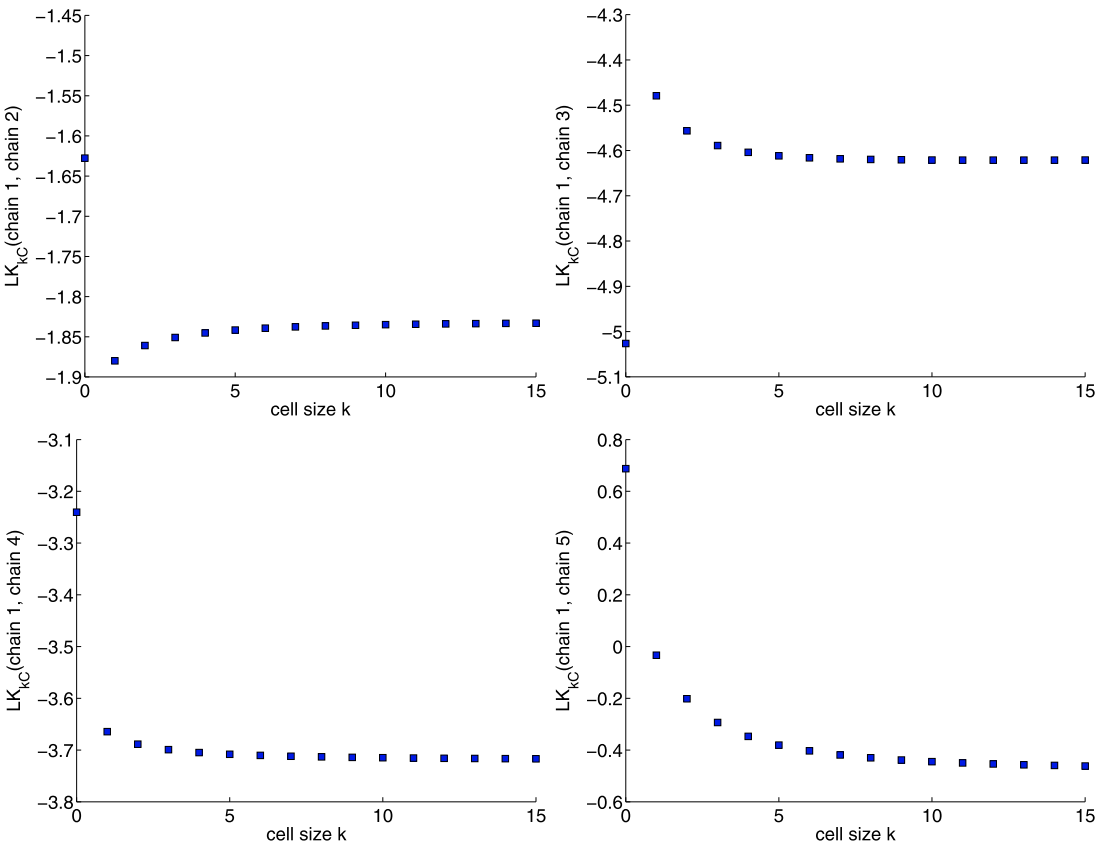

Fig. 16. Approximations of the periodic linking number of chain 1 with chains 2, 3, 4 and 5 in a PE frame. The point at $k = 0$ corresponds to the local periodic linking number. The point at $k = 1$, corresponds to the cell periodic linking number and for $k \geq 2$, $LK_{kC}(I, J)$, is computed by increasing the chain cell of I_0 by one in each direction at every iteration. Thus, as k increases, LK_{kC} becomes a better approximation of LK_P.

respectively. The mean absolute difference is 1.57 and 1.52 respectively. This shows that the local periodic linking number retains similar but distinct information for open and closed chains.

8.2. Comparison of the local and cell periodic linking number to the (global) periodic linking number

In this section we compare the local and cell periodic linking number to the global periodic linking number. To do this, for each PE frame we compute LK_C for an increasing size of chain cell. Let LK_{kC} denote the cell periodic linking number for a chain cell increased by k cells in each direction to form a larger cell. Notice that as k increases, more and more images are taken into consideration in the computation of LK_{kC} symmetrically around the central cell, and, thus, LK_{kC} tends to LK_P. In order to reduce computational cost, we use the reduced frames which approximate the polymer configurations. Our results indicate that $LK_{kC} \approx LK_C$, $\forall k$. Fig. 16(a)–(d) shows the linking of a chain with other chains in a melt. For cell size 0, the data points correspond to the local periodic linking number of I with J, $LK(I, J)$. For cell size 1 the data points correspond to the cell periodic linking number of I with J, $LK_C(I, J)$. For cell size greater than one the data points show $LK_{kC}(I, J)$, $k = 2, \ldots, 15$.

We observe that for all pairs of chains, LK_{kC} converges to a limiting value, as expected that LK_{kC} tends to LK_P. Also we notice that almost for all pairs of chains, LK_C is within an error of 0.1 from the limiting value. This suggests that LK_C is a good approximation of LK_P. So, we expect that $LK_C(I, J) \approx LK_C(J, I)$, since $LK_C(I, J) \approx LK_P(I, J) = LK_P(J, I) \approx LK_C(J, I)$. Moreover, since $LK_C \approx LK_P$, we expect that the dependence of LK_C on $SC(I)$ in the case of open chains is weak.

Our numerical results indicate that the number of images used for the computation of LK, k, are related to the number of images used for the computation of LK_C, m, by $\langle m \rangle \approx 10\langle k \rangle$, in accordance with the predictions in Remark 43 for $n = 1000$, $b = 1$, $l = 62.35$. We find $\langle |LK_C| \rangle - \langle |LK| \rangle = -0.0072$. Therefore, on extracting average information from the melt, both measures give similar averages. A more informative quantity however, is the mean absolute difference between the two measures, which is equal to $\langle |LK_C - LK| \rangle = 0.4020$ for this system. This suggests that there exist some pairs of chains for which the values can differ significantly. Indeed, we observe that $\langle |LK_C(I, J)| - 1 \leq |LK(I, J)| \leq |LK_C(I, J)| + 1$. This indicates that the local entanglement is similar, but different than the global entanglement.

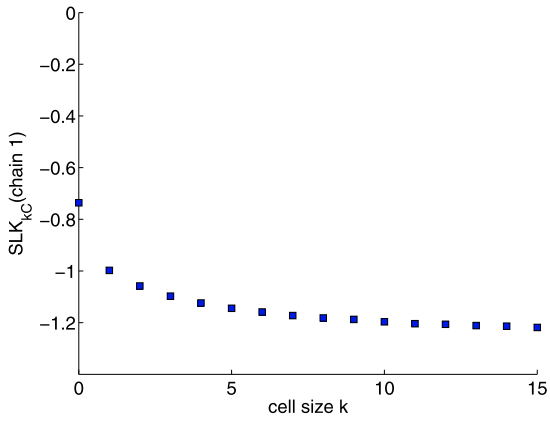

Fig. 17. Approximations of the periodic linking number with self-images of chain 1 in a PE frame. The point at $k = 0$ corresponds to the local periodic linking number with self-images. The point at $k = 1$, corresponds to the cell periodic linking number with self-images and for $k \geq 2$, $SLK_{kC}(I, J)$, is computed by increasing the chain cell of I_0 by one in each direction at every iteration. Thus, as k increases, SLK_{kC} becomes a better approximation of SLK_P.

By computing LK and LK_C after performing end-to-end closure of the chains, the numerical results show that the two measures coincide (results not shown here). By definition, we know that for closed chains $LK_P = LK_C$, but it is possible that $LK \neq LK_P$. Thus, our results suggest that, for closed chains, for most practical purposes, one may consider that $LK = LK_C = LK_P$.

Fig. 17 shows the cell periodic linking number with self-images of I, for increasing cell size, $SLK_{kC}(I)$. Again, the data point at cell size 0 is the local periodic linking number with self-images, $SLK(I)$. The data point at cell size 1 is the cell periodic linking number with self-images, $SLK_C(I)$ and the data points at larger cell size are $SLK_{kC}(I), k = 3, \ldots, 15$. The data are very similar to that of the periodic linking number of I and J. We observe that $SLK_{kC}(I)$ converges to a limiting value and, as expected that $SLK_{kC}(I)$ tends to $SLK_P(I)$. We notice that $|SLK_C(I)| \approx |SLK_{16C}(I)| - 0.2$ and $|SLK(I)| = |SLK_C(I)| - 0.3$. Thus, SLK_C is a good approximation of SLK_P and SLK captures similar but different information than SLK_C.

9. Conclusions

Systems employing PBC are often used in applications. Due to the PBC, measuring the entanglement in these systems is more complicated. In this study we defined the periodic linking number, LK_P, and the periodic self-linking number, SL_P, as measures of entanglement of chains in a system employing PBC and we studied their properties. Systems employing one, two or three PBC are related to 3-manifolds, ST, $T^2 \times I$ and T^3, respectively. In the case of closed chains, LK_P is an integer topological invariant which is equal to the intersection number of two closed chains in ST, $T^2 \times I$ or T^3, respectively (Proposition 44). Also, it can be computed using only one simulation cell (Proposition 8). In the case of open or infinite chains (the latter correspond to homologically non-trivial chains in ST, $T^2 \times I$ or T^3, respectively), LK_P is an infinite summation which we proved converges (Theorems 18, 24, 33). For open and infinite chains LK_P is a real number that is a uniformly continuous function almost everywhere of the chains coordinates.

For the purpose of applications to polymers, where the short range interactions may be more relevant, we defined two approximations of the periodic linking number, the cell periodic linking number, LK_C, and the local periodic linking number, LK, and we applied them to PE melt samples. The numerical results suggest that LK and LK_C capture similar entanglement information, but LK_C provides a better approximation of LK_P than LK.

Acknowledgements

The author wishes to express her sincere thanks to Professor K. Millett and to Professor S. Lambropoulou for their close guidance and supervision of this research, as well as for the motivation of new ideas, and for very useful and detailed discussions, which contributed fundamentally to the realization of these results. The author wishes to express her sincere thanks to Professor D.N. Theodorou and Dr. C. Tzoumanekas who motivated this research with their work and helped with fruitful discussions.

This research has been co-financed by the European Union (European Social Fund – ESF) and Greek National Funds through the Operational Program “Education and Lifelong Learning” of the National Strategic Reference Framework (NSRF) – Research Funding Program: THALES: Reinforcement of the interdisciplinary and/or inter-institutional research and innovation.

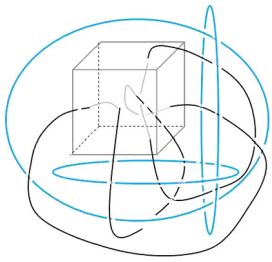

Fig. 18. In the case of 3 PBC, there are three auxiliary curves that represent the Borromean rings. Surgery along the Borromean rings gives T^3.

Appendix A. Identification spaces

We notice that a generating cell with one, two, or three PBC defines an *identification space* that is created by identifying the opposite faces of the cell with respect to the PBC. This space is the solid torus, $ST = S^1 \times D$, in the case of one PBC, the thickened torus, $T^2 \times I = S^1 \times S^1 \times I$, in the case of two PBC, or the three torus, $T^3 = S^1 \times S^1 \times S^1$, in the case of three PBC respectively. Upon identification of the cell with respect to the PBC all the arcs of a generating chain, say i, get connected to form a closed or open knotted curve in the identification space, ST, $T^2 \times I$ or T^3, in case of one, two or three PBC respectively, which we shall call *identification chain* and shall be denoted as $\bar{I}$.

The identification of two opposite faces can be realized via a simple arc that does not intersect the cell joining the middle points of the opposite faces. This arc shall be called *generic closing arc*. Giving natural orientations, front–back, right–left and top–bottom to the faces of the cell, it induces a natural orientation on the generic closing arcs. For each generating chain, say i, in the cell, we define a *closing arc*, as an oriented arc that connects a pair of corresponding endpoints of i on opposite faces of the cell, such that it does not intersect the cell, it is parallel to the corresponding generic closing arc and such that it inherits the orientation of the arcs of i that it connects. Then, the arcs that compose the generating chain i together with all closing arcs get connected to form one curve in $\mathbb{R}^3$ that we shall call *realized chain*, and shall be denoted as $\bar{i}$ (see Fig. 18).

Note that the realized chain $\bar{i}$ is not sufficient to unambiguously represent, in $\mathbb{R}^3$, the identification chain $\bar{I}$ in the identification space. In order to do this we use auxiliary curves to represent the identification space, following the method of [87], see also [56]. Namely, by contracting the cell to a point, an oriented generic closing arc with that point bounds a disc. A simple closed curve piercing that disc at the center once with positive orientation shall be called an *auxiliary curve*. In this manner, we define the auxiliary curves α_1, α_2, α_3 for the three pairs of opposite faces. In the case of two PBC, there are only two auxiliary curves, which form the Hopf link, and in the case of three PBC, the three auxiliary curves form the Borromean rings [79]. Let L denote the link in $\mathbb{R}^3$ that is formed by the auxiliary curves, that is, $L = \alpha_1$ or $\alpha_1 \cup \alpha_2$ or $\alpha_1 \cup \alpha_2 \cup \alpha_3$. Then we can unambiguously represent the identification chain $\bar{I}$ by the *mixed realized link* $\bar{i} \cup L$ in $\mathbb{R}^3$ (see Fig. 18).

Appendix B. Linking numbers from the cell

As we discussed in the introduction, the periodic system consists in an infinite number of chains. So, measuring the linking number of all the pairs of chains in the system requires an infinite calculation. However, infinitely many pairs of chains are in the same relative position, thus their linking is the same. We would like to compute the linking number of all the different pairs of chains. On the other hand we know that the periodic system is generated by one cell, containing only a finite number of generating chains. These give rise to a finite number of identification chains in the identification space, to a finite number of realized chains in $\mathbb{R}^3$ and to a finite number of free chains in the periodic system. We would like to extend the Gauss linking number to chains in PBC and retain its main properties. Namely, that it is symmetric, that, when the generating chains in the cell form closed chains in the periodic system, it is a topological invariant and that, when the generating chains in the cell form open chains in the periodic system it is a continuous function of the chains coordinates. Let us examine the different definitions of linking number that occur for these different types of chains. These give a number of alternatives that will lead to the appropriate definition of linking in PBC. Namely:

Linking between two generating chains, $L(i, j)$. Ideally, one would like to measure the linking in the system directly from the cell. Indeed, let i, j be two generating chains in the cell. These may not form a link, since each one may consist of many disconnected arcs. Let $i_1, \ldots, i_k$ denote the arcs that compose the generating chain i, and let $j_1, \ldots, j_l$ denote the arcs that compose the generating chain j. Then one can compute the linking integral over i and j by summing up the linking numbers of each pair of arcs. That is, we define the *generating linking number* as $L(i, j) = \sum_{m=1}^{k} \sum_{n=1}^{l} L(i_m, j_n)$. We notice that this is finite, but it may not be a topological invariant even if the generating chains were closed (see Fig. 19 for an illustrative example). Moreover, this measure of entanglement would not capture the global entanglement between any two complete unfoldings of the two generating chains in the periodic system.

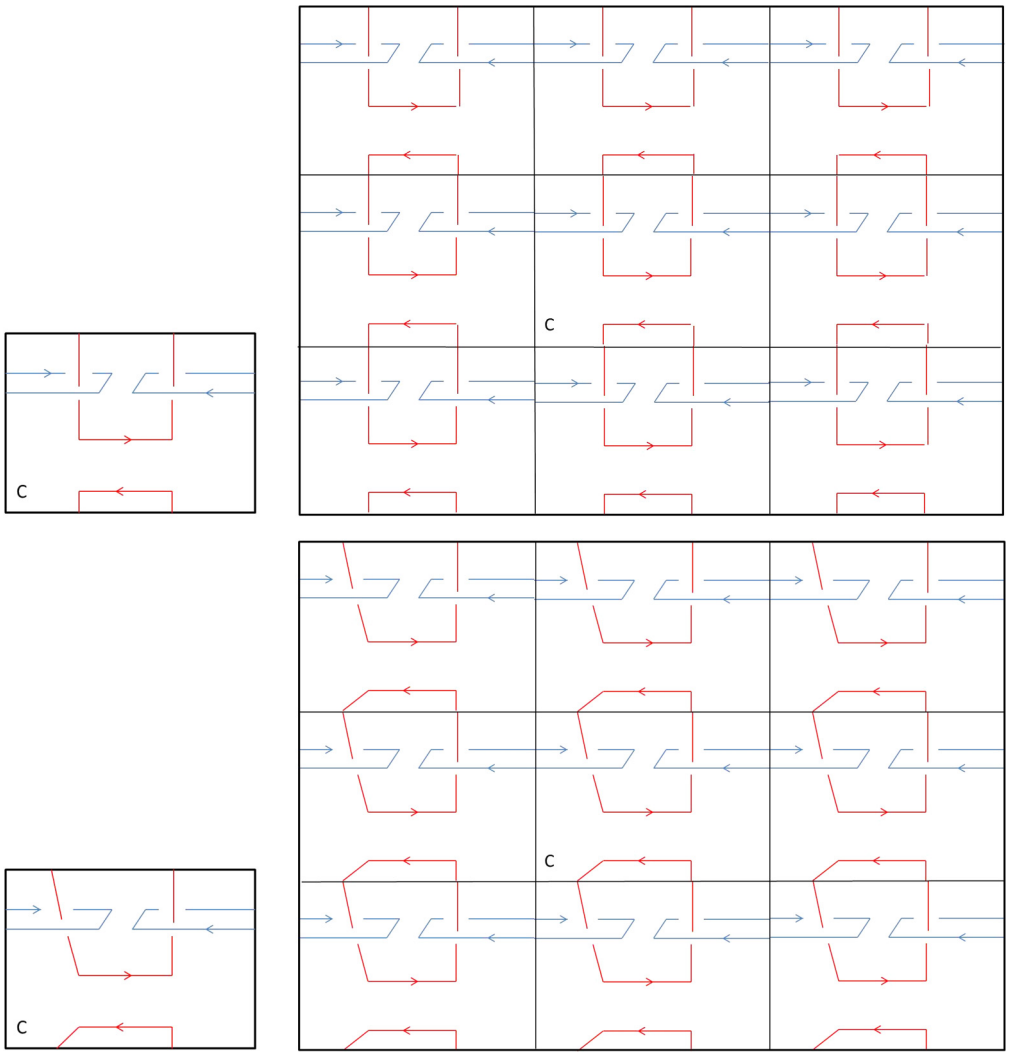

Fig. 19. Example of two cells which generate topologically equivalent closed chains in the periodic system. Above is shown a cell with generating chains i and j formed by the arcs: $e_{i,1} = \{(0.3, 0.5, 0.4), (0.3, 0.5, 1)\}$, $e_{i,2} = \{(0.3, 0.5, 0), (0.3, 0.5, 0.2), (0.9, 0.5, 0.2), (0.9, 0.5, 0)\}$, $e_{i,3} = \{(0.9, 0.5, 1), (0.9, 0.5, 0.4), (0.3, 0.5, 0.4)\}$ and $e_{j,1} = \{(0.7, 0.3, 0.5), (1, 0.3, 0.5)\}$, $e_{j,2} = \{(0, 0.3, 0.5), (0.5, 0.3, 0.5), (0.5, 0.8, 0.5), (0, 0.8, 0.5)\}$, $e_{j,3} = \{(1, 0.8, 0.5), (0.7, 0.8, 0.5), (0.7, 0.3, 0.5)\}$, respectively. Then, $L(i, j) = 0.0932$. Below is shown a topologically equivalent system, where j is replaced by j' formed by the arcs: $e_{j',1} = \{(0.7, 0.3, 0.5), (1, 0.1, 0.5)\}$, $e_{j',2} = \{(0, 0.1, 0.5), (0.5, 0.3, 0.5), (0.5, 0.8, 0.5), (0, 0.8, 0.5)\}$ and $e_{j',3} = \{(1, 0.8, 0.5), (0.7, 0.8, 0.5), (0.7, 0.3, 0.5)\}$. Then, $L(i, j') = 0.0759 \neq L(i, j)$, indicating that the linking number between two closed generating chains is not a topological invariant.

Linking between two realized chains, $L(\bar{i}, \bar{j})$. Two realized chains, $\bar{i}$, $\bar{j}$, form a 2-component link in $\mathbb{R}^3$ for which we can compute their usual linking number, $L(\bar{i}, \bar{j})$, that we call *realized linking number*. This is a topological invariant for closed and infinite generating chains. However, we notice that for infinite generating chains the corresponding realized chains are intrinsically linked with the auxiliary curves that represent the identification space, so we need to take into consideration also the linking of $\bar{i}$, $\bar{j}$ with the auxiliary link that represents the identification space [87,76,77]. This is not going to be pursued here. In the case of open generating chains $L(\bar{i}, \bar{j})$ is not even well-defined since the Gauss linking integral of open chains depends strongly on the geometry of the chains. Thus, $L(\bar{i}, \bar{j})$ will attribute different values for different choices of closing arcs, even if the generating chains are fixed.

Linking between two identification chains, $int(\sigma, J)$. Two identification chains, $\bar{I}$, $\bar{J}$, form a 2-component link in the identification space. Then we can define their linking number, called *identification linking number*, as $int(\sigma, \bar{J})$, where σ denotes a homological surface (a 2-chain) whose boundary is $\bar{I}$, and "*int*" denotes the intersection number between $\bar{J}$ and σ. This is meaningful and well-defined only in the case of closed generating chains. In the case of open chains it is not possible to define a 2-chain with boundary an open identification chain. In the case of infinite generating chains a more complex definition of intersection number, relative to the identification space, can be used in order to measure their linking.

Notice that all the linking numbers defined above are clearly symmetric and finite, but they fail to retain main properties of the Gauss linking number.

Appendix C. Connecting LK_P with the linking number in identification spaces

In this section we relate the periodic linking number of two closed free chains to the linking numbers of related configurations. We will show that the periodic linking number of two closed free chains coincides with the linking number of two closed chains that lie in another manifold than $\mathbb{R}^3$.

There is a correspondence between the periodic system and the identification space via a covering map. Let M denote the identification space (ST, $T^2 \times I$ or T^3). Then $\mathbb{R}^3$ is the universal cover of M, so, there is a local homeomorphism $p : \mathbb{R}^3 \to M$ such that $p(I_u) = \bar{I}$ and $p(J_v) = \bar{J}$ for all images I_u of I and all images J_v of J. Then there exist induced homomorphisms $p_1^* : H_1(\mathbb{R}^3) \to H_1(M)$ and $p_2^* : H_2(\mathbb{R}^3) \to H_2(M)$. Thus, homologically trivial elements in $\mathbb{R}^3$ are mapped to homologically trivial elements in M.

We notice that, if the free chains I, J in $\mathbb{R}^3$ are closed, their images can be viewed as 1-cycles which represent trivial elements in $H_1(\mathbb{R}^3)$. Thus $\bar{I}$, $\bar{J}$ represent also trivial elements in $H_1(M)$, so there exist 2-chains $\sigma_{\bar{I}}$, $\sigma_{\bar{J}}$ in T^3 for which $\partial\sigma_{\bar{I}} = \bar{I}$ and $\partial\sigma_{\bar{J}} = \bar{J}$.

For two 1-cycles in an oriented 3-manifold, we can define their intersection number as the algebraic sum of intersections between the one 1-cycle and the 2-chain in the 3-manifold that is bounded by the other [88]. This number is equal to the linking number between the two cycles seen as curves in $\mathbb{R}^3$ [88].

For our case of closed free chains, the following holds:

Proposition 44. *Let I, J denote two closed free chains in a system with PBC. Then*

$$LK_P(I, J) = int(\sigma, \bar{J}) = L(\bar{i}, \bar{j}), \tag{C.1}$$

where σ denotes the 2-chain in T^3 with boundary $\bar{I}$ and int denotes the intersection number of a 2-chain with a 1-cycle.

Proof. Let Σ denote the 2-*chain* in $\mathbb{R}^3$ whose boundary is I_0. Then $\partial\sigma = \bar{I} = p(I_0) = p(\partial\Sigma) = \partial p(\Sigma)$. Thus $p(\Sigma)$ is homologous to σ, and by definition of the intersection number we know that $int(\sigma, \bar{J}) = int(p(\Sigma), \bar{J})$. Thus each intersection point of $\bar{J}$ with σ lifts to exactly one point in Σ and one point on an image of J. So $LK_P(I, J) = \sum_v L(I, J_v) = \sum_v int(\Sigma, J_v) = int(\sigma, \bar{J})$.

Since both $\bar{I}$, $\bar{J}$ represent trivial elements in $H_1(M)$, then $int(\bar{J}, \sigma_{\bar{I}}) = L(\bar{i}, \bar{j})$. □

Using the same method as in the proof of Proposition 8 we can provide a combinatorial proof of Proposition 44 for systems employing one or two PBC. First we will need the following Lemma:

Lemma 45. *A generating chain i is closed if and only if there is an even number of intersection points on each face, and half of them are starting points of arcs in the cell and half are endpoints of arcs in the cell.*

Proof. Let us project the periodic system on the xy-plane. Then with probability one the projection of I_0 is a collection of simple closed curves, say b_i, in the xy-plane which share one or more common points (the self-intersections of the projection of I_0). By Jordan's theorem, each one of these curves divides the xy-plane into an interior and exterior region. The projections of the x- and y-faces of the cells of the periodic system are lines, say ϵ_x, ϵ_y, parallel to the x- and y-axis. If a line coming from the exterior region, intersects a curve and enters the interior region, then it must cross it again in order to return to the exterior region. Thus a line may intersect a curve b_i an even number of times, half towards the interior of the region that b_i bounds, and the other half towards the exterior. For a line ϵ_x (resp. ϵ_y) parallel to the x-axis (resp. y-axis), each intersection corresponds to an intersection of an arc of I_0 with the x-face (resp. y-face) of the cell in which it lies in the periodic system. Then the translation of this arc of I_0 in the generating cell intersects the x-face (resp. y-face) of the generating cell. In order to see the result for the z-faces, we follow the same thinking by projecting the periodic system towards the zy-plane. □

Alternative proof of Proposition 43 for one and two PBC. Let us project the realized chains to the xy-plane. We can transform the x- and y-closing arcs so that when projected towards $\vec{k}$, they do not intersect the projection of the cell. Then,

$$L(\bar{i}, \bar{j}) = \frac{1}{2} \sum_{c \in cr(\bar{i}, \bar{j})} sign(c) = \frac{1}{2} \Big(\sum_{c \in cr(i,j)} sign(c) + \sum_{\substack{c \in cr(\text{closure arcs } i, \\ \text{closure arcs } j)}} sign(c) \Big), \tag{C.2}$$

where cr is defined as in the proof of Proposition 8. Let us focus on the second term. By the definition of closing arcs follows that to this term contribute only the crossings between the x-closing arcs of $\bar{i}$ (or $\bar{j}$) and y-closing arcs of $\bar{j}$ (or $\bar{i}$). Also, by the definition of closing arcs follows that the projection of each x-closing arc of $\bar{i}$ (or $\bar{j}$) intersects the projection of

every y-closing arc of $\bar{j}$ (or $\bar{i}$) exactly once and either the projection of all the x-closing arcs are "over" the projection of the y-closing arcs or they are all "under". By Lemma 45 for each x-closing arc of $\bar{i}$ there exists another x-closing arc of $\bar{i}$ with the opposite orientation. Since they both intersect a y-closing arc of $\bar{j}$ (if there is one), and they are both over or under it, the algebraic sum of these crossings is zero. Thus

$$L(\bar{i},\bar{j}) = \frac{1}{2}\sum_{c\in cr(i,j)} sign(c) = \Big(L(i,j)\Big)_{xy}. \tag{C.3}$$

By Proposition 8 follows that $LK_P(I,J) = \Big(L(i,j)\Big)_{xy} = L(\bar{i},\bar{j})$. □

By Proposition 44 and Corollary 10 we have the following connection of SL_P to the self-linking number in identification spaces:

Corollary 46. *Let I denote a closed free chain in PBC and $\bar{i}$ the corresponding realized chain, then $SL_P(I) = Sl(\bar{i})$.*

Proof. Let $\bar{i}$ and $\bar{i}_\epsilon$ denote the realized chains of the free chains I and I_ϵ respectively. Then by definition of I_ϵ, the arcs of $\bar{i}_\epsilon$ inside the cell are the normal push-offs of $\bar{i}_\epsilon$. We can choose the closure arcs of $\bar{i}_\epsilon$ so that they are also the normal pusf-offs of the closure arcs of $\bar{i}$. Thus $\bar{i}_\epsilon$ is also the variation free curve of $\bar{i}$. We have that

$$SL_P(I) = LK_P(I,I_\epsilon) = L(\bar{i},\bar{i_\epsilon}) = Sl(\bar{i}). \qquad \square \tag{C.4}$$

References

[1] M. Doi, S.F. Edwards, The Theory of Polymer Dynamics, Clarendon Press, Oxford, 1986.
[2] L.J. Fetters, D.J. Lohse, D. Richter, T.A. Witten, A. Zirkel, Connection between polymer molecular weight, density, chain dimensions, and melt viscoelastic properties, Macromolecules 27 (1994) 4639.
[3] L.J. Fetters, D.J. Lohse, S.T. Milner, W.W. Graessly, Packing length influence in linear polymer melts on the entanglement, critical, and reptation molecular weights, Macromolecules 32 (1999) 6847.
[4] M. Kröger, S. Hess, Rheological evidence for a dynamical crossover in polymer melts via nonequilibrium molecular dynamics, Phys. Rev. Lett. 85 (2000) 1128–1131.
[5] R. Everaers, S.K. Sukumaran, G.S. Grest, C. Svaneborg, A. Sivasubramanian, K. Kremer, Rheology and microscopic topology of entangled polymeric liquids, Science 303 (2004) 823.
[6] M. Kröger, Shortest multiple disconnected path for the analysis of entanglements in two- and three-dimensional polymeric systems, Comput. Phys. Commun. 168 (2005) 209–232.
[7] S. Shanbhag, M. Kröger, Primitive path networks generated by annealing and geometrical methods: insights into differences, Macromolecules 40 (2007) 2897.
[8] C. Tzoumanekas, D.N. Theodorou, Topological analysis of linear polymer melts: a statistical approach, Macromolecules 39 (2006) 4592–4604.
[9] M. Kröger, J. Ramirez, H.C. Öttinger, Projection from an atomistic chain contour to its primitive path, Polymer 43 (2002) 477–487.
[10] P.S. Stephanou, C. Baig, G. Tsolou, V.G. Mavrantzas, M. Kröger, Quantifying chain reptation in entangled polymer melts, J. Chem. Phys. 132 (2010) 124904.
[11] M. Kröger, H. Voigt, On a quantity describing the degree of entanglement in linear polymer systems, Macromol. Theory Simul. 3 (1994) 639–647.
[12] Z1 is available online at http://www.complexfluids.ethz.ch/Z1.
[13] N.C. Karayiannis, M. Kröger, Combined molecular algorithms for the generation, equilibration and topological analysis of entangled polymers: methodology and performance, Int. J. Mol. Sci. 10 (2009) 5054–5089.
[14] M. Rubinstein, R. Colby, Polymer Physics, Oxford University Press, 2003.
[15] H.K. Moffatt, The degree of knottedness of tangled vortex lines, J. Fluid Mech. 35 (1969) 117–129.
[16] H.K. Moffatt, R.L. Ricca, Helicity and the Calugareanu invariant, Proc. R. Soc. Lond. Ser. A 439 (1992) 411–429.
[17] K. Bajer, Abundant singularities, Fluid Dyn. Res. 36 (2005) 301–327.
[18] H. von Helmholtz, On integrals of the hydrodynamical equations, which express vortex-motion, Crelle's J. 55 (1858) 485–513.
[19] L. Woltjer, A theorem on force-free magnetic fields, Proc. Natl. Acad. Sci. USA 44 (1958) 489–491.
[20] R. Betchov, Semi-isotropic turbulence and helicoidal flows, Phys. Fluids 7 (1961) 925–926.
[21] U. Frisch, A. Pouquet, J. Léorat, A. Mazure, Possibility of an inverse cascade of magnetic helicity in magnetohydrodynamic turbulence, J. Fluid Mech. 68 (1975) 769.
[22] A. Brandenburg, K. Subramanian, Astrophysical magnetic fields and nonlinear dynamo theory, Phys. Rep. 417 (2005) 1.
[23] C. Rorai, D. Rosenberg, A. Pouquet, P.D. Minnini, Helicity dynamics in stratified turbulence in the absence of forcing, Phys. Rev. E 87 (2013) 063007.
[24] J.B. Taylor, Relaxation of toroidal plasma and generation of reverse magnetic fields, Phys. Rev. Lett. 33 (1974) 1139.
[25] R. Marino, P.D. Minnini, D. Rosenberg, A. Pouquet, Emergence of helicity in rotating stratified turbulence, Phys. Rev. E 87 (2013) 033016.
[26] K.R. Sreenivasan, C.M. White, The onset of drag reduction by dilute polymer additives, and the maximum drag reduction asymptote, J. Fluid Mech. 409 (2000) 149–164.
[27] F. Edwards, Statistical mechanics with topological constraints: I, Proc. Phys. Soc. 91 (1967) 513–519.
[28] F. Edwards, Statistical mechanics with topological constraints: II, J. Phys. A, Gen. Phys. 1 (1968) 15–28.
[29] L.H. Kauffmann, Knots and Physics, Ser. Knots Everything, vol. 1, World Scientific, 1991.
[30] V. Jones, A polynomial invariant of knots via von Neumann algebras, Bull. Am. Math. Soc. 12 (1985) 103–112.
[31] P. Freyd, D. Yetter, J. Hoste, W. Lickorish, K.C. Millett, A. Ocneanu, A new polynomial invariant for knots and links, Bull. Am. Math. Soc. 12 (1985) 239–246.
[32] K. Iwata, S.F. Edwards, New model of polymer entanglement: localized gauss integral model, J. Chem. Phys. 90 (1989) 084567.
[33] K. Foteinopoulou, N.C. Karayiannis, M. Laso, M. Kröger, L. Mansfield, Universal scaling, entanglements and knots of model chain molecules, Phys. Rev. Lett. 101 (2008) 265702.
[34] J. Qin, S.T. Milner, Counting polymer knots to find the entanglement length, Soft Matter 7 (2011) 10676–10693.

[35] C. Micheletti, D. Marenduzzo, E. Orlandini, Polymers with spatial or topological constraints: theoretical and computational results, Phys. Rep. 504 (2011) 1–73.
[36] A. Stasiak, V. Katritch, L. Kauffman, Ideal Knots, Ser. Knots Everything, vol. 19, World Scientific, Singapore, 1999.
[37] E. Flapan, When Topology Meets Chemistry: A Topological Look at Molecular Chirality, Cambridge University Press, 2000.
[38] K.C. Millett, A. Dobay, A. Stasiak, Linear random knots and their scaling behavior, Macromolecules 38 (2005) 601–606.
[39] K.C. Millett, B. Sheldon, Tying Down Open Knots, Ser. Knots Everything, vol. 36, 2005, pp. 203–217.
[40] K.F. Gauss, Werke Kgl. Ges. Wiss. Gött. (1877).
[41] H.K. Moffatt, The energy spectrum of knots and links, Nature 347 (1990) 367–369.
[42] E. Panagiotou, K.C. Millett, S. Lambropoulou, The linking number and the writhe of uniform random walks and polygons in confined space, J. Phys. A 43 (2010) 045208.
[43] Y. Diao, R.N. Kushner, K.C. Millett, A. Stasiak, The average crossing number of equilateral random polygons, J. Phys. A, Math. Gen. 36 (2003) 11561–11574.
[44] J. Arsuaga, M. Vazquez, P. McGuirk, S. Trigueros, D.W. Sumners, J. Roca, DNA knots reveal a chiral organization of DNA in phage capsids, Proc. Natl. Acad. Sci. USA 102 (2005) 9165–9169.
[45] J. Arsuaga, Y. Diao, M. Vazquez, Mathematical methods in DNA topology: applications to chromosome organization and site-specific recombination, in: C.J. Benham, S. Harvey, W.K. Olson, D.W. Sumners, D. Swigon (Eds.), Mathematics of DNA Structure, Functions and Interactions, vol. 40, Springer Science + Business Media, New York, 2009, pp. 7–36.
[46] A. Dobay, J. Dubochet, K.C. Millett, P. Sottas, A. Stasiak, Scaling behavior of random knots, Proc. Natl. Acad. Sci. 100 (2003) 5611–5615.
[47] Y. Diao, C. Ernst, K. Hinson, U. Ziegler, The mean-squared writhe of alternating random knot diagrams, J. Phys. A, Math. Theor. 43 (2010) 495202.
[48] Y. Diao, A. Dobay, A. Stasiak, The average inter-crossing number of equilateral random walks and polygons, J. Phys. A, Math. Gen. 38 (2005) 7601–7616.
[49] J. Portillo, Y. Diao, R. Scharein, J. Arsuaga, M. Vazquez, On the mean and variance of the writhe of random polygons, J. Phys. A, Math. Theor. 44 (2011) 275004.
[50] J.I. Sulkowska, E.J. Rawdon, K.C. Millett, J.N. Onuchic, A. Stasiak, Conservation of complex knotting and slpiknotting in patterns in proteins, Proc. Natl. Acad. Sci. USA 109 (2012) E1715.
[51] E. Panagiotou, K.C. Millett, S. Lambropoulou, Quantifying entanglement for collections of chains in models with periodic boundary conditions, in: Topological Fluid Dynamics, Procedia IUTAM 7 (2013) 251–260.
[52] E. Panagiotou, M. Kröger, K.C. Millett, Writhe and mutual entanglement combine to give the entanglement length, Phys. Rev. E 88 (2013) 062604.
[53] E. Panagiotou, M. Kröger, Pulling-force-induced elongation and alignment effects on entanglement and knotting characteristics of linear polymers in a melt, Phys. Rev. E 90 (2014) 042602.
[54] K.C. Millett, E.J. Rawdon, Energy, ropelength, and other physical aspects of equilateral knots, J. Comput. Phys. 186 (2003) 426–456.
[55] M.S. Berger, Magnetic helicity in a periodic domain, J. Geophys. Res. 102 (1997) 2637.
[56] H.R. Morton, S. Grishanov, Doubly periodic textile structures, J. Knot Theory Ramif. 18 (2009) 1597–1622.
[57] E. Panagiotou, C. Tzoumanekas, S. Lambropoulou, K.C. Millett, D.N. Theodorou, A study of the entanglement in systems with periodic boundary conditions, Prog. Theor. Phys. Suppl. 191 (2011) 172–181.
[58] G. Calugreanu, Sur les classes d'isotopie des noeuds tridimensionnels et leurs invariants, Czechoslov. Math. J. 11 (1961) 588–625.
[59] T. Banchoff, Self-linking numbers of space polygons, Indiana Univ. Math. J. 25 (1976) 1171–1188.
[60] F.B. Fuller, The writhing number of a space curve, Proc. Natl. Acad. Sci. USA 68 (1971) 815–819.
[61] J.H. White, Self-linking and the Gauss integral in higher dimensions, Am. J. Math. 91 (1969) 693–727.
[62] F.B. Fuller, Decomposition of the linking number of a closed ribbon: a problem from molecular biology, Proc. Natl. Acad. Sci. USA 75 (1978) 3557–3561.
[63] P.T. Bateman, On the representations of a number as the sum of three squares, Proc. Lond. Math. Soc. 71 (1950) 70–101.
[64] T. Estermann, On the representations of a number as a sum of three squares, Proc. Lond. Math. Soc. 3 (1959) 575–594.
[65] E. Grosswald, Representations of Integers as Sums of Squares, Springer-Verlag, 1985.
[66] C.G.J. Jacobi, Fundamenta Nova Theoriae Functionum Ellipticarum, Sumtibus Fratrum Borntraeger, 1829.
[67] S. Cooper, M. Hirschhorn, On the number of primitive representations of integers as sums of squares, Ramanujan J. 13 (2007) 7–25.
[68] E. Landau, Handbuch der Lehre von der Verteilung der Primzahlen, Teubner, Leipzig, 1909.
[69] F. Chamizo, E. Christobal, A. Ubis, Visible lattice points in the sphere, J. Number Theory 126 (2007) 200–211.
[70] W. Duke, Hyperbolic distribution problems and half-integral weight mass forms, Invent. Math. 92 (1988) 73–90.
[71] W. Duke, R. Schulze-Pillot, Representation of integers by positive ternary quadratic forms and equidistribution of lattice points on ellipsoids, Invent. Math. 99 (1990) 49–57.
[72] E.P. Golubeva, O.M. Fomenko, Assymptotic distribution of lattice points on the three-dimensional sphere, J. Sov. Math. 52 (1990) 3036–3048.
[73] J. Bourgain, P. Sarnak, Z. Rudnik, Local statistics of lattice points on the sphere, arXiv:1204.0134, 2012, 15 pp.
[74] D. Hensley, The number of lattice points within a contour and visible from the origin, Pac. J. Math. 166 (1994) 295–304.
[75] F. Chamizo, H. Iwaniec, On the sphere problem, Rev. Mat. Iberoam. 11 (1955) 417–429.
[76] D. Cimazoni, V. Turaev, A generalization of classical invariants of links, Osaka J. Math. 44 (2006) 1–31.
[77] U. Kaisre, Link Theory in Manifolds, Springer, 1997.
[78] R. Schneiderman, Stable accordance of knots in 3-manifolds, Algebr. Geom. Topol. 10 (2010) 373–432.
[79] P. Kirk, C. Livingston, Knot invariants in 3-manifolds and essential tori, Pac. J. Math. 197 (2001) 73–96.
[80] D. DeTurk, H. Gluck, Electrodynamics and the gauss linking integral on the 3-sphere and the hyperbolic 3-space, J. Math. Phys. 49 (2008) 023504.
[81] D. DeTurk, H. Gluck, Linking, twisting, writhing and helicity on the 3-sphere and in hyperbolic 3-space, J. Differ. Geom. 94 (2013) 87–128.
[82] L.H. Kauffmann, Virtual knot theory, Eur. J. Comb. 20 (1999) 663–691.
[83] V.I. Arnold, The asymptotic Hopf invariant and its applications, Sel. Math. Sov. 5 (1986) 4.
[84] C. Tzoumanekas, F. Lahmar, B. Rousseau, D.N. Theodorou, Topological analysis of linear polymer melts: a statistical approach, Macromolecules 42 (2009) 7474.
[85] E.J. Hanse van Rensburg, D.W. Sumners, E. Wasserman, S.G. Whittington, Entanglement complexity of self-avoiding walks, J. Phys. A, Math. Gen. 25 (1992) 6557.
[86] P. Virnau, Y. Kantor, M. Kardar, Knots in globule and coil phases of a model polyethylene, J. Am. Chem. Soc. 127 (2005) 15102.
[87] S. Lambropoulou, C.P. Rourke, Markov's theorem in 3-manifolds, Topol. Appl. 78 (1997) 95–122.
[88] H. Seifert, W. Threlfall, A Textbook of Topology, Pure Appl. Math., 1985.